REPORT DOCUMENTATION PAGE

Form Approved
OMB No. 0704-0188

1. REPORT DATE *(DD-MM-YYYY)*	2. REPORT TYPE	3. DATES COVERED *(From - To)*
06-10-2010	Technical Paper	

4. TITLE AND SUBTITLE

Implementations Strategies for In-Space Macron Propulsion

5a. CONTRACT NUMBER

5b. GRANT NUMBER

5c. PROGRAM ELEMENT NUMBER

6. AUTHOR(S)
Jacob Schonig

5d. PROJECT NUMBER

5f. WORK UNIT NUMBER
50260542

7. PERFORMING ORGANIZATION NAME(S) AND ADDRESS(ES)

Air Force Research Laboratory (AFMC)
AFRL/RZSA
10 E. Saturn Blvd.
Edwards AFB CA 93524-7680

8. PERFORMING ORGANIZATION REPORT NUMBER

AFRL-RZ-ED-TP-2010-414

9. SPONSORING / MONITORING AGENCY NAME(S) AND ADDRESS(ES)

Air Force Research Laboratory (AFMC)
AFRL/RZS
5 Pollux Drive
Edwards AFB CA 93524-7048

10. SPONSOR/MONITOR'S ACRONYM(S)

11. SPONSOR/MONITOR'S NUMBER(S)
AFRL-RZ-ED-TP-2010-414

12. DISTRIBUTION / AVAILABILITY STATEMENT

Distribution A: Approved for public release; distribution unlimited (PA #10506).

13. SUPPLEMENTARY NOTES
Master's Thesis, University of Colorado, Colorado Springs, CO.

14. ABSTRACT

A Macron Launched Propulsion (MLP) system has been derived from electric propulsion technology to provide the ability to accelerate macrons (i.e. a macroscopic particle with an approximate mass of 1 gram) as a means of thrust for in-space propulsion. Macron propulsion technology can potentially accelerate macrons to speeds upwards of 10km/s with a corresponding specific impulse (Isp) of 1,000s and a thrust of 10N. The data presented in this paper outlines the performance parameters of a MLP system and serves as a guide for spacecraft operators to effectively implement and utilize a macron propulsion system. All spacecraft propulsion systems have the potential to adversely impact the space environment. The research conducted within the study supports the claim that a macron propulsion system's level of impact on the space environment is no greater than current operational propulsion methods. If implemented in the most precautious manner, a macron propulsion system is theoretically capable of operating in the space environment with a near zero level of impact. Macron propulsion technology has numerous distinct performance parameters and the potential to be implemented as a primary in-space propulsion system capable of conducting numerous orbital maneuvering scenarios with minimal space environment impact.

15. SUBJECT TERMS

16. SECURITY CLASSIFICATION OF:			17. LIMITATION OF ABSTRACT	18. NUMBER OF PAGES	19a. NAME OF RESPONSIBLE PERSON
					Mr. Marcus Young
a. REPORT	b. ABSTRACT	c. THIS PAGE			19b. TELEPHONE NUMBER *(include area code)*
Unclassified	**Unclassified**	**Unclassified**	SAR	98	N/A

IMPLEMENTATION STRATEGIES FOR IN-SPACE MACRON PROPULSION

by

JACOB ANDREW SCHONIG

B.S., United States Air Force Academy, 2009

A thesis submitted to the Graduate Faculty of the

University of Colorado at Colorado Springs

in partial fulfillment of the

requirements for the degree of

Masters of Mechanical Engineering

Department of Mechanical and Aerospace Engineering

2010

The views expressed in this article are those of the author and do not reflect the official policy or position of the United States Air Force, Department of Defense, or the U.S. Government.

This thesis for a Masters of Mechanical Engineering degree by

Jacob Andrew Schonig

has been approved for the

Department of Mechanical and Aerospace Engineering

By

_____

Andrew Ketsdever, Chair

_____

Steven Tragesser

_____

Scott Trimboli

_____

Date

Schonig, Jacob Andrew (M.S., Mechanical Engineering)

Implementation Strategies for In-Space Macron Propulsion

Thesis directed by Associate Professor Andrew D. Ketsdever

Recent advances in energy storage and solid-state switching enabled the use of peristaltic, pulsed inductive acceleration of non-ferritic particles for spacecraft propulsion. Macron Launched Propulsion (MLP) systems electromagnetically accelerate gram-sized aluminum particles (i.e. macrons) to achieve exit velocities between 5 and 10km/s with corresponding specific impulses between 500 and 1,000s. Research was conducted to formulate possible implementations of this technology and analyze this system's potential impact on the orbital debris environment. Ultimately, the firing angle, exit velocity, and altitude combination at which a macron is fired determines a macron's trajectory and dictates the level of impact upon the orbital debris environment. Macrons which are placed into orbital trajectories are highly undesirable and possess adequate destructive capability via hypervelocity impacts to cause a catastrophic failure on even the most heavily shielded spacecrafts.

Research supports the implementation of macron propulsion technology as a multi-purpose orbital maneuvering system but cautions the use of a macron propulsion system in a manner that could result in macrons entering into stable Earth orbital trajectories. Furthermore, the implementation of a macron propulsion system as a means of constant momentum exchange of mass between satellites enables sustainable tandem satellite formations with a theoretically infinite operational lifetime.

Macron propulsion technology is applicable to a wide variety of orbital maneuvering scenarios and is relevant to contemporary and future space operations. Traditional propulsion methods (i.e. solid rocket motors) are widely implemented and can have a tremendously impact the space environment. Macron propulsion technology can be implemented as a primary in-space propulsion system with potentially no impact on the space environment.

DEDICATION

To those who have always supported, mentored, and believed in me.

ACKNOWLEDGMENTS

This work was supported by the Advanced Concept Group of the Air Force Research Laboratory's Propulsion Directorate (Edwards AFB, CA). Satellite Tool Kit™ software courtesy of Analytic Graphics Inc. (AGI). On an organizational level, the author wishes to thank the United States Air Force and the University of Colorado at Colorado Springs, specifically the Department of Mechanical and Aerospace Engineering, for their acceptance and support.

Simply stated, Dr. Andrew Ketsdever is an invaluable and irreplaceable mentor who has insurmountably contributed not only to the development of this paper but also to the author's personal, professional, and academic development. Dr. Ketsdever is well deserving of the author's unwavering gratitude, trust, and respect. In addition, the author wishes to thank the Dr. Taylor Lilly for his priceless and significant contributions to the academic development of the author and his willingness to always aide others. Furthermore, Dr. David Kirtley's contributions to the development of this paper through numerous fruitful conversations and guidance must be recognized.

The support provided by Sarah Schonig to the development of this paper is incomparable and undeniable. Sarah's never ending support, understanding, and love provides the foundation for the author's personal and professional development. No words can describe the author's admiration and respect for Sarah's lifelong efforts and commitments.

TABLE OF CONTENTS

TABLES

Table

FIGURES

Figure

NOMENCLATURE

ρ	=	atmospheric density
F	=	force of thrust
v	=	macron exit velocity
f	=	firing frequency
ΔV	=	change in velocity
ΔV_s	=	change in velocity for simple plane change
θ	=	inclination change angle
C_d	=	coefficient of drag
A	=	cross-sectional area
V_i	=	spacecraft initial velocity
F_d	=	force of drag
I_{sp}	=	specific impulse
m_i	=	initial spacecraft mass
m_f	=	final spacecraft mass
m_x	=	mass of object x
g_0	=	Earth's acceleration due to gravity
μ	=	Earth's gravitational parameter
n	=	angular velocity
a	=	semi-major axis
R	=	radius
z_x^*	=	distance from centerline orbit to object x
Δy	=	change in satellite separation distance
α_{xy}	=	acceleration force in the direction from object x to y
t_t	=	thickness of target or impacting surface
$t_{t\,min}$	=	minimum thickness of target or impacting surface
d_c	=	crater diameter
D_c	=	crater depth
d	=	diameter
d_p	=	particle diameter
$d_{p\,max}$	=	maximum defeatable particle diameter
ρ_t	=	density of impacting target or surface
ρ_p	=	density of particle
v_p	=	velocity of particle
α_p	=	particle impact angle with respect to surface normal
$\lambda, \beta, \gamma, \xi, \kappa, \delta, \upsilon$	=	calibration constants
K_1	=	calibration factor

CHAPTER 1

INTRODUCTION

A Macron Launched Propulsion (MLP) system has been derived from electric propulsion technology to provide the ability to accelerate macrons (i.e. a macroscopic particle with an approximate mass of 1 gram[1]) as a means of thrust for in-space propulsion. Macron propulsion technology can potentially accelerate macrons to speeds upwards of 10km/s with a corresponding specific impulse (Isp) of 1,000s and a thrust of 10N. Isp is a measure of the total impulse per unit weight of propellant and is one of several key performance parameters when analyzing a propulsion system. Modeling suggests a highly efficient MLP thruster with no ionization losses can achieve efficiencies upwards of 90% while operating between 500 and 1,000s of Isp. With these performance parameters, macron propulsion technology could successfully fill the void of a highly efficient electric propulsion (EP) system which operates between 500 and 1,000s of Isp, as seen in Figure 1,[2] while maintaining a relatively high thrust level. Figure 1 displays typical Isp and efficiency ranges for various EP systems. Satellite mission designers are interested in the development of a responsive spacecraft propulsion system that maintains high efficiencies and thrust. Because of the well known trade-off between thrust and Isp in traditional EP systems, there is an interest in a high power EP system that operates at a moderate Isp (i.e. 1,000s) with reasonably high thrust levels (i.e. 10N). In comparison to traditional EP systems, a MLP system is highly efficient and displays a noticeable increase in both Isp and thrust levels from resitojet and arcjet technologies.

A. Focus of this Study

This study seeks to provide a technical system analysis of potential implementations of macron propulsion technology and the corresponding impact of a MLP system on the space environment. The study and development of macron propulsion technology has been initiated due to a MLP system's capability of expanding the operational performance range of EP technology. Currently, MSNW, LLC has developed a preliminary MLP system which allows for extensive experimentation and validation of performance

parameter predictions.[3] Before a MLP system can be integrated into the space mission architecture, a comprehensive analysis of the system's overall impact on the space environment is warranted. Specifically, the overall goal of this research is to determine the impact that a fired macron can have on the orbital debris environment, the potential hazards imposed by a fired macron on other orbiting spacecraft, and formulating possible implementations of macron propulsion technology.

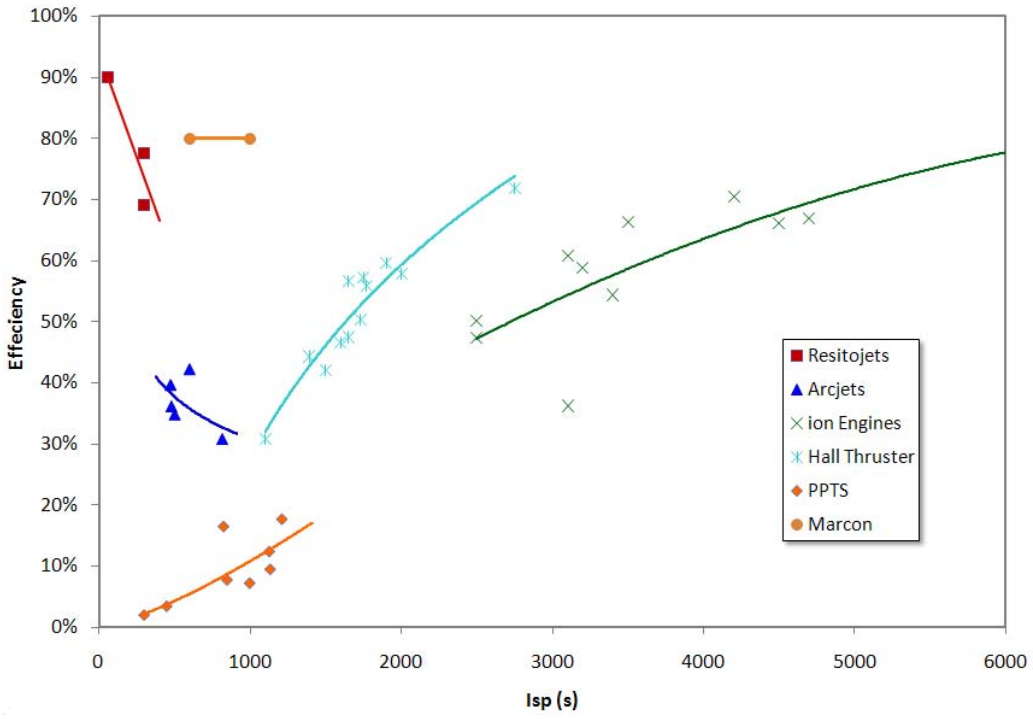

Figure 1. Typical efficiencies for various EP methods[2]

The knowledge gained from this study will provide insights into the advantages, disadvantages, and general operational boundaries of macron propulsion technology from an overall space environment perspective. This study will investigate possible implementations of a MLP system as a means of orbital maneuvering. A primary goal of all conducted research in this study is to define an operational realm of orbital maneuvers that are practical and enhanced through the implementation of macron propulsion technology. The insights gained from a MLP system's analysis will identify the current macron propulsion technology design space while simultaneously aiding decision makers in the determination of a MLP system's level of merit and applicability to contemporary space operations.3

B. Technical Review of MLP System

The MLP system investigated in this study utilizes peristaltic, pulsed inductive acceleration techniques of non-ferritic particles to electromagnetically accelerate macrons to speeds between 5 and 10km/s. Pulsed induction is an acceleration mechanism based on the repulsive force exerted on a magnetically induced conductor by employing a series of one or more pulsed coils. Since this process is inductive, no direct mechanical or electrical connection with the projectile is required resulting in an increased overall system lifetime capable of high firing frequencies. The maximum exit velocity of a macron fired from a MLP system is thus determined by the intrinsic behavior of the projectile's (i.e. macron's) material conductivity, density, induced current sheet thickness, and number of stages of the propulsion system. The maximum exit velocity achievable through this approach is independent of the magnetic waveform and is primarily limited by the material characteristics of the macron. Ultimately, heating of the macron due to the magnitude of the induced currents can cause vaporization if a macron's material properties are unfavorable. Aluminum was chosen as the material of choice due to its excellent operating parameters and low cost. In its simplest manifestation, the physics of the MLP system are similar to those employed in a plasma-based Pulsed Inductive Thruster (PIT) and a Magnetically Accelerated Plasmoid (MAP) thruster.[4] Figure 2 depicts a MLP system capable of achieving the energy and power requirements to launch a 1g macron with an exit velocity of 10km/s.[3]

Figure 2. Six staged MLP system (*Shown are solid-state switching, parallel capacitors, fiber-optic trigger and data acquisition unit, and macron launcher)*[3]

The mission benefits of a propulsion system based on the acceleration of macrons are far reaching. The primary efficiency loss in a MLP thruster is a result of Ohmic heating of the projectile. Therefore, macrons are ejected from the thruster without significant heat transfer to the thruster's walls minimizing the amount of thermal management required for the overall system. Similarly, this technology is uniquely suited to be implemented as a primary, in-space propulsion system applicable for power levels greater than 10kW and can provide high thrust to power ratios of greater than 200mN/kW at 800s of specific impulse.[3] These performance parameters allow for a very rapid response to necessary orbital maneuvers. A MLP system's performance capabilities can reduce transfer times by enabling multi-day orbital maneuvering in contrast to the traditional multi-month plasma EP maneuvers. Furthermore, the traditional benefits of a pulsed EP system also apply: exceptional variability in thrust and power levels, variable Isp, and high specific power.

Figure 3 displays key performance parameters for traditional EP systems.[5] Figure 3(A) shows the specific mass (i.e. the system's mass required for a unit of power) versus Isp (i.e. the system's ability to convert propellant into directionalized thrust). One goal of all EP systems is to minimize specific mass while maximizing Isp. In this regard, macron propulsion technology provides an increase in operational capabilities by increasing Isp while continuing to minimize specific mass with respect to resistojets and arcjets. Figure 3(B) shows the thrust to power ratio of various EP systems versus Isp which is a measure of how efficiently an EP system can convert electrical power into thrust.

The power input required for any propulsion system is a function of the system's force of thrust, Isp, and efficiency. For a given input power, a trade-off between thrust and Isp generally exists for all EP systems as shown in Eq. (1). To increase the force of thrust of an EP system, Isp values are usually decreased which drives a decrease in system efficiency and vice versa. A key attribute of macron propulsion technology is the ability to alter thrust and Isp values relatively independent of system efficiency. With respect to traditional EP systems, a MLP system is capable of increasing Isp with minimal reductions to the thrust to power ratio. This represents an increase in the operational capabilities of EP systems. A detailed description of the MLP system under investigation can be found in Ref. [3].

$$P_{in} = \frac{1}{2}\eta^{-1} F g_0 Isp \tag{1}$$

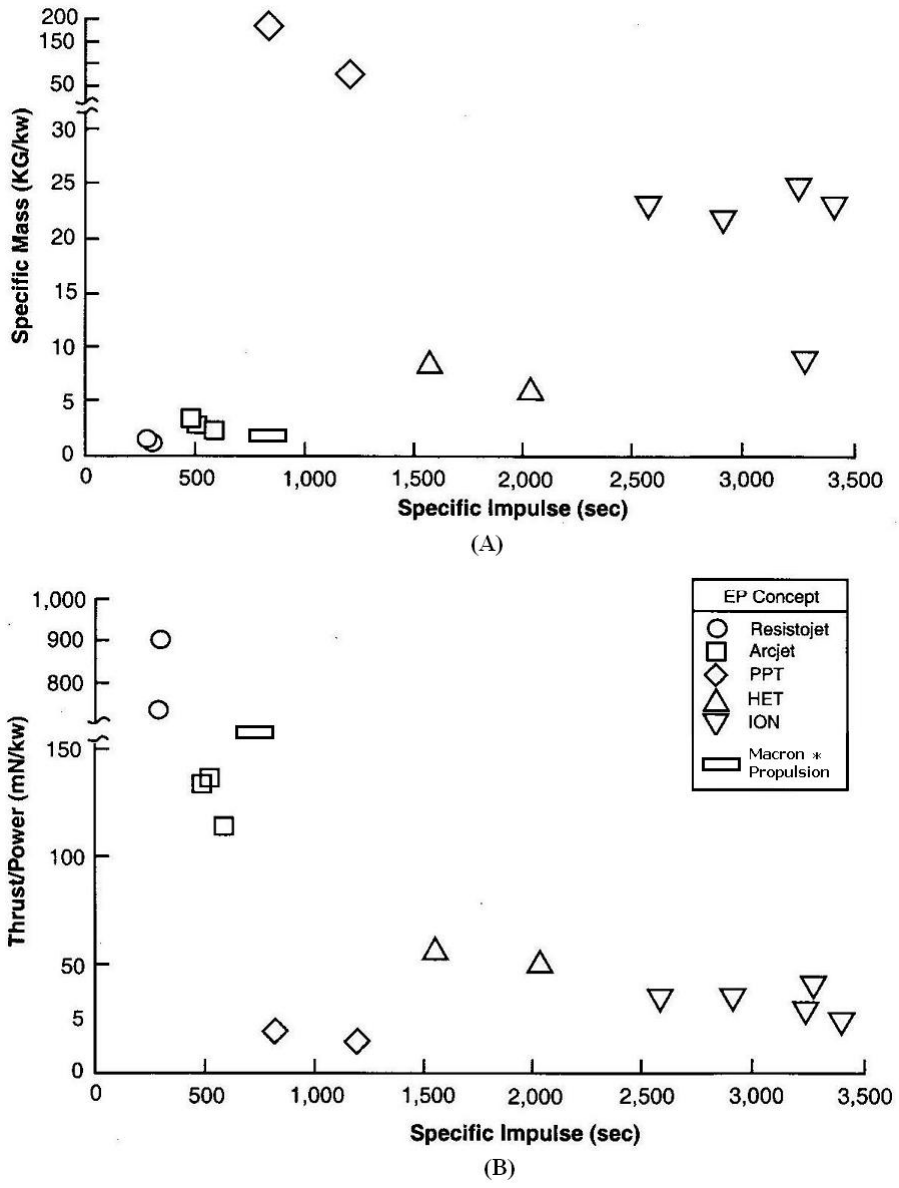

Figure 3. (A) specific mass and (B) thrust to power ratios of traditional EP systems versus Isp [5]

**Macron propulsion data added by author*

CHAPTER 2

CHARACTERIZATION OF THE MMOD ENVIRONMENT

Before an analysis of a MLP system's impact on the space environment can be fully understood, a basic level of understanding of the characteristics and threats (i.e. hypervelocity impacts) imposed by the Micrometeoroid and Orbital Debris (MMOD) environment is required. Once a macron is fired from a MLP system, it will become a self-governing space object subjected to the full extent of the laws of astrodynamics (i.e. space environment motion). Refs. [6, 7, and 8] give a complete overview of astrodynamics concepts.

If a fired macron is placed into an Earth orbital trajectory, it will be classified as an orbital debris object and adversely impact the space environment by increasing both the number of MMOD particles and the probability of a MMOD object collision with a satellite. Therefore, all orbital macrons will negatively impact space operations. Orbital debris mitigation and prevention measure are crucial because space operations and exploration are vital to our national, civil, and commercial interests. The sources (i.e. potentially a MLP system) must be addressed and minimized to ensure a continuation of space operations.

A. Micrometeoroid and Orbital Debris Environment

Extensive research has been conducted to characterize the MMOD environment by the collective works of Refs. [9, 10, 11, and 12]. The two primary sources of space debris are naturally occurring micrometeoroids and human created orbital debris. Micrometeoroids are, by definition, considered any solid particle larger than an atom but smaller than an asteroid traveling through the universe.[13] Typically, micrometeoroids are composed of interplanetary ice or rock particles. In contrast, orbital debris particles are unnaturally occurring objects that result from human presence in space. All orbital debris can be categorized in five general classifications: fragmentation, nonfunctional spacecrafts, rocket bodies, mission related debris, and debris from unknown sources.

In general, fragmentation particles are produced through spacecraft collisions, deterioration, and break-ups and account for 40% of the all orbital debris.[9] The size and number of fragments released is dependent on the energy and nature of the fragmentation process. In general, fragmentation debris is assumed to account for a debris particle diameter range between 0.1mm and 1m.[10] Nonfunctional spacecrafts account for 25.3% of the orbital debris environment and consist of decommission spacecrafts.[9] Rocket bodies from spent upper stages account for 19.4% of the orbital debris environment. Mission related debris accounts for 13.3% of the orbital debris environment and includes explosive bolts, vehicle shrouds, solid rocket motor debris, and sodium potassium (i.e. coolant) droplets.[9] The remaining 2% of the orbital debris comes from unknown sources.[9] The size range of orbital debris is vast and contains three general classifications: small, medium, and large size particles. Small particles are less than 1mm in diameter, medium particles are between 1mm and 10cm in diameter, and large particles are greater than 10cm in diameter.

Current ground based space surveillance technology is capable of detecting and tracking orbital debris particles with diameters greater than 1cm. Therefore, the production of orbital debris particles smaller than 1cm in diameter is highly undesirable due to the current limitations of space debris tracking technology which does not allow for adequate tracking of sub-centimeter diameter orbital debris particles. Large particles are tracked and catalogued using ground based sensors and optical telescopes. Medium particles are tracked and catalogued by the Haystack radar. Small particles are undetectable using ground based technology and rely on in-situ measuring techniques (i.e. examining the small particle damage on spacecrafts that are returned to Earth).

The MMOD flux (i.e. the amount of space debris passing through a given area at a given time) experienced by a satellite is directly proportional to the probability of a MMOD particle impacting a satellite.[11] As MMOD flux increases, so too does the probability that a satellite experiencing a MMOD related collision. Therefore, in order to assess the threat level imposed by a MMOD particle on a satellite, it is necessary to quantify the MMOD flux in the particular region of space in which the satellite operates. Due to increased space operations, the orbital debris flux in LEO is greater than the micrometeoroid flux. Therefore, orbital debris accounts for the majority of the LEO collision hazards. Figure 4 shows the approximate MMOD flux according to particle size in LEO.[14] The number density of micrometeoroids in

GEO is slightly less than in LEO; however, Figure 4 is a reasonably accurate approximation of the micrometeoroid flux for all altitudes less than or equal to GEO. In GEO, the orbital debris flux is relatively insignificant as compared to the micrometeoroid flux. A general equation which calculates the micrometeoroid flux and the representative mass density distribution experienced by a spacecraft are given in Ref. [15] and Appendix A.

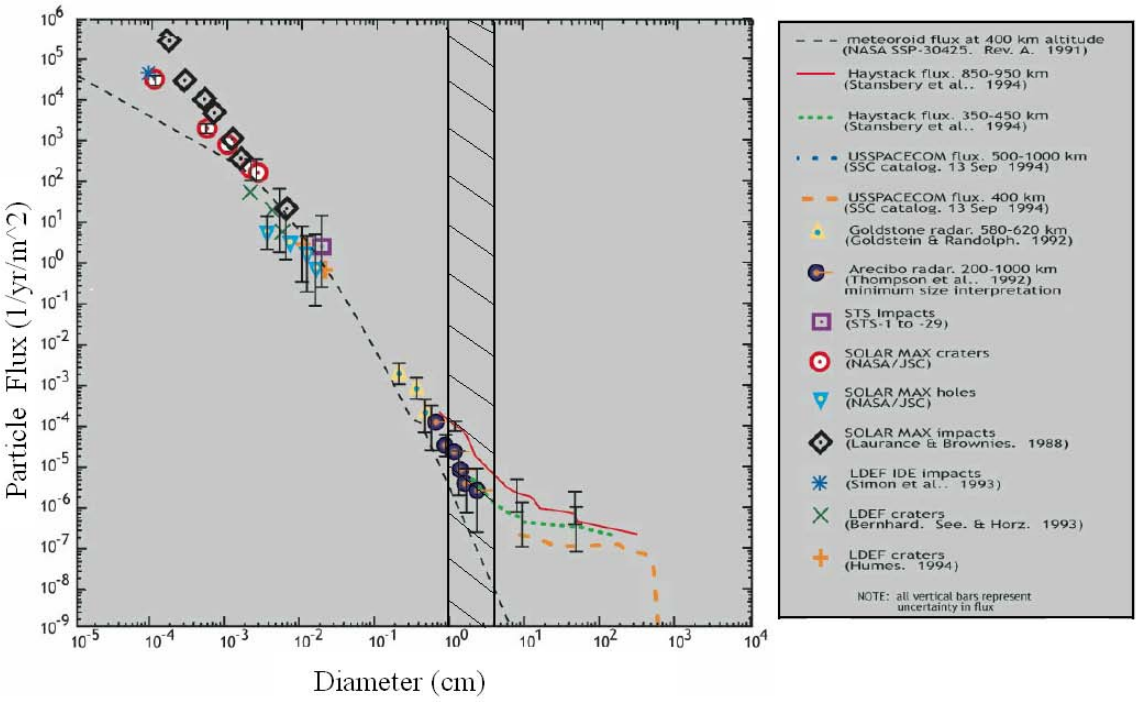

Figure 4. MMOD flux according to particle size[14]

The most significant difference between the micrometeoroid and orbital debris particle populations are the relative mass distribution of debris particles. The majority of orbital debris mass is found in objects greater than 1cm in diameter; whereas, the majority of mass of micrometeoroid debris is found in particles less than 0.1mm in diameter. In other words, orbital debris particles tend to be large (i.e. greater than 10cm in diameter) while micrometeoroid particles tend to be small (i.e. less than 0.1mm in diameter). This distribution of space debris mass is sufficient to cause the orbital debris environment to be more hazardous than the micrometeoroid debris environment for spacecraft operating below 2,000km altitude. The greatest concentration of orbital debris occurs at inclinations of 60, 80, and 100deg for LEO altitudes ranging between 350 and 2,000km with peak particles concentrations at 1,000km altitude. The orbital inclination of an object refers to the relative angle between the object's orbital plane and the

equatorial plane. Figure 5 shows the MMOD density of cataloged debris objects according to particle size between LEO and GEO.[16] As seen in Figure 5, the number density of MMOD objects is highly dependent on object size and orbital altitude. In general, the growth and decay trends remain relatively independent of particle size for altitudes less than or equal to GEO.

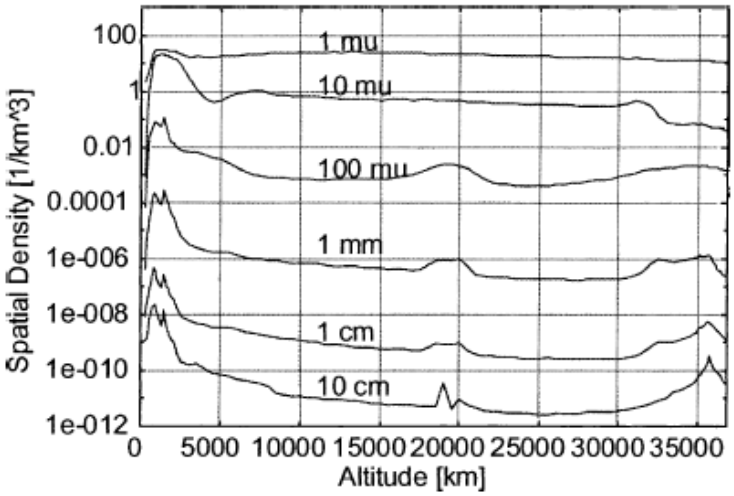

Figure 5. MMOD density for various orbital altitudes according to particle size[16]

Mathematical modeling of the orbital debris particle distribution predicts that collision fragmentation will cause the collective mass of sub-centimeter diameter particles to grow at twice the rate of the total accumulation of mass in Earth orbit. Over the past 10 years, the total mass accumulation in orbit has increased at an average rate of 5% per year, indicating that the population of small debris particles should be expected to increase at roughly 10% per year.[12,17,18]

The international space community recognizes the steady and continual growth of space debris as a global issue which must be addressed by both passive and active measures. Due to a lack of regulations and accountability, all space-faring nations have adversely contributed to the orbital debris population. The current accumulation treads of orbital debris particles are leading the global community on an unsustainable path that will result in space debris saturation of numerous orbital altitudes primarily located in the mission critical realm of LEO. This places strict requirements on the implementation of a MLP system in the space environment. All fired macrons have the potential to adversely impact the orbital debris environment and therefore, a MLP system must be operated in a manner which minimizes space environment impact (i.e. macron orbital trajectories).

C. Hypervelocity Impacts

Hypervelocity impacts (HVIs) are traditionally defined as any impact occurring with a relative velocity approximately greater than 3km/s.[19] However, this definition is merely a rule of thumb. The technical definition of a HVI is any impact of sufficient velocity that during the brief moments of collision both the particle and the impacting surface react as if they were fluids. In other words, the impact process is dominated by inertia versus material strength properties.[20] Furthermore, impact damage is essentially independent of both the angle of impact and particle density.[21]

Spacecrafts which operate in the densely populated orbital debris altitude regime between 350 and 2,000km experience a steady orbital debris particle flux which strongly increases with decreasing particle sizes as seen in Figure 4. The most probable impact velocities for orbital debris particles with operational satellites are between 1 and 15km/s and between 5 and 30km/s for meteoroids.[10] The majority of LEO orbital debris particles maintain velocities approximately equal to 7.7km/s with an average relative velocity with respect to other space objects (i.e. collision velocity) of approximately 12km/s for near circular orbits and up to 16km/s for highly eccentric orbits.[12] The exact collision velocity is a function of the angle between the two object's velocity vectors and is independent of object size or mass. Kessler's velocity function is one method of calculating the directionality of orbital debris impacts and their respective velocity distribution.[12,18,22] Kessler's velocity function describes the relative number of MMOD impacts between a range of collision velocities averaged over all orbital altitudes. The non-normalized collision velocity distribution relative to a spacecraft with a given inclination is given in Appendix B. The resulting velocity distribution of MMOD objects of various inclinations is shown in Figure 6.[12] In general, as the inclination of a satellite is increased, the range of probable collision velocities and particle fluxes decrease while the average collision velocity increases; therefore, increasing the probability of a HVI occurring at a given inclination's maximum probable collision velocity.

The resulting damage from a HVI can reasonably be predicted by a series of damage equations that are empirically derived to simulate the desired impact scenario (i.e. various particle mass and velocity combinations). Therefore, all sets of damage equations are specifically calibrated for a given impact scenario and operate under scenario specific assumptions. In general, damage equations are derived to determine if a given impact will exceed the ballistic limit of the impacting surface (i.e. will a particle

penetrate the impacting surface). The damage equations presented in Appendix B and Ref. [23] assume spherical aluminum particles impacting a single-wall surface composed of standard space-faring materials (i.e. aluminum, titanium, stainless steel, and other monolithic metal structures).

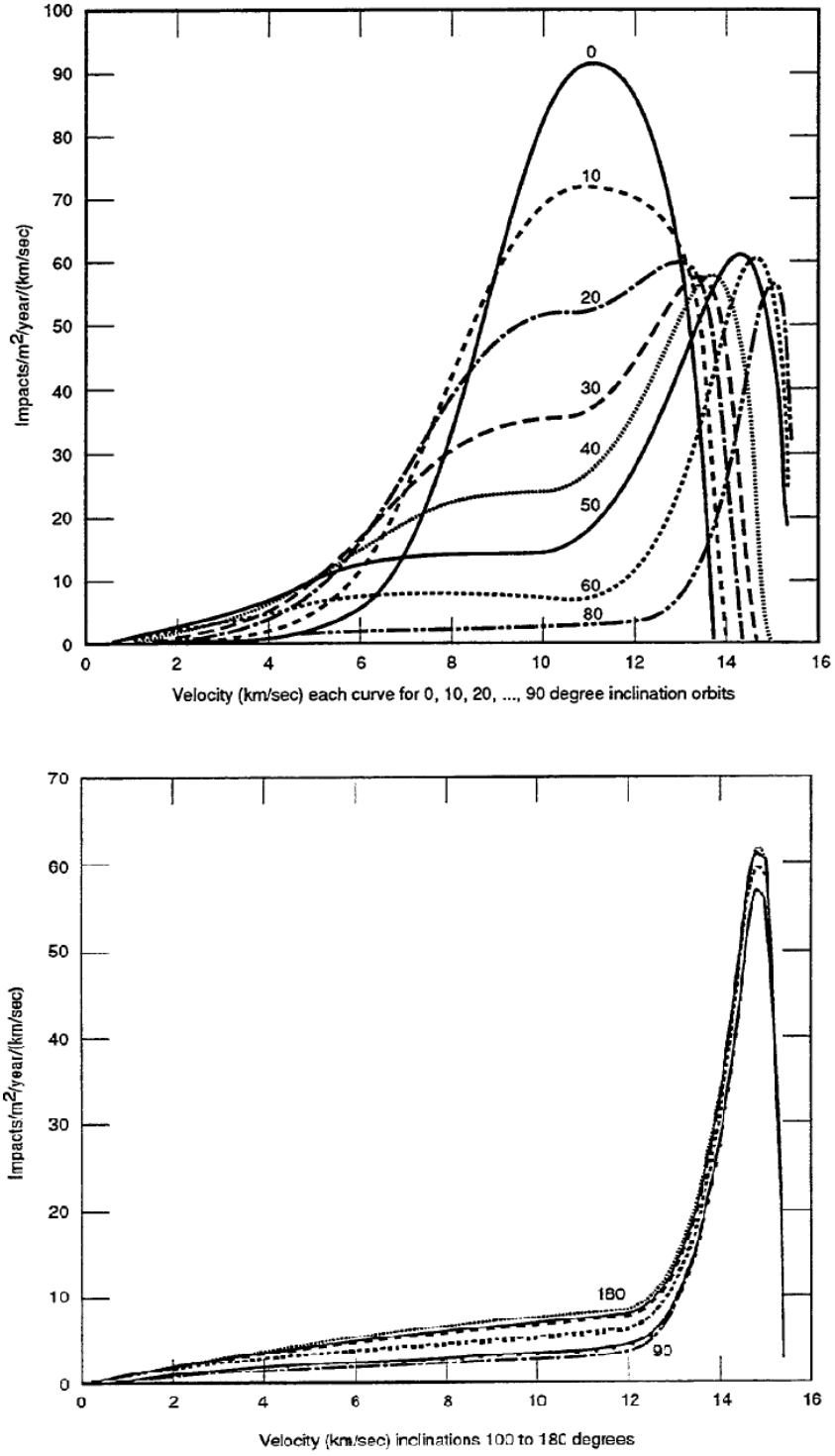

Figure 6. Kessler's velocity function for various satellite inclinations[15]

There are three primary classifications of satellite failures caused by HVIs: functional, critical, and catastrophic. A functional failure results when a single non-mission critical component is damaged. A critical failure occurs when a mission critical component is damaged but does not result in complete spacecraft or mission failure. A catastrophic failure occurs when the sustained damage results in mission failure and complete destruction of the spacecraft.[9]

In general, the consequences of HVIs with MMOD particles can range from small surface craters for small impacting debris particles (i.e. less than 1mm in diameter) to complete penetration for medium size debris (i.e. a macron) objects and partial or complete destruction via shockwaves for large impacting debris particles (i.e. greater than 10cm in diameter). Small debris particle impacts are most frequent in occurrence but they are also most insignificant in terms of spacecraft damage potential. Large debris particle impacts primarily result in catastrophic destruction of a spacecraft but are extremely rare in occurrence due to relatively small population size and because large debris particles are easily detected and avoided.

If a debris particle is able to penetrate the surface of a spacecraft, there are numerous subsequent consequences. When a HVI occurs with sufficient energy to cause complete penetration of the surface material, a debris cloud composed of the impacting particle and surface materials is created and spread inward and radially outward in the shape of a cone as seen in Figure 7. This radially distributed debris cloud causes degradation of surface, thermal, window, and mirror coatings which effects both the optical and thermal properties of a spacecraft in addition to increasing the small particle MMOD population size. Once a particle has penetrated the surface of a spacecraft, it will be exposed to the inner subsystems which if damaged, could result in critical or catastrophic failure.[9] The vast majority of satellites incorporate shielding protective measures to counter the effects of HVIs. At a minimum, shielding is installed on mission critical components (e.g. fuel tanks, batteries, critical circuitry, and other explosive pressure vessels) which would result in a catastrophic failure if damaged.

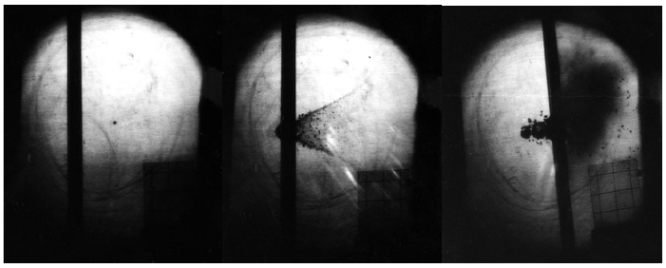

Figure 7. Debris cloud resulting from a 1cm diameter Al-particle HVI[9]

Medium debris particle collisions (i.e. orbital macron collisions) are the greatest challenge for spacecraft designers due to a combination of the large population size of medium size MMOD particles and their corresponding destructive capabilities.[9] Spacecraft shielding can dramatically decrease the damage of an impacting particle which correlates to an increased operational lifetime. However, even the most advanced shielding technologies are still limited in capability. Figure 8 shows the performance of various operational shielding methods: a single aluminum plate, a two-plate Whipple shield, and a stuffed Whipple shield. A standard Whipple shield is composed of two or more layers of solid alloy plates with various separation distances between each plate. This configuration allows for a distribution of the impacting energy over a greater surface area while simultaneously providing several layers of redundancy which is often necessary for medium size debris particle impacts. A stuffed Whipple shield fills the voids between each plate with a high strength material (e.g. Kevlar or Nextel).[23]

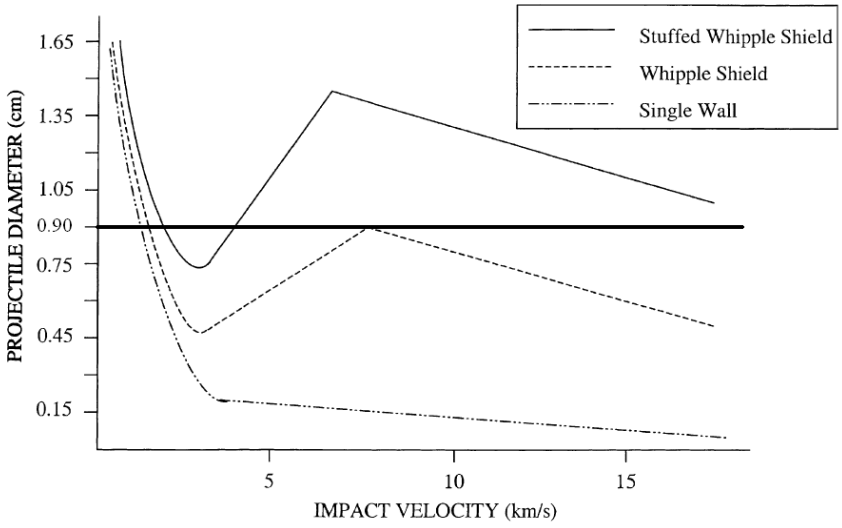

Figure 8. Effectiveness of various shielding methods *(aluminum bumper and inner wall1.27 and 4.38mm thick, respectively)*

As highlighted in Figure 8, all shielding methods experience decreased protective capabilities at sub-hypervelocities. A 1g macron (i.e. 0.8991cm in diameter) can penetrate a Whipple and a single-wall shield regardless of collision velocity. Only a stuffed Whipple shield can defend against a 1g orbital macron collision. Although counterintuitive, stuffed Whipple shields can be penetrated by a range of sub-HVIs (i.e. approximately 2 to 4km/s) but not true HVIs with orbital macrons due to the nature of material interactions during a HVI.

In general, shielding is not present on all surfaces of a spacecraft. The optimal scenario for a HVI is for the impacting particle to strike a shielded area while the worst-case scenario is for an impact to occur on an unshielded portion of the spacecraft. If a macron collides with an orbiting spacecraft, complete penetration can occur regardless of where the macron strikes. Therefore, all macrons placed into orbital trajectories will have adequate potential to cause a catastrophic failure regardless of spacecraft protective measures.

D. Potential MLP System Effects on MMOD Environment

The primary threat imposed by MMOD particles are HVIs with operational satellites. Therefore, stray or unaccounted for macrons orbiting the Earth with high relative velocities can have a tremendous impact on space operations. The most heavily populated orbital debris altitude regimes are located in LEO between 900 and 1,000km in altitude, where there is an average population of 100 cataloged MMOD objects for every 10km altitude band.[11] The second most populated altitude regime is between 1,400 and 1,500km.[9] LEO orbital altitudes are vital to space operations and provide a port of entry into the space environment. Despite the numerous advantages of LEO, satellites in LEO are 100 times more likely to collide with a MMOD particle than satellites in semisynchronous (i.e. MEO) or GEO orbits.[9]

The probability of an orbital collision is primarily dependant on the satellite's orbital altitude, size, lifetime, and orbital inclination. Spacecraft size plays an obvious role in collision probability. The larger a satellite (i.e. spacecraft or debris particle), the greater the probability that the satellite will experience a collision due to the MMOD flux's dependency on an object's cross-sectional area. Similarly, the longer a satellite stays in orbit, the greater the probability the satellite will experience a collision within its lifetime due to the MMOD flux's dependency on an object's time in orbit. Orbital collisions are a significant threat to operational satellites and occur at an alarming rate.

According to Figure 6, a macron fired into a prograde orbital trajectory will experience relative velocities with other orbiting satellites approximately between 1 and 15km/s with an average impact velocity of approximately 12km/s.[24] In general, collision velocities increase with eccentricity. Likewise, retrograde orbital objects experience significantly larger collision velocities than prograde orbital objects (i.e. greater than 13km/s) due to the vast majority of satellites being in prograde orbits. Satellite velocity vectors are constantly changing throughout an orbit and are position (i.e. time) specific. Therefore, to accurately predict the collision velocity between two objects, knowledge of the time, location, and the orbital parameters of both colliding objects must be known.

Any increase in the orbital debris population size is obviously undesirable and any increase beyond the naturally occurring micrometeoroid flux should be avoided. Fired macrons that remain in orbit (i.e. do not reenter or escape) will adversely contribute to the orbital debris environment by increasing the population of medium sized debris particles. The shaded area in Figure 4 represents the current macron radius range under consideration in this study. Through this size range, orbital debris is substantial. Above this size range, orbital debris tends to dominate the MMOD particle flux, and below this size range, MMOD particles are undetectable through ground based surveillance techniques.

For the orbital maneuvering scenarios analyzed in this study, all macrons placed into orbital trajectories will have an orbital inclination ranging between 25 and 81deg for LEO firings (i.e. 400km altitude). According to Figure 6, the most probable collision velocities associated with orbital inclinations between 25 and 81deg are approximately 13 to 15km/s, respectively. According to the Meteoroid and Space Debris Terrestrial Reference model created in the year 2001(MASTER-01),[16] the total number of MMOD objects in LEO is approximately 5.46×10^{13} objects and the combined number of MMOD objects in MEO and GEO is approximately 7.415×10^{15} objects. Therefore, a single macron placed into an orbital trajectory has minimal impact on the overall number of MMOD objects or the MMOD flux experienced by a satellite. Likewise, according to the MASTER-01 model, the number of 1cm diameter MMOD objects in LEO is approximately 189,461 objects and the combined number of 1cm diameter MMOD objects in MEO and GEO is approximately 384,484 objects. Similarly, one macron (i.e. 1cm diameter MMOD object) placed into an orbital trajectory will not have a significant effect on the overall 1cm diameter MMOD environment.

The damage which can result from HVIs are significant and necessitate both active (e.g. operating a MLP system only in non-orbital trajectory firing angles) and passive (e.g. spacecraft shielding) orbital debris mitigation practices. At hypervelocity speeds, the impact of a 1cm in diameter aluminum sphere releases the same energy as an exploding hand-grenade which can have equally devastating consequences to a spacecraft.[10] The energy density of stick (i.e. 140g) of dynamite is approximately 12.5MJ/kg.[25] The energy density of a 1g macron with a collision velocity of 10km/s is approximately 50MJ/kg. Therefore, an orbital macron has the potential to be four times more destructive than dynamite. HVIs with MMOD objects are an ever present threat to spacecrafts. History, as well as experimental data, has shown that the damage incurred by a MMOD collision can have adequate potential to cause a catastrophic failure to even the most heavily shielded spacecraft.

The earliest recorded orbital debris collision was in 1981 when ground based tracking systems recorded Cosmos 1275 spontaneously break-up into 300 separate pieces one month after its launching.[26] Cosmos 1487 experienced a similar anomaly in 1993. Olympus-1, a European Space Agency (ESA) satellite, received a confirmed collision during a meteor show in 1993 which resulted in catastrophic failure.[27] In 1996, a French microsatellite (i.e. satellite mass between 10 and 100kg) named Cerise collided with an explosion fragment of an Ariane-1 H-10 upper stage booster which had been in orbit for over a decade.[28] In 2006, a Russian Express-AM11 communication satellite catastrophically collided with an unconfirmed object believed to be orbital debris.[29] The most recent orbital collision occurred in 2009 between a nonoperational Russian satellite (Cosmos-2251) and a U.S. satellite (Irridium-33) which resulted in catastrophic damage of the operational Irridium-33 satellite.[30]The Long Duration Exposure Facility (LDEF) was commissioned in 1984 and was in LEO for 69 months. During LDEF's operational lifespan, it experienced a MMOD flux of approximately 140 significant impacts/m^2/year.[31] MMOD collisions have become an accepted reality for space operations and as a result, spacecraft designers have developed techniques to protect satellites from and minimize the consequences of a MMOD particle collision. However, the goal of this study is to provide operational criteria and implementation strategies for a MLP system in a manner which does not contribute to the orbital debris environment growth rate.

CHAPTER 3

MACRON ORBITAL ANALYSIS

Typically, the impact of a propulsion system's exhaust plume on the space environment can be hard to characterize; however, the effects of a macron propulsion system's exhaust plume (i.e. fired macrons) are readily apparent and can be significant. With every firing of a MLP system, a solid macroscopic particle is released into the space environment with a potentially catastrophic impact. This chapter investigates the possible trajectory outcomes of a fired macron, for numerous firing scenarios. The end goal of the orbital analysis is to provide a clear and tangible understanding of the possible macron trajectory outcomes and their corresponding probabilities of occurrence. The motivation of this research is to quantify the impact of an operational MLP system on MMOD environment.

A. Trajectory Analysis

The three primary parameters which determine the final trajectory of a macron are the direction, velocity, and altitude at which a macron is fired. Therefore, comprehensive models were created to simulate all firing angle (i.e. 0 to 360deg) and exit velocity (i.e. 5 to 10km/s) combinations for various firing altitudes. Satellite Tool Kit™ (STK) was used to determine the resulting trajectories of all fired macrons. STK software is a general-purpose modeling and analysis software for space systems which incorporates spatial mechanics and integrated visualization.[32] At its core, STK solves the second-order equations of motions through a variation of Cowell's formulation and Runge-Kutta numerical techniques.[33] All simulations neglect the possibility of a fired macron colliding with a neighboring spacecraft prior to achieving its final trajectory. A near term collision analysis would need to be conducted prior to all firing sequences to ensure, for example, that a macron on an escaping trajectory does not collide with a satellite along its trajectory.

STK simulations were designed to predict the trajectory of a 1g macron being fired from a circularly orbiting satellite with an initial inclination of 0deg from various firing altitudes. No perturbation

forces were considered (e.g. drag or solar radiation pressure); therefore, trajectory outcomes are a direct result of the two-body equation of motion. Macrons were modeled as solid aluminum spheres and three primary firing altitudes were investigated: 300, 20,000 and 35,786km (LEO, MEO, and GEO, respectively). Individual simulations were created for all firing angles across a two-dimensional plane parallel to the Local Vertical-Local Horizon (LVLH) of Earth with the principle coordinate system based on the velocity vector in the x-direction (i.e. RAM) as seen in Figure 9. Only firing angles within this plane were simulated since maneuvering outside of this plane is typically inefficient for the maneuvers investigated in this study.

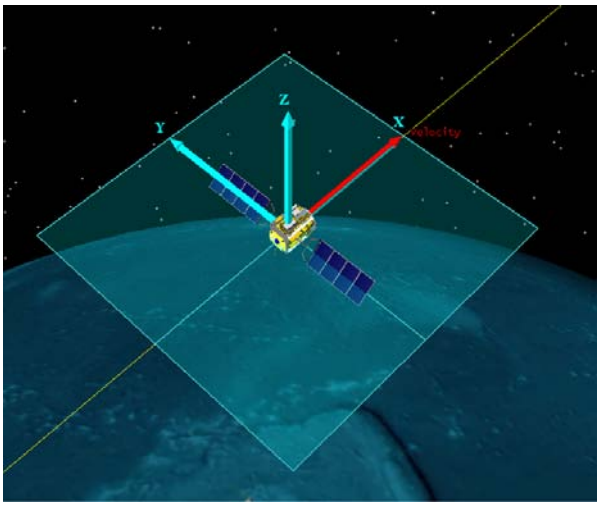

Figure 9. Macron firing plane

In general, when conducting an orbital altitude transfer, maneuvering in the anti-RAM direction is most efficient. A preliminary and overarching analysis of fired macron trajectories was conducted by fixing the firing angle of a propulsion system to the anti-RAM direction while varying the firing altitude and thruster Isp values. The Isp of a propulsion system is directly related to the exit velocity of the exhaust particles which allows for trajectory determination. This preliminary trajectory analysis study provides insights into the nature of the exhaust plume trajectories for all classifications of propulsion system's (i.e. chemical, electric, and macron propulsion systems). Figure 10 show preliminary trajectory analysis based on various propulsion systems Isp values for firing altitudes between LEO and GEO assuming perfectly directionalized exhaust flow in the anti-RAM direction with no third-body or atmospheric drag effects. Table 1 outlines the typical Isp ranges for various propulsion systems.

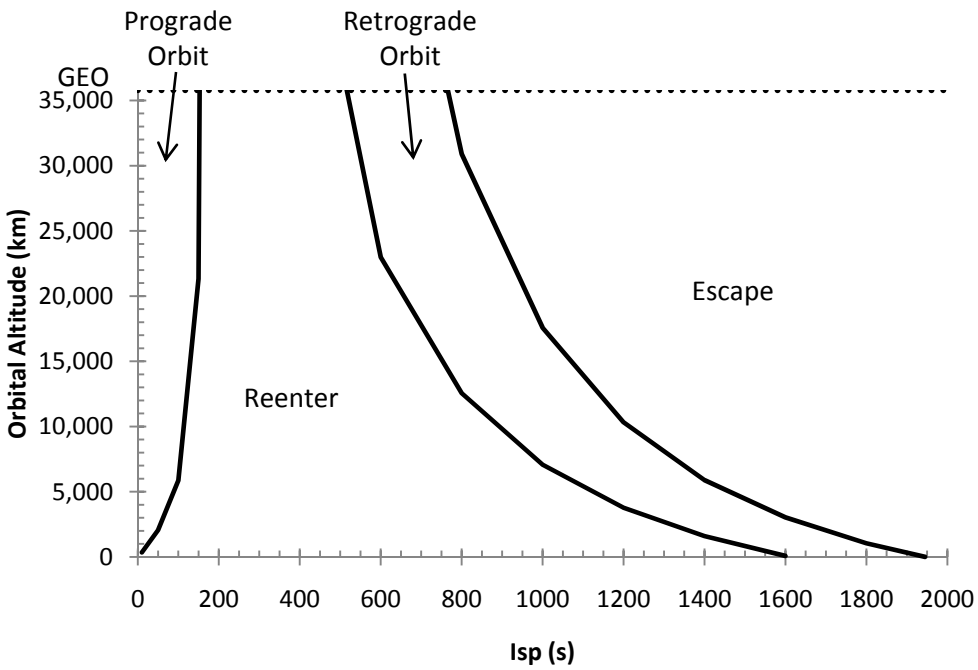

Figure 10. Preliminary anti-RAM exhaust plume trajectories for various Isp values

Propulsion Type	Isp (s)
Chemical	200-450
Resistojet	200-350
LOX/LH_2	440-460
Arcjet	400-1000
Macron Propulsion	800-1000
Solid Pulsed Plasma	600-2000
Hall Thruster	1500-2000
Ion Engine	1500-5000
Magnetoplasma Dynamic	2000-5000

Table 1. Typical Isp ranges for various propulsion systems.

Figure 10 and Table 1 combined highlight a disadvantage of a MLP system as compared to chemical and various EP (e.g. Hall thruster, ion engine, and magnetoplasma dynamic) systems. The relatively low Isp values achieved by chemical propulsion systems ensure that all anti-RAM exhausted matter will be placed on reentry trajectories. Similarly, EP systems are capable of achieving sufficiently high Isp values to ensure that all anti-RAM exhausted matter is placed on escape trajectories. MLP systems

operate in the prime Isp range to produce orbital trajectories which is highly undesirable due to the potentially hazardous impacts a single macron can have on space operations.

STK orbital trajectory simulations showed that third-body (i.e. moon) gravitational effects were generally negligible. However, at very specific firing angle, exit velocity, and altitude combinations, macrons have the potential to enter into highly elliptical orbits with a radius of apogee (i.e. a satellite's furthest point from Earth) approximately equal to or greater than the altitude of the Earth-Moon Lagrangian Point 1 (i.e. approximately 3.235×10^5km). These orbits are referred to as lunar sphere of influence (LSOI) orbits and required three-body orbital analysis. Over time, STK simulations have shown the vast majority of the LSOI orbits ultimately enter into an escape or reentry trajectory due to a constant cycle of lunar perturbations. Furthermore, LSOI orbital effects are most notable at lower (i.e. 5 to 9km/s) exit velocities and are minimal at higher (i.e. greater than 10 km/s) exit velocities.

Due to third-body gravitational effects, all trajectory analysis simulations were conducted using STK with a standardized Epoch time (i.e. scenario start time) to ensure constant relative positioning of the moon. All resulting trajectories were grouped into four categories (escape, reenter, orbit, or LSOI) as shown in Figure 11 where 0deg points in the RAM direction and 180deg points in the anti-RAM direction. For the purposes of this study, only firing angles, exit velocities, and altitude combinations resulting in minimally stable orbits (i.e. complete at least one symmetrical orbit before degrading) were considered to be orbital trajectories.

With the exception of a few firing scenarios, all macrons fired with any component of their velocity in the RAM direction escaped. In LEO, all macrons fired solely in the anti-RAM direction, the most efficient direction to thrust when altering an orbit's size or shape, are placed on a reentry trajectories. These firing angle and altitude combinations will become significant when analyzing possible implementations of a MLP system because the resulting trajectories minimize the level of impact a macron can have on the orbital debris environment. Likewise, for GEO maneuvers, all macrons fired with an exit velocity greater than or equal to 8km/s will escape regardless of firing angle, potentially minimizing a macron's level of impact. All firing angles highlighted in red in Figure 11 represent orbital trajectories and in turn trajectories (i.e. firing angles) which should be avoided.

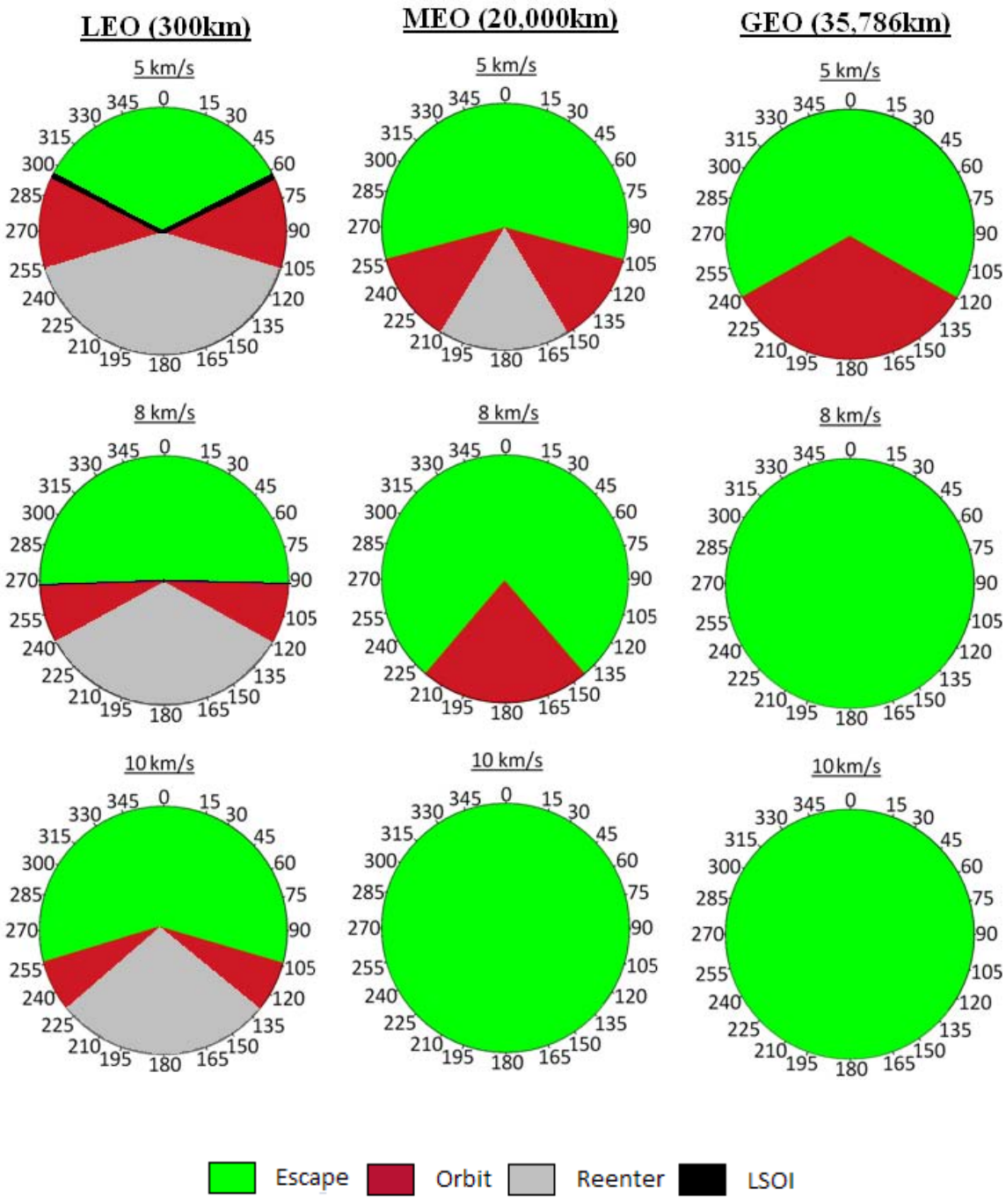

Figure 11. Macron trajectories for all possible firing angle, exit velocity, and altitude combinations

B. Orbital Trajectories

For all firing angle, exit velocity, and altitude combinations which result in orbital trajectories, knowledge of the corresponding orbital lifetime can be vital to space operations and to the determination of orbital debris effects. Orbital lifetime data can outline a general distinction between stable (i.e. large orbital lifetime) and unstable (i.e. small orbital lifetime) orbital trajectories. Knowledge concerning the orbital stability of a fired macron can aide a spacecraft operator's decision-making abilities by increasing their knowledge of the potential consequences of given maneuver (i.e. firing scenario). For example, if a pertinent spacecraft maneuver dictates a specific firing angle, exit velocity, and altitude combination that results in an orbital trajectory of a fired macron, an understanding of the resulting orbital trajectory (e.g. stable or unstable) could potentially effect a spacecraft operator's ultimate decision as to whether or not to conduct the given orbital maneuver. If the resulting orbital lifetime is on the order of a few days, it may be an acceptable risk for spacecraft operators to take in order to ensure mission success. However, if the resulting orbital lifetime equates to thousands of years, a more informed decision may result in the implantation of alternative propulsion (i.e. less impactful) methods in order to ensure continued space operations in the future. The ultimate goal of the orbital lifetime research conducted, is to provide spacecraft operators with additional information on the potential space environment impacts when the outcome of a firing scenario maneuver results in an orbital trajectory of a fired macron.

1. Force of Drag

The orbital lifetime of a satellite is dependent on a series of retarding forces which include atmospheric drag, solar radiation pressure, and third-body gravitational forces. For the purposes of this study, atmospheric drag was the only dissipative force considered in the computation of orbital lifetime calculations. The atmospheric drag experienced by a satellite is highly dependent on the satellite's orbital altitude, area to mass ratio, and eccentricity. The force of drag on an object is a result of the atmospheric density (ρ), the object's velocity (v), the object's coefficient of drag (C_d), and the cross-sectional area (A) of the spacecraft. The exact force of drag can be calculated by the following equation

$$F_d = \frac{1}{2}\rho v^2 c_d A \tag{2}$$

Atmospheric density continually fluctuates and it is not linear with altitude. Atmospheric density plays a vital role in the determination of the force of drag experienced by a satellite as seen in Eq. (2). One primary source of atmospheric density fluctuation occurs as a result of the sun's approximate 11yr solar cycle. During times of maximum solar activity (i.e. solar max), the Earth's atmosphere is heated and expanded which increases the density of the atmosphere at a given altitude. An increased atmospheric density correlates to an increased force of drag on satellites. The opposite is true during times of minimum solar activity (i.e. solar min). When the atmosphere cools and contracts, atmospheric densities decrease which in turn decreases the force of drag experienced by satellites. In LEO, the atmospheric density and, in turn, the force of drag is important. In GEO, the atmospheric density is so low that drag is not a factor. Orbital altitudes greater than 600km can have orbital lifetimes ranging from tens, hundreds, thousands to even millions of years for objects in GEO.[9,34] The eccentricity of an orbit determines both the altitude of perigee (i.e. point of closest passage to Earth) and apogee which defines the atmospheric density regime for a given satellite. A satellite in an elliptical orbit with the same average altitude as a circular orbit will degrade more rapidly due to the increased force of drag experienced near perigee. Furthermore, the area to mass ratio of a satellite effects its overall ballistic coefficient (BC) as seen in Eq. (3).

$$BC = \frac{m}{C_d A} = \frac{\rho \boldsymbol{V_{ol}}}{C_d \boldsymbol{A}}; \quad \left(\frac{kg}{m^3}\right)\left(\frac{\boldsymbol{m^3}}{\boldsymbol{m^2}}\right) \tag{3}$$

Eq. (3) highlights an object's BC's dependency on the ratio of volume to area. However, increasing the radius of a solid object will unproportionally increase both the volume and cross-sectional area of an object. To determine which is more effected by a change in radius (i.e. volume or cross-sectional area) an examination of the units is helpful. The volume of an object increases at a rate of radius cubed whereas, the cross-sectional area increases at a rate of radius squared. Therefore, the BC of an object increase with any increase in radius (i.e. cross-sectional area). Combining Eqs. (2) and (3) results in the force of drag and BC being inversely proportion as seen in Eq. (4). In summary, increasing a satellite's cross-sectional area or decreasing its mass will result in a decreased BC, an increased force of drag, and a decreases orbital lifetime and vice versa.

$$F_d = \frac{1}{2}\frac{mv^2}{BC} \quad (4)$$

2. Orbital Lifetimes

Orbital lifetime calculations were conducted for all firing scenarios that resulted in orbital trajectories. The orbital lifetime of a macron can be viewed as being proportional to its potential impact on the orbital debris environment. Likewise, the greater the orbital lifetime, the more stable the orbit. As with all orbital lifetime predictions, there is an intrinsic amount of error due to the inaccuracies associated with predicting the highly variable space weather which effects the atmospheric densities at a given altitude.[35]

Two orbital lifetime models were created using MATLAB. The first code integrated the force due to atmospheric drag throughout an orbit (i.e. integrated drag force code) while the second code utilized the Equations of Variation (i.e. EOV code). In both codes, third-body and other Earth perturbation forces (e.g. J2) were neglected. The only external forces applied were the forces due to atmospheric drag and Earth's gravity. Macrons were modeled as spheres which effectively directionalized the force of drag in the anti-RAM direction. For simplicity, atmospheric drag was considered to be negligible at orbital altitudes greater than 2,000km.[36] Atmospheric density data was obtained through the Naval Research Laboratory's Mass Spectrometer and Incoherent Scatter radar model derived from empirical data released in the year 2000 (NRLMSIS-00)[37] for solar minimum, maximum, and mean periods. This data was incorporated into both MATLAB drag models on an 11yr solar cycle. Orbital lifetimes are susceptible to changes in the solar cycle due to the solar cycle's effects on the atmospheric density values at a give altitude.[38] All MATLAB simulations were started with F10.7 values corresponding to solar mean values which is accurate for an epoch in the year 2009. The F10.7 index is a measure of the solar radio flux per unit frequency at a wavelength of 10.7 cm and is an excellent indicator of overall solar activity. Each MATLAB code terminated once the macron's altitude of perigee equaled the radius of the Earth (i.e. reentry) or once an orbital lifetime calculation reached 1,000 years. Orbital lifetimes greater than 1,000 years were considered to be permanent and stable orbits.

The accuracy of the EOV code was compared against the integrated drag force code as seen in Figure 12. Both MATLAB codes produced similar results; however, computational times varied drastically with the EOV code being significantly more practical to utilize. Therefore, the EOV code was applied to all

subsequent orbital lifetime calculations. An analysis was conducted to determine the optimal time step of the EOV code. Reduced time steps allow for greater accuracy but at the cost of an increased computation time. A parametric time step study was conducted and yielded a standardized time step of 60s based on the accuracy of the results obtained which can be viewed in Appendix D. The resulting orbital lifetime data from the EOV code is shown in Figure 13.

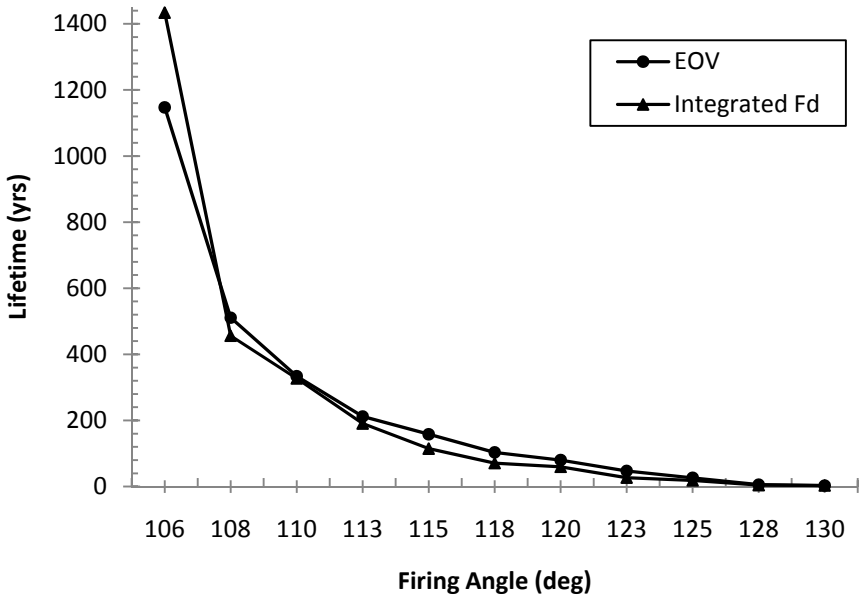

Figure 12. Accuracy comparison between EOV and Integrated Force of Drag codes

As expected, when firing altitudes are increased, the resulting orbital lifetimes also increase. As seen in Figure 11, the range of firing angles displayed in Figure 13 correspond to orbital trajectories. For each exit velocity and firing altitude combination, the smallest firing angle represents the boundary between reentry and orbital trajectories and the largest firing angles represent the boundary between orbital and escape trajectories. In terms of firing angle, the altitude at which a macron is fired has little effect on the orbital-escape boundary angles but has a large effect on the reentry-orbital boundary angle.

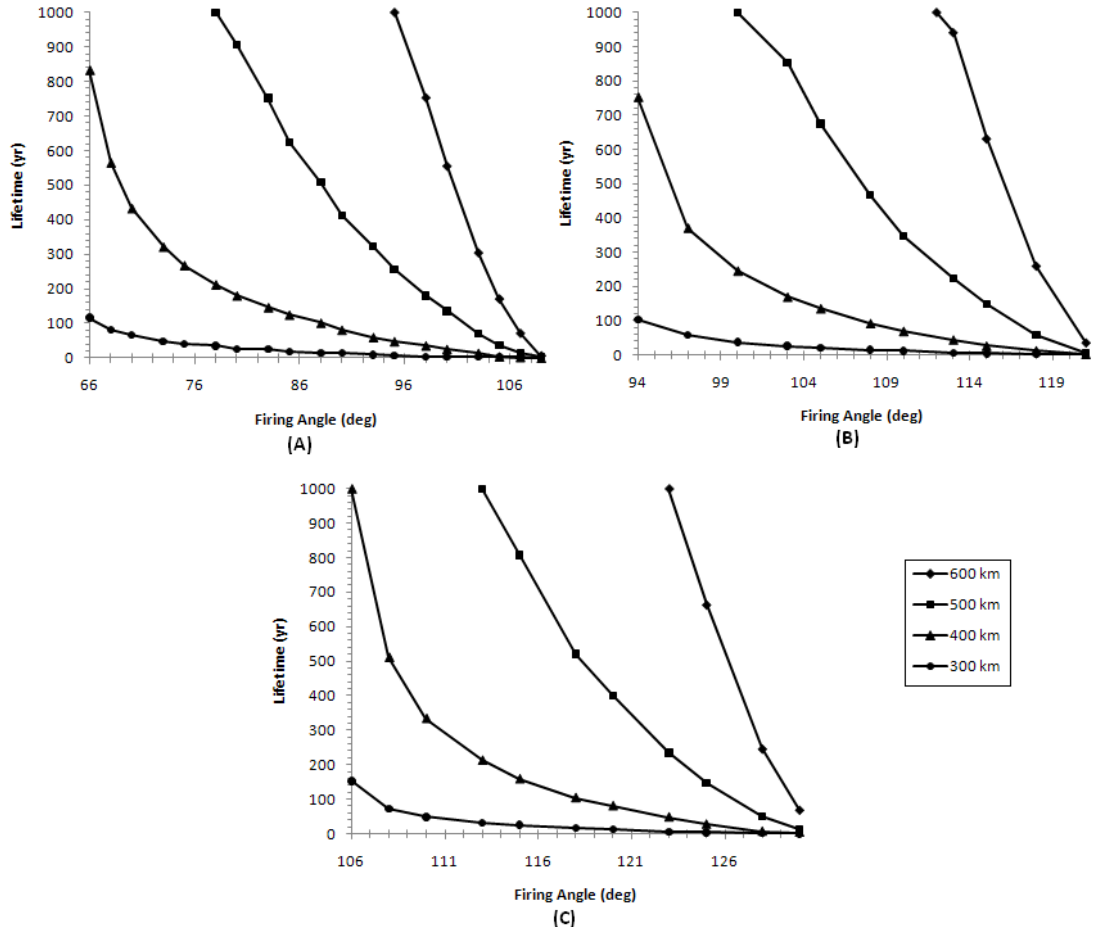

Figure 13. EOV code orbital lifetimes versus macron firing angles as a function of firing altitude for various system configurations ((A) *1g-7.07km/s (B) 10g-2.24km/s (C)1g-10km/s)*

3. Macron Size Effects

The force of drag on a macron is a direct result of the atmospheric density and a macron's orbital velocity, coefficient of drag, and cross-sectional area. For the purposes of this study, exit velocities were bound between 5 and 10km/s and the overall shape of a macron was defined as spherical with a coefficient of drag of 2; therefore, the only unconstrained variable in the force of drag equation is a macron's cross-sectional area. The theoretical coefficient of drag for a spherical satellite, assuming defuse reflection (i.e. $C_d = 2$), was used throughout all orbital lifetime calculations.[39] For a given mass, the cross-sectional area can be altered by using a different material (i.e. varying material density) or by varying the structural geometry (e.g. solid spheres, hollow spheres, cylinders, etc.) of a macron. However, due to the interactions which occur between a macron and the MLP system, aluminum macrons were chosen specifically because

of material conductivity and cost benefits. Refer to Ref. [3] for further information concerning the selection process of a macron's material. Therefore, the only practical way to alter the force of drag on a macron is to change its geometry. Any increase in cross-sectional area or a decrease in mass will decrease the object's BC which increases the force due to drag and decreases orbital lifetimes, as previously derived.

Orbital lifetime data presented in Figure 13 simulated a constant macron cross-sectional area based on the assumption that each macron was a solid aluminum sphere with a mass of 1g (i.e. a diameter of 0.891cm). Figure 14 illustrates the effects of an increased cross-sectional area on a macron's orbital lifetime while keeping mass constant. Using a hollow sphere geometry, it is possible to maintain a macron's spherical geometry and constant overall mass (i.e. 1g) while varying its radius (i.e. cross-sectional area). As expected, any increase in the macron's cross-sectional area decreases the resulting orbital lifetime. A decreased orbital lifetime reduces a macron's level of impact on the orbital debris environment. However, an increase in the cross-sectional area of each macron by utilizing a hollow sphere geometry would equate to an overall decrease in propellant storage density (i.e. increased propellant storage volume).

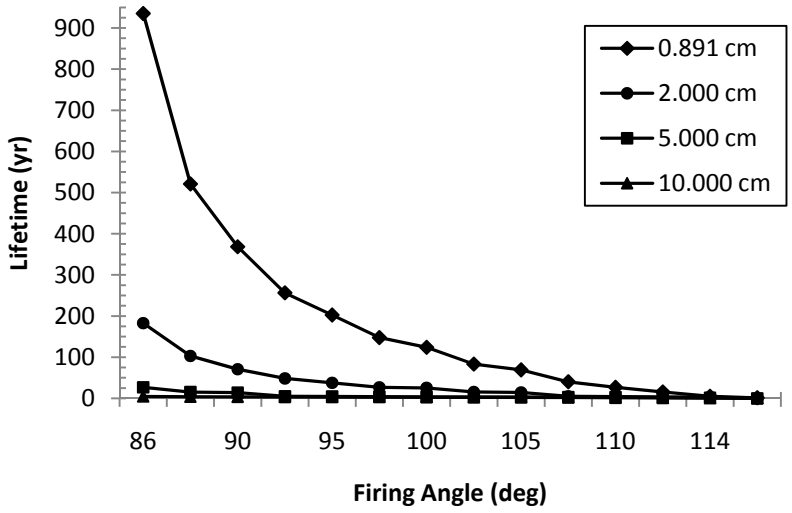

Figure 14. Cross-sectional area affects on orbital lifetimes as a function of macron diameter

For a standard LEO to GEO transfer using solid aluminum spheres, the required propellant volume is approximately $0.15m^3$. For the same transfer using hollow aluminum spheres with a 2.5cm radius, the required propellant volume is approximately $23.7m^3$. Due to the volume of a sphere being dependent on the

radius cubed, the volume of a macron will increase in a cubic manner for any increase in cross-sectional area. Therefore, a trade-off between a macron's cross-sectional area (i.e. propellant storage density) and orbital lifetime exists. For missions that require a satellite to minimize overall spacecraft volume, solid macrons are more beneficial because they minimizing overall propellant volume; however, due to the increase in orbital lifetime associated with smaller macrons, caution must be taken to prevent orbital trajectories. Missions that have no spacecraft size limitations should use larger macrons to minimize orbital lifetimes and decrease the potential space environment impact for all conducted maneuvers.

CHAPTER 4

ORBITAL MANEUVERS USING MACRON PROPULSION

Three primary in-space maneuvering scenarios were created using STK's Astrogator™ tool kit to analyze a MLP system's ability to alter an orbit. The three orbital maneuvering scenarios of interest were intra-LEO transfers (i.e. 400 to 600km altitude), LEO to GEO transfers, and GEO inclination changes. For all scenarios, theoretical performance predictions were calculated using Hohmann transfer and simple plane change (SPC) assumptions, respectively, and were compared with STK simulated data to provide performance prediction insights.

Three macron mass and exit velocity combinations were used throughout all orbital maneuvering simulations and are shown in Table 2. An initial spacecraft mass of 1,000kg was also used for all STK simulations. The mass and exit velocity combination of a macron determines the energy required per firing. Figure 15 shows a general prediction of the number of macrons required to perform a maneuver based on the required change in velocity, ΔV. Multiplying the number of macrons required by the respective mass of a macron results in the amount of propellant mass required for a given ΔV.

KE (kJ)	Mass (g)	Diameter (cm)	Ve (km/s)	F (N)	Isp (s)
25	1	0.891	7.07	7.07	720.8
	10	1.920	2.24	22.36	227.9
50	1	0.891	10.00	10.00	1,019.4

Table 2. Macron exit velocity and mass combinations

A primary goal in the implementation of any propulsion system is to provide the capability to conduct all desired maneuvers without adversely impacting the space environment. Thus, maneuvering scenarios that place macrons on reentry or escape trajectories are desired. In LEO, reentry trajectories are more desirable than escaping trajectories because when a LEO fired macron is placed on an escaping trajectory, it must traverse over 35,000km of altitude, highly populated with spacecraft, without experiencing a collision. The opposite is true for GEO maneuvers (i.e. escaping trajectories are more

desirable than reentry trajectories). Less desirable scenarios result in macrons being placed into unstable Earth orbital trajectories which degrade quickly due to drag. Highly undesirable maneuvering scenarios place macrons into stable Earth orbital trajectories.

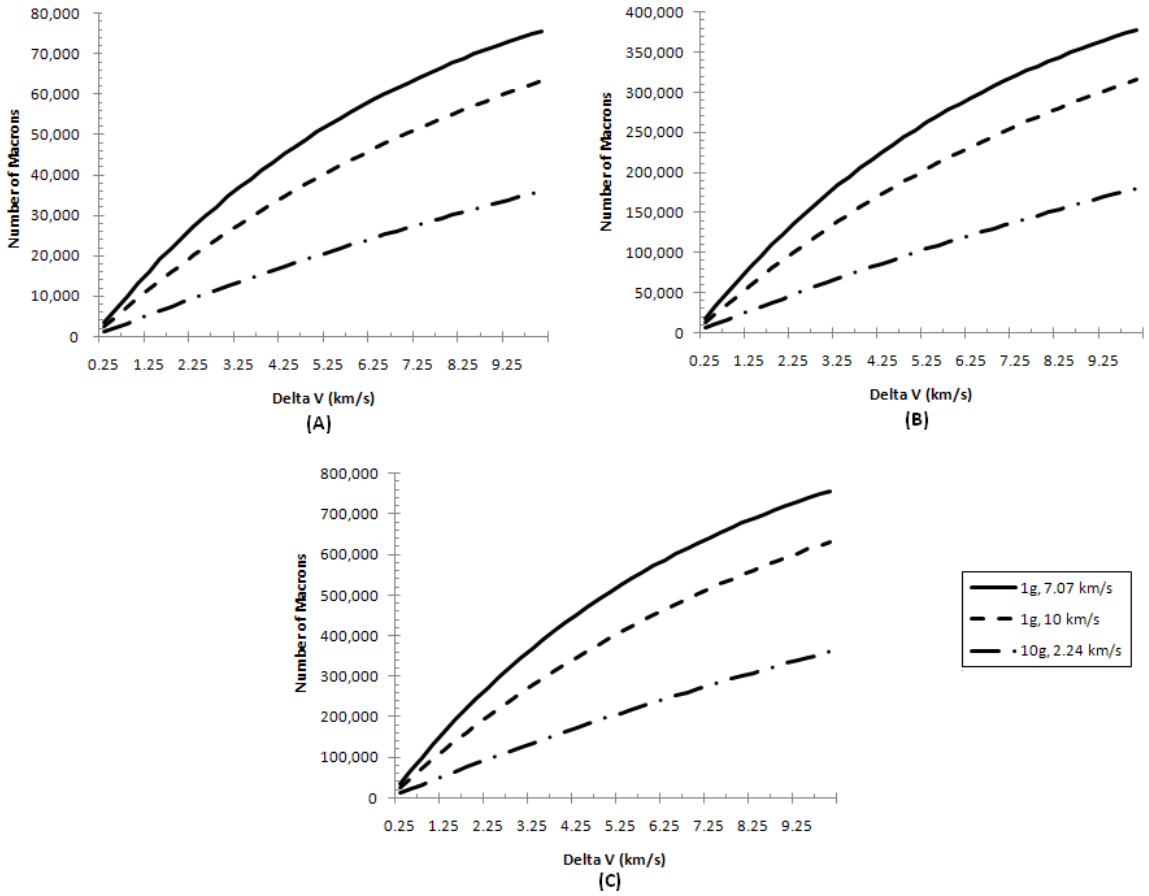

Figure 15. Number of macrons required per ΔV for various satellite masses

((A)100kg, (B) 500kg, (C) 1,000kg)

A. Intra-LEO Transfers

Three intra-LEO transfer simulations were created using STK and the macron mass and exit velocity combinations shown in Table 2. Each intra-LEO transfer scenario consisted of a series of finite (i.e. 1,000 to 2,000s) burns centered about either perigee or apogee over a several orbit period and assumed a constant spacecraft mass. In practice, a maneuvering spacecraft will experience mass losses due to propellant expenditure which increases the thruster's impulse throughout a maneuver. A variable satellite mass was not considered for intra-LEO transfers and therefore, the results obtained can be considered a

worst-case scenario. However, due to relatively minimal burn durations and required propellant masses, modeling an intra-LEO transfer as a constant mass system still provides a reasonably accurate ΔV prediction due to minimal maneuvering inefficiencies.

Theoretically, the most efficient way to increase a spacecraft's altitude is to perform a Hohmann transfer. Hohmann transfer calculations utilize coplanar and co-apsidal orbits and instantaneous thrust assumptions. The maneuvering inefficiencies associated with conducting a non-impulsive Hohmann transfer were minimized by centering each finite burn over its point of interest (i.e. perigee or apogee) and by minimizing the ratio of burn time to overall maneuver time.[40] A comparison of the number of macrons required to conduct an intra-LEO transfer can be seen in Table 3.

One source of error associated with the STK simulations is due to non-perfectly circularized final orbits. All STK scenarios achieved at least a 99.9% circularized final orbit (i.e. eccentricity less than or equal to 0.001). Achieving a perfectly circularized final orbit would require an increased amount of propellant (i.e. number of macrons). The corresponding ΔV associated with this error is approximately 11.5m/s. The overall increase in the number of macrons required to compensate for this additional ΔV is dependent on the MLP system configuration and the satellite mass. For a 1,000kg satellite using a 1g-7.07km/s (i.e. Isp = 720.8s) configuration, completely circularizing an orbit requires approximately 1,600 additional macrons, a 10g-2.24km/s (i.e. Isp = 227.9s) configuration requires approximately 1,150 additional macrons, and a 1g-10km/s (i.e. Isp = 1019.4s) configuration requires approximately 500 additional macrons.

Configuration	1g-7.07km/s	10g-2.24km/s	1g-10km/s
Hohmann	15,654	4,950	11,069
MLP Trajectory	15,776	4,995	11,100

Table 3. Numbers of macrons required to complete an intra-LEO transfer

B. LEO to GEO Transfers

The implementation of a MLP system as a LEO (i.e. 400km altitude) to GEO (i.e. 35,786km altitude) transfer propulsion system was also considered. The notional MLP system is capable of operating with varying macron mass, exit velocity, and firing frequencies. The operational power range of the MLP system is between 25 to 250kW with a max energy per firing of 25kJ. These power and energy levels

equate to a potential system firing frequency between 1 and 10Hz. At these firing frequencies, modeling the overall system as either a long duration finite burn or numerous impulsive burns did not have a major effect on the total number of macrons required to complete a transfer. These simulations merely represent different system configurations and modeling techniques with identical outcomes. Due to the complexity and long computation times of modeling a LEO to GEO transfer as numerous impulsive burns, the long duration finite burn method was adopted for all subsequent STK simulations. Numerous impulsive burn simulations were created to continually apply an instantaneous burn to the satellite followed by a period of propagation (i.e. f^{-1}) until the final orbit was achieved. Long duration finite burns averaged the thrust of a given macron over the total time between firings (i.e. f^{-1}) and applied the resulting force as a constant spacecraft thrust until the final orbit was achieved.

Simulations were setup to model an updating mass satellite transfer, which takes into account mass losses due to propellant expenditure, from LEO to GEO using various transfer methods (i.e. Hohmann and spiral trajectories). A theoretical minimum number of macrons required to complete a LEO to GEO transfer was calculated using Hohmann transfer assumptions with propellant masses determined by the ideal rocket equation (IRE), Eq. (5). STK simulations of a MLP system's trajectory resulted in a high thrust, LEO to GEO spiral transfer trajectory which thrusts through MEO, propagates to GEO, and then thrusts again to circularize the final orbit as seen in Figure 16. For comparison, the amount of propellant mass required to conduct a low thrust (i.e. traditional EP), spiral trajectory was also calculated using MLP system Isp values and a standard rule of thumb to calculate the required ΔV for a low thrust spiral transfer which can be seen in Eq. (6).[41] Table 4 displays the number of macrons required to complete a LEO to GEO transfer using a Hohmann transfer, a low thrust spiral trajectory and a high thrust spiral trajectory (i.e. MLP system trajectory).

$$\Delta V = I_{sp} g_o ln\left(\frac{m_i}{m_f}\right) \tag{5}$$

$$\Delta V_{total} = V_i - V_f \tag{6}$$

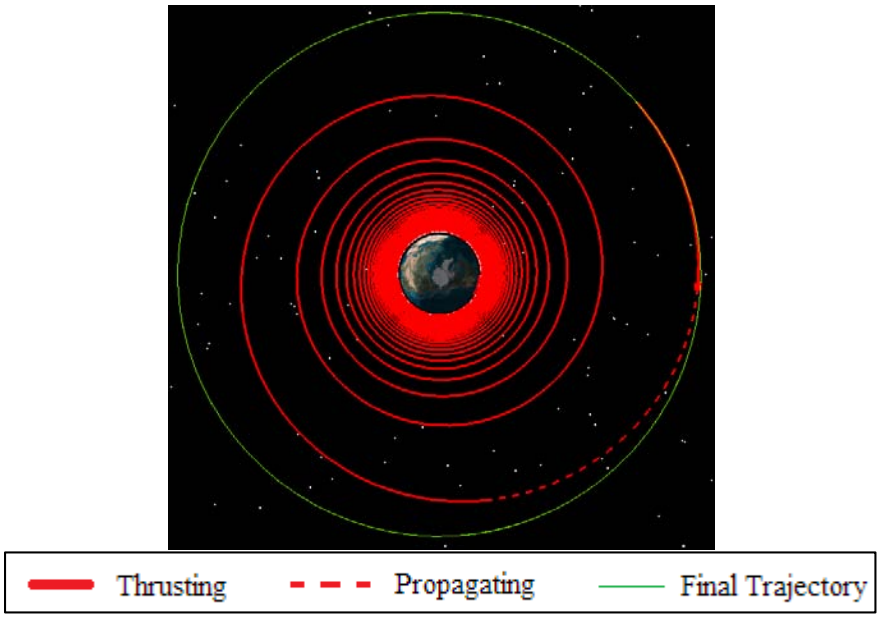

Figure 16. LEO to GEO high thrust spiral trajectory

Configuration	1g-7.07km/s	10g-2.24km/s	1g-10km/s
Hohmann + IRE	420,477	NA	319,855
High Thrust Spiral (MLP Trajectory)	478,708	NA	368,822
Low Thrust Spiral	650,071	NA	459,670

Table 4. Number of macrons required for LEO to GEO transfer

For both viable MLP system configurations (i.e. 1g-7.07km/s and 1g-10km/s), STK predicts approximately a 15% increase in propellant mass as compared to Hohmann transfer assumptions. However, for a 10g-2.24km/s configuration, a MLP system requires a larger propellant mass than the overall spacecraft mass making the maneuver impossible to perform using this particular MLP system configuration.

In general, solid rocket motors (SRMs) (i.e. chemical propulsion) perform LEO to GEO transfers utilizing trajectories similar to Hohmann transfers; whereas, low thrust EP systems utilize spiral trajectories. A LEO to GEO Inertial Upper Stage (IUS) SRM requires 9,709kg of propellant whereas, a MLP system only requires a propellant mass of 478kg or 368kg, depending on system configuration, as seen in Table 5. This reduction in propellant mass is a result of the increased Isp values of a MLP system as compared to a chemical propulsion system. A traditional EP system conducts a LEO to GEO transfer using

a low thrust, spiral trajectory which place a satellite into an almost completely circularized final orbit without utilizing propagation or multiple burn techniques. A Stationary Plasma Thruster (SPT) (i.e. Hall thruster) achieves approximately 86mN of thrust with 1,600s of Isp.[42] As seen in Table 5, when conducting a LEO to GEO transfer, a SPT-100 requires approximately 65kg of xenon propellant and requires a transfer time of approximately 4.4 months[42] as compared to a MLP system's overall transfer time of 6.35 days. In summary, a LEO to GEO transfer using a MLP system requires less propellant mass than chemical propulsion systems but requires increased transfer times. As compared to traditional EP systems, a MLP system requires an increased amount of propellant but achieves a LEO to GEO transfer 95% faster.

Propulsion System	Propulsion Type	Propellant Mass (kg)	Transfer Time
IUS	Chemical	9,709	5.3 hr
MLP	Macron (EP)	479 or 369	6.35 days
SPT-100	Plasma (EP)	65	4.4 months

Table 5: Comparison of LEO to GEO transfers using various propulsion systems

Of the three macron mass and exit velocity combinations, a 10g-2.24km/s MLP system configuration has the lowest Isp of 227.9s, as seen in Table 2. Figure 17 shows the number of macrons required to transfer a given satellite mass (i.e. all mass excluding propellant mass) from LEO to GEO for both the Hohmann-IRE and STK simulations of a MLP system's trajectory.

The optimal MLP system configuration to complete a LEO to GEO transfer minimizes both the energy per firing and the number of macrons required while avoiding orbital trajectories. The lowest energy configuration which results in the ideal situation of reentry trajectories in LEO and escaping trajectories in GEO requires a 1g-8km/s MLP system configuration as seen in Figure 11. However, a LEO to GEO transfer requires a MLP system to continuously operate throughout the LEO, MEO, and GEO regimes. In MEO, anti-RAM firings with an exit velocity of 8km/s results in retrograde orbital trajectories. According to Figure 10 and Figure 11, a LEO to GEO transfer is the only maneuver investigated in this study that will produce orbital trajectories when conducting a maneuver in the most efficient manner (i.e. anti-RAM firing). Orbital trajectories, while maneuvering through MEO using a 1g-8km/s MLP system configuration,

can be avoided by either increasing the energy per firing (i.e. increasing the exit velocity) or utilizing off-axis thrusting techniques.

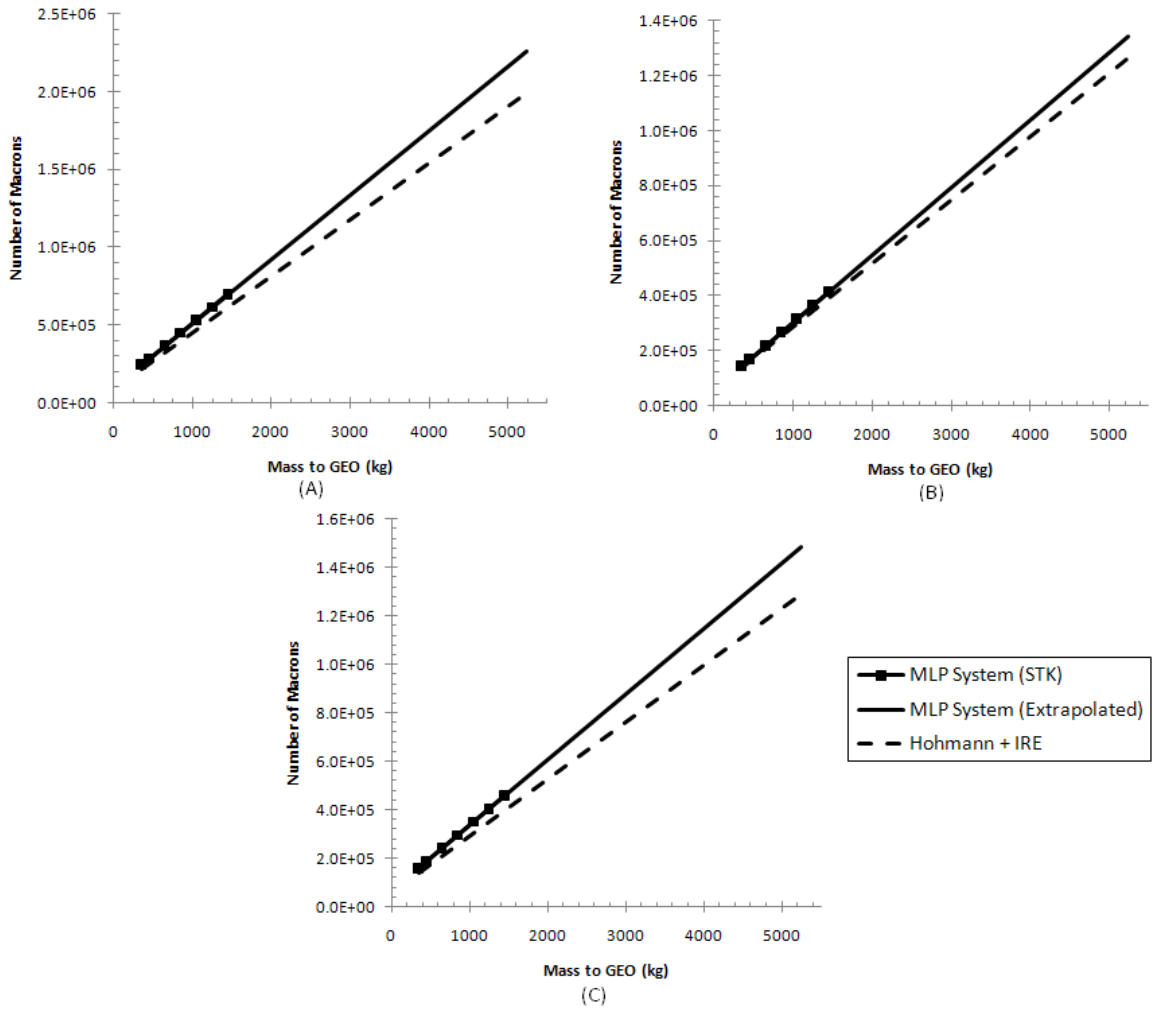

Figure 17. Number of macrons required to transfer a given mass from LEO to GEO using various MLP system configurations (*(A) 1g-7.07km/s (B) 10g-2.24km/s (C)1g-10km/s)*

Increasing the exit velocity to 10km/s would result in escape trajectories for all MEO anti-RAM fired macrons. Off-axis thrusting requires precise pointing accuracy, satellite slew rate compensation, an increased number of macrons, and knowledge of the resulting macron trajectory for all firing angles, exit velocities, and altitude combinations. Off-axis thrusting will induce a satellite slew rate which can be compensated for via symmetric firings across the RAM axis or a secondary attitude control system. Symmetric firings across the RAM axis would require a MLP system to rotate its firing angle after each

firing. Figure 18 provides trajectory analysis for various altitude and firing angle combinations for a 1g-8km/s MLP system configuration. Conducting off-axis maneuvers in the most efficient manner would require a MLP system to utilize the range of firing angles represented by the orbit-escape boundary line in Figure 18. In order to ensure that all macrons are placed on the desired (i.e. escape) trajectory, a MLP thruster pointing accuracy of less than 1deg would be required.

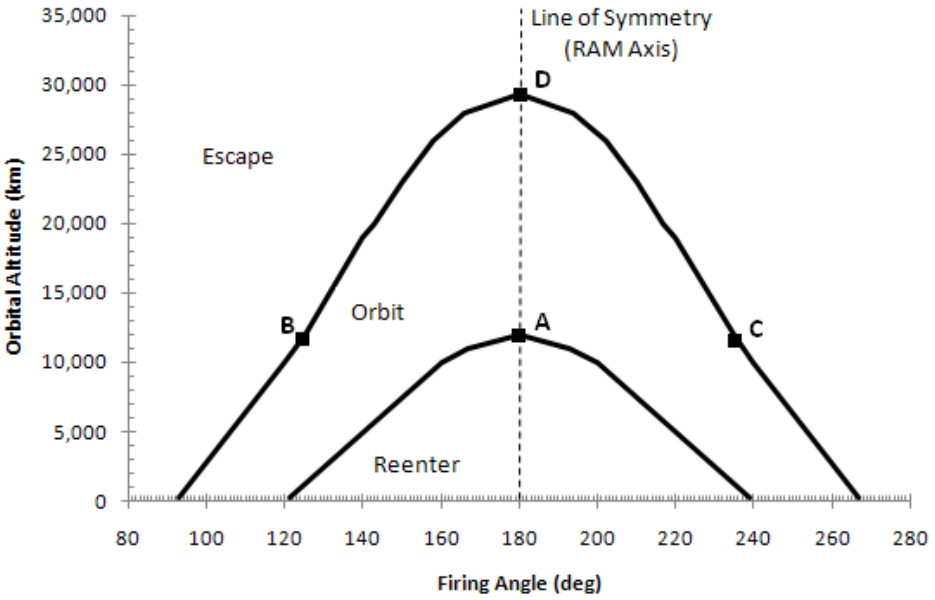

Figure 18. Macron trajectory for a LEO to GEO transfer

Point: A (180deg, 12,004km), B (125deg, 12,004km), C (235deg, 12,004km), D (180deg, 29,382km)

For example, to conduct a LEO to GEO transfer without changing the MLP system configuration (e.g. 1g-8km/s), the following thrusting sequence is required. Thrust in the anti-RAM direction (i.e. 180deg) from LEO up to an altitude of 12,004km (point A in Figure 18). Off-axis thrusting is required from altitudes of 12,004 to 29,382km (i.e. the altitudes corresponding to the line connecting points A and D in Figure 18). Off-axis thrusting must commence at an altitude of 29,382km to avoid orbital trajectories. The most efficient firing angles for off-axis thrusting are the boundary angles represented by the escape-orbit boundary line in Figure 18. These boundary angles maximize the thrust in the anti-RAM direction and minimize off-axis thrust components. The change in firing angle between Points B and C in Figure 18 is 110deg. In this configuration, a MLP system must be capable of a firing angle change rate of 110deg/s for a 1Hz system, or two MLP systems could be used to reduce the required firing angle change rates. At an

altitude of 29,382km, normal thrusting in the anti-RAM direction may be resumed, with all macrons being placed on escape trajectories, until GEO is achieved.

To complete a LEO to GEO transfer thrusting only in the anti-RAM direction (i.e. worst-case scenario for orbital debris environment impact) approximately 160,360 macrons would be placed in orbital trajectories. Assuming the spacecraft conducting the LEO to GEO transfer was launched from Kennedy Space Center (i.e. inclination = 28.5deg), all 160,360 macrons will experience relative collision velocities of approximately 13km/s according to Figure 6. For perspective, the 2007 Chinese ASAT test resulted in approximately 2 million 0.1 to 1cm diameter debris particles and over forty thousand 1 to 10cm diameter debris particles.[43] The Iridium-Cosmos collision in 2009 resulted in 1,313 debris particles.[44]

Table 6 and Table 7 combined categorize both the MMOD particle and mass contributions according to object size. Assuming the number of particles calculated by the MASTER-01 model (i.e.) for MEO and GEO regimes and that on average MMOD objects smaller than 1cm in diameter have a density of $2.8 g/cm^3$ and objects larger than 1cm diameter have a density of $2.8d^{-0.74}$ g/cm^3, [45] it is possible to determine the mass growth rate effects of conducting a LEO to GEO transfer maneuvering solely in the anti-RAM direction. According to the MASTER-01 model and relative MMOD particle densities, there is approximately $8.13 \times 10^5 kg$ of orbital debris in MEO and GEO. The nominal MMOD mass growth rate is approximately 5% a year[12,17,18]; therefore, a single LEO to GEO transfer using anti-RAM fired 1g macrons has minimal effects on the yearly mass growth rate of all MMOD objects in MEO and GEO. However, a single LEO to GEO transfer using anti-RAM fired 1g macrons will increase the mass of 1cm diameter MMOD objects in MEO and GEO (i.e. 4,509kg) by approximately 3.5%. In terms of MMOD mass, a single LEO to GEO transfer would have a negligible impact on the overall MMOD mass in MEO and GEO (i.e. $1.71 \times 10^6 kg$).

In terms of the MMOD environment impact, one LEO to GEO transfer thrusting only in the anti-RAM direction would have minimal impact on the total number of MMOD objects in MEO and GEO (i.e. 7.415×10^{15} objects). However, a single LEO to GEO transfer only firing in the anti-RAM direction would increase the number of 1cm diameter MMOD objects in MEO and GEO (i.e. 384,484 objects) by approximately 42%. In terms of MMOD flux, a single LEO to GEO transfer would have a negligible impact on the overall MMOD flux environment in MEO and GEO (i.e. 7.36×10^{15} objects).

Orbit Regime	>1 μm	>10 μm	>0.1 mm	>1 mm	>1 cm	>10 cm	>1 m	Total Count
LEO	3.39E+13	2.06E+13	6.30E+10	1.39E+08	189,461	9,679	2,256	**5.46E+13**
MEO+GEO	7.23E+15	1.33E+14	4.78E+11	1.92E+08	384,484	8,153	2,014	**7.36E+15**
LEO→GEO	7.26E+15	1.54E+14	5.41E+11	3.31E+08	573,945	17,832	4,270	**7.41E+15**

Table 6: Number of orbital debris particles according to particle size and altitude (*MASTER-2001 reference population for May 2001)*[10]

Orbit Regime	>1 μm	>10 μm	>0.1 mm	>1 mm	>1 cm	>10 cm	>1 m	Total Mass (kg)
LEO	0.4	242	739	1,630	2,222	20,657	876,165	**901,655**
MEO+GEO	84.8	1,565	5,606	2,252	4,509	17,401	782,179	**813,596**
LEO→GEO	85.1	1,806	6,345	3,882	6,732	38,058	1,658,344	**1,715,252**

Table 7: Orbital debris mass contributions according to particle size and altitude

In summary, a single worst-case LEO to GEO transfer will have minimal impact on the overall MMOD flux due to a relatively insignificant contribution to the overall number and mass of MMOD particles but will have a significant impact on the overall mass growth rate of 1cm diameter MMOD objects in MEO and GEO. In terms of numbers, small MMOD particles (i.e. less than 1cm diameter) account for the vast majority (i.e. greater than 99%) of MMOD objects. However, in terms of mass, large particles (i.e. greater than 1cm diameter) account for the vast majority (i.e. 99%) of the overall MMOD mass. Therefore, the addition of 160,360 medium size MMOD particles represents an increase in the mass of all 1cm diameter MMOD objects with negligible impact on the overall MMOD flux. This impact can theoretically be negated by increasing exit velocities through MEO or utilizing off axis thrusting techniques.

C. GEO Inclination Changes

The last orbital maneuver analyzed in this study was a GEO inclination changing maneuver. To achieve an inclination change, the standard maneuvering procedure is to thrust in the coplanar and orthogonal direction to RAM (i.e. 90 or 270deg from RAM) at either the ascending or descending node, respectively. As seen in Figure 11, inclination changing maneuvers will result in orbital or reentry trajectories in LEO, depending on the exit velocity, and solely reentry trajectories for MEO and GEO

firing, regardless of exit velocity. Therefore, GEO inclination changing maneuvers, if conducted properly, minimize the potential for a macron to effect the space environment.

Using simple plane change (SPC) assumptions, instantaneous burns at either the ascending or descending node in the direction orthogonal to RAM and parallel to the LVLH plane (i.e. 90 or 270deg), and the IRE (i.e. updating satellite mass), a theoretical number of macrons required to complete an inclination changing maneuver in GEO can be calculated through the use of the Eq. (5) combined with Eq. (7).

$$\Delta V_s = 2V_i sin\left(\frac{\theta}{2}\right) \tag{7}$$

The results from Eq. (7) were compared against the simulated results created within STK as seen in Figure 19. All GEO inclination changing simulations were modeled as long duration, non-constant mass, finite burns centered on either the ascending or descending node over a several orbit period. STK scenarios were developed using three different firing frequencies to verify a convergence of the data to the theoretically computed predictions. The burn time per ascending or descending node passage was held constant at 2,000s with varying firing frequencies of 1, 5 and 10Hz. A 2,000s burn duration requires the inclination changing maneuver to begin 3,072km before either the ascending or descending node and end 3,072km after the node. As the burn duration increases, small maneuvering inefficiencies are incurred due to thrusting at a location other than the ascending or descending node, as expected. However, the overall burn distances associated with a 2,000s burn is relatively insignificant as compared to the circumference of GEO. As the firing frequencies are increased, the overall time to complete a maneuver decreases. Decreasing the firing frequency requires an increased number of burns to complete the same transfer which equates to an increased number of orbits (i.e. time) to complete the maneuver. The results of varying firing frequencies are summarized in Figure 20.

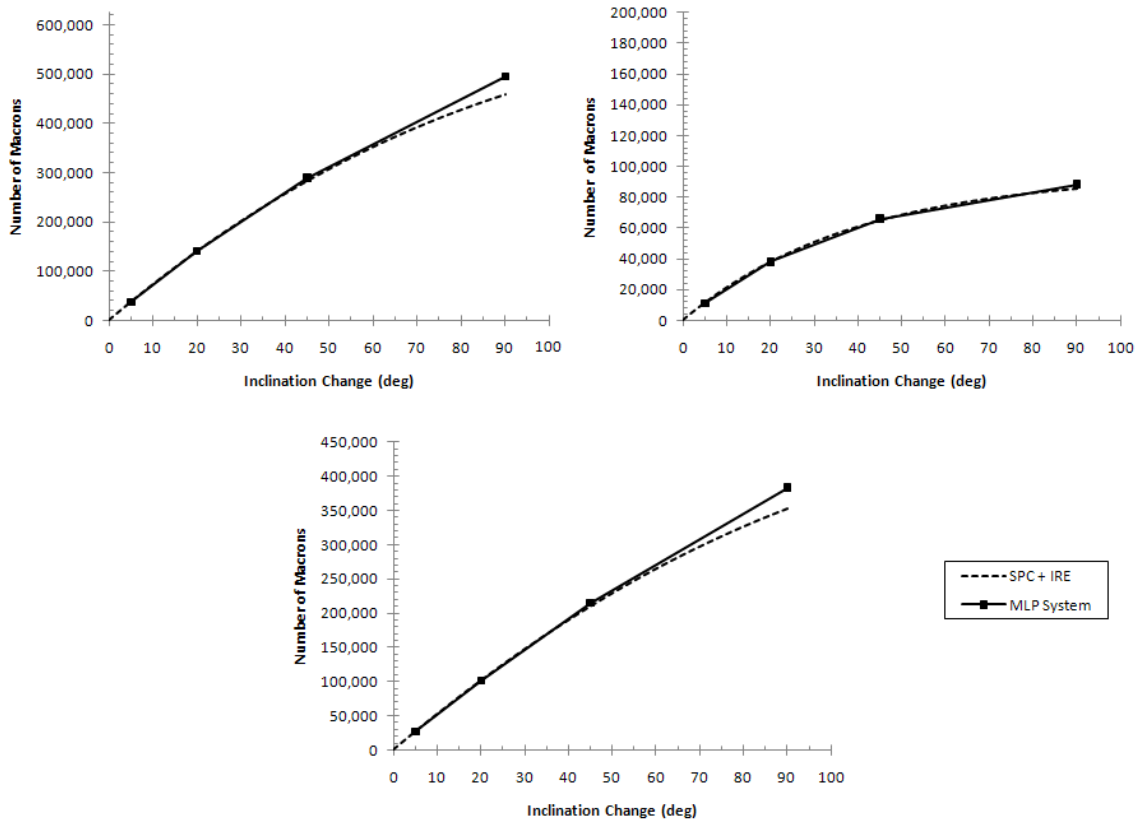

Figure 19. Number of macrons required to complete a given inclination change at GEO for various MLP system configurations (*(A) 1g-7.07km/s (B) 10g-2.24km/s (C) 1g-10km/s)*

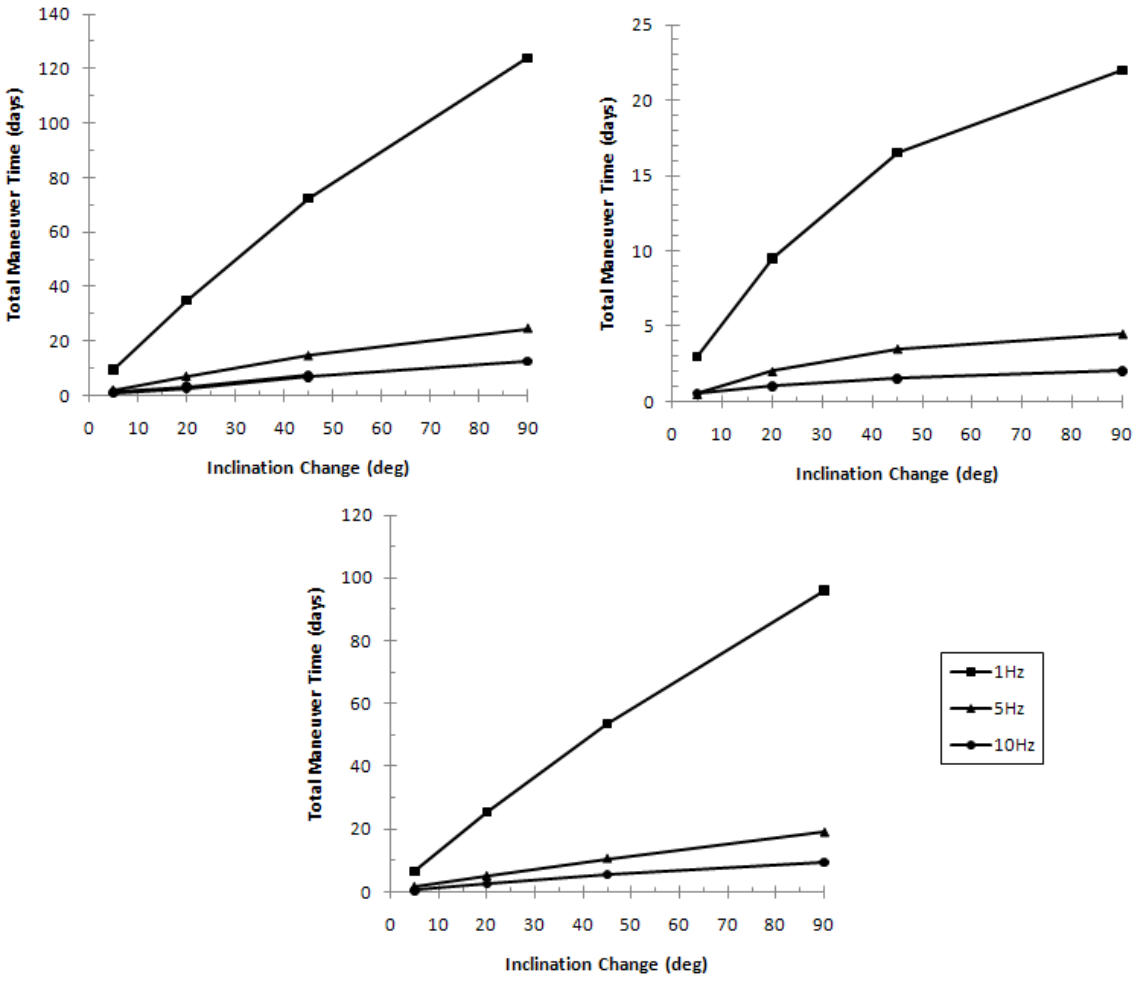

Figure 20. Total time to complete a GEO inclination change as a function of firing frequency for various MLP system configurations (*(A) 1g-7.07km/s (B) 10g-2.24km/s (C) 1g-10km/s)*

CHAPTER 5

CONSTANT THRUST UTILIZING MACRON PROPULSION

In addition to orbital maneuvers, macron propulsion technology can be implemented in a variety of other maneuvering scenarios. Based on the analysis conducted in Chapter 4, a MLP system can also be implemented as a GEO phasing or GEO to GEO rendezvous orbital maneuvering system. The remainder of this chapter is dedicated to analyzing the implementation of a MLP system in a momentum exchange manner to create constantly spaced satellite formations. The underlying concept of momentum exchange relies on one satellite creating an impulse of momentum (i.e. imparting momentum on a mass) which is then captured by another satellite and redirected back towards the first satellite to provide a constant thrust scenario.[46] Reference [47] provides a thorough analysis of satellite formation station-keeping utilizing momentum exchange tactics.

A. Concept Overview

An in-depth concept overview of tandem (i.e. side by side) satellite formations can be found in Ref. [46]. The concept presented in this chapter evaluates the implementation of a MLP system in a manner which provides a momentum exchange through mass (i.e. macron) streams as a means of maintaining a tandem satellite formation. A stream of macrons is created by one satellite and directed towards the receiving satellite. The receiving satellite collects the macron stream and redirects the macrons back towards the originating satellite to begin a cyclical process. A conceptual drawing of the overall concept might look like Figure 21 in which two spacecrafts in polar orbits are imaging the Earth's surface. The tandem satellites use streams of continuously exchanged macrons to produce the force needed to maintain a constant separation distance.

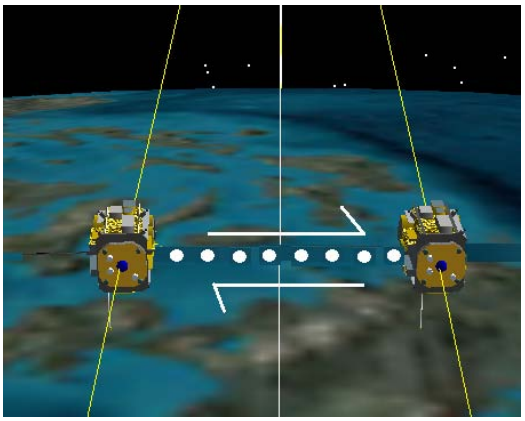

Figure 21: Momentum exchange concept for formation flying satellites

In the past decade, the advantage of satellite formations to the field of remote sensing has given rise to several proposals for their implementation. The first tandem satellite formation to fly will likely be a pair of satellites known as TarraSAR-X and Tandem-X.[48,49] TarraSAR-X was launched in June 2007 to a nominal 514km altitude polar orbit. The companion satellite, Tandem-X, is expected to be launched in 2010. These satellites will provide the first bi-static synthetic aperture radar (SAR)[50,51] platform in space. Tandem formations are expected to provide topographic image resolution on the order of 1cm.[52] To achieve a tandem formation both satellites are placed into offset polar orbits. Due to the ever-changing separation distances, tandem satellite formations in unpowered flight do not produce uniform observations because the satellites are unable to achieve a constant separation distance throughout all orbits. A consistent baseline is important for certain missions where timely detection of surface changes are necessary.

Since both unpowered tandem satellites are each in polar orbits around the center of the Earth, their orbits cross twice every orbital period and the satellites tend to converge on each other unless a continuous separation force counteracts this convergence. A polar orbiting tandem satellite formation in unpowered and powered (i.e. actively thrusting) flight can be viewed in Figure 22. A constant momentum exchange of macrons between tandem satellites can provide the required repulsive force necessary to maintain the satellite formation for a theoretically infinite lifetime.

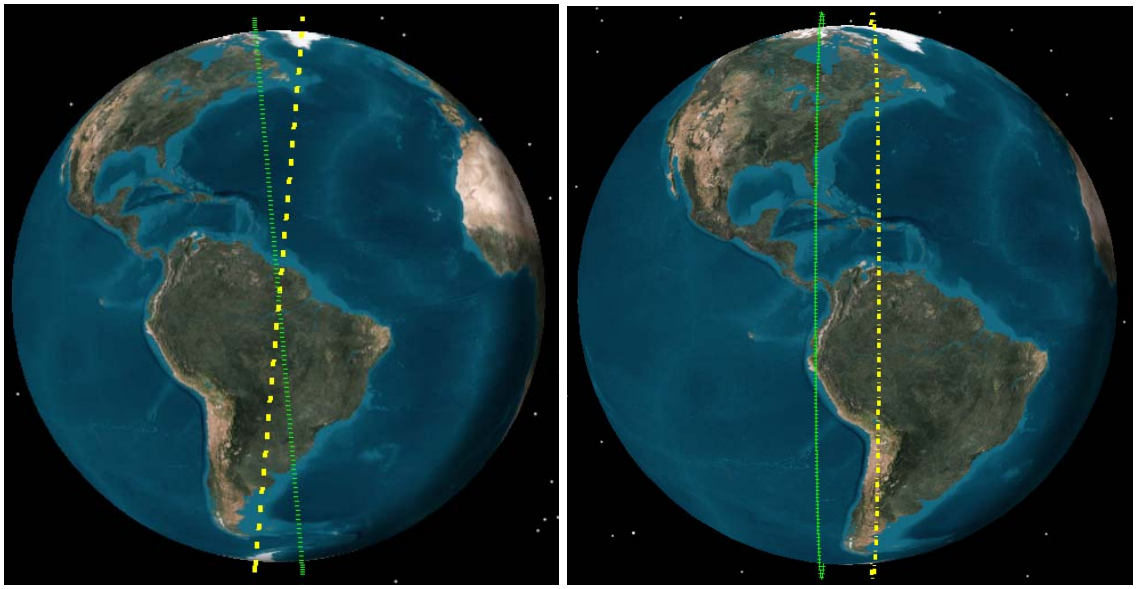

(A) (B)

Figure 22. Orbit tracks for tandem satellites in (A) unpowered and (B) powered flight

B. Macron Propulsion System Implementation

In terms of space environment impact, macron propulsion technology's greatest downfall is the expulsion of a macroscopic particle with potentially kilojoules worth of energy into the space environment. Conversely, the expulsion of energetic mass is the crucial characteristic which makes a MLP system ideal for an in-space momentum exchange device. By equipping both satellites in a tandem formation with a MLP system and a macron collection device, it is theoretically possible to create a constant momentum exchange of mass between each satellite by firing and capturing macrons to and from the opposing satellite, respectively, thereby eliminating the potential for macrons to stay in orbit.

The magnitude of the force required to keep a satellite in a non-Earth centered orbit is a function of the orbital altitude, separation distance from the centerline of Earth (i.e. one half the separation distance between the satellites), and the mass of each satellite. There are two viable methods to determine the exact force required to sustain tandem flight. The first method involves splitting the force of gravity into its respective vector components in the radial and tangential directions. The component of gravity that acts in the tangential direction is equal and opposite in magnitude to the force required to sustain tandem flight. The second method utilizes the Clohessy-Wilshire equations and is represented by Eq. (8). [47] Equation (8) is only valid for radiation or mass momentum exchange when the mass flow is small compared to the

overall satellite mass and when the transit time between satellites is small compared to the overall orbital period.[47] The acceleration force in the direction from satellite 1 to satellite 2 is represented by α_{12} and z^*represents one half the separation distance between each satellite.

$$\alpha_{12} = m_1 n^2 z_1^* = m_1 \frac{\mu}{a^3} z_1^* \tag{8}$$

Figure 23 shows the required thrust for one satellite to maintain tandem flight for various satellite masses and orbital altitudes with a constant separation distance of 1km (i.e. $z^* = 0.5$km). For LEO tandem satellite formations, the required thrust to maintain a 1km separation distance is between 10mN and 1N per satellite for all considered satellite masses (i.e. 10 to 1,000kg). This required range of forces correlates to a 1g macron being fired with an exit velocity between 10m/s and 1km/s, respectively, with a 1Hz firing frequency. These parameters are well within the operational range of a MLP system. Figure 24 shows the required thrust per satellite to maintain a desired tandem flight separation distance assuming each satellite has a mass of 100kg.

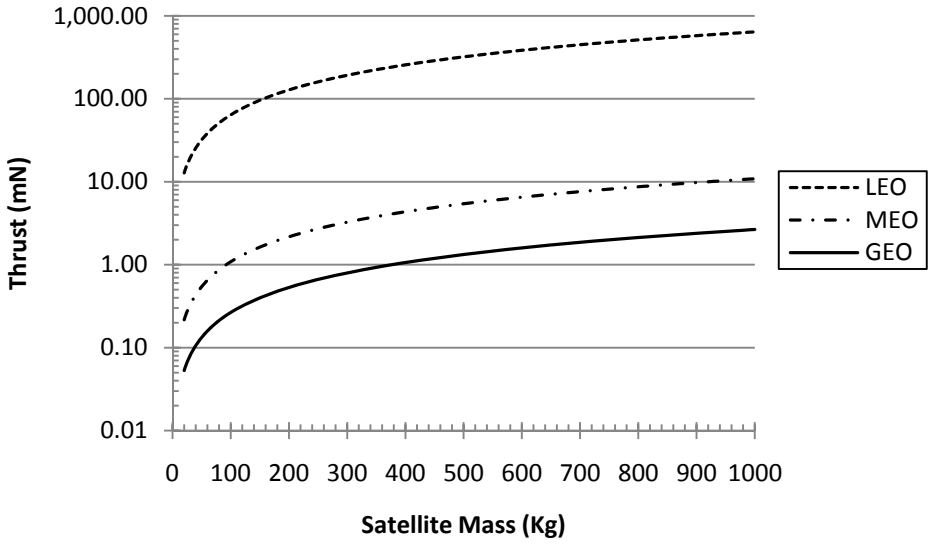

Figure 23. Required thrust per satellite to maintain tandem flight with a 1km separation distance for various satellite masses and orbital altitudes

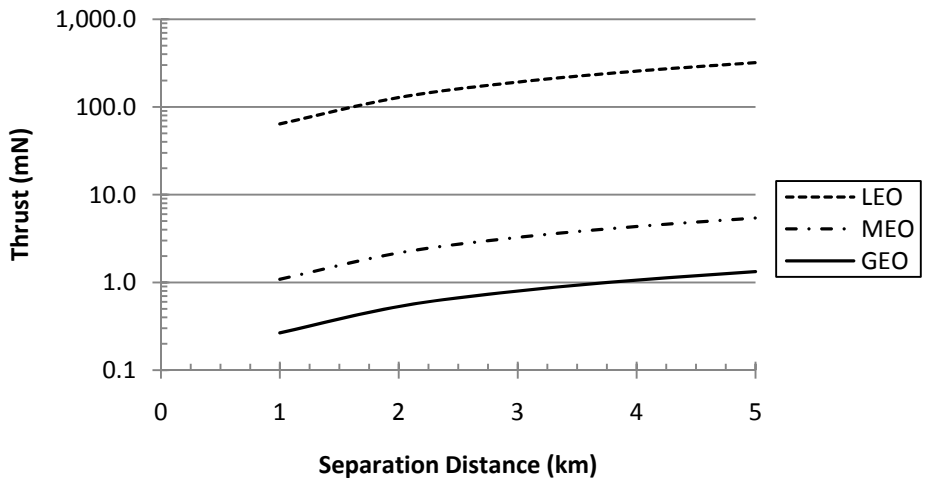

Figure 24. Required thrust per satellite to maintain tandem flight with a given separation distance for a 100kg satellite in various orbital altitudes

C. Trajectory Perturbations

Once a macron is fired, it will immediately enter into an Earth centered orbit. For the exit velocities under consideration (i.e. 10m/s to 1km/s), all fired macrons will be placed on orbital trajectories of varying sizes with inclinations near 90deg. A fired macron will follow its orbital trajectory until it is captured by the opposing satellite at which time the macron will impart the required station-keeping momentum onto the capturing satellite. During the time of transit required for a macron to travel from one satellite to another, it will experience perturbation forces, primarily drag, that will alter the macron's orbital trajectory. Understanding and quantifying the effects of drag on a macron's orbital trajectory is fundamental not only to the collection of a macron by the opposing satellite but also to the prevention of a macron from becoming orbital debris (i.e. a macron that is not collected). Increased satellite separation distances and decreased firing velocities will correlate to an increased transit time.

A MATLAB code (i.e. miss distance code) was created to simulate the effects of drag on a macron's trajectory during transit periods between satellites and can be viewed in Appendix E. The miss distance code was created to assume no third-body perturbation effect. The ultimate goal of the miss distance code was to quantify and directionalize the miss distance of a fired macron at the time of collection. A macron was considered to be collected when the position vector component in the direction tangent to the Earth's surface and orthogonal to the RAM direction (i.e. the y-axis in Figure 25) was

equivalent to that of the capturing satellite. Once the collection criteria was met, the distance between the capturing satellite's center of mass and the macron's center of mass was recorded and represents the overall miss distance for a given firing velocity and satellite separation distance combination. The overall miss distance quantity is significant because it will ultimately determine the required size of the macron collector (i.e. the radius of the collection device). Satellite separation distances were varied between 1 and 3km due to the advantages that these separation distances provide to remote sensing operations.

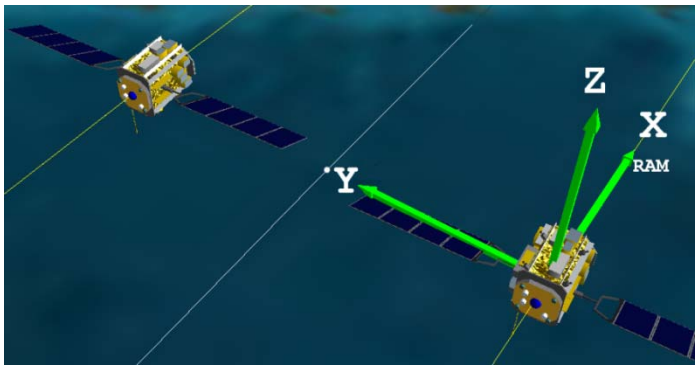

Figure 25. Tandem satellite formation reference frame

The overall miss distance data provided by the code during a time of solar mean can be viewed in Figure 26. Due to orbital mechanics, all macrons will impact the capturing satellite with a velocity vector that does not point solely in the desired y-direction. This creates an off axis (i.e. x- or z-axis) thrust component. Simulations have shown that off-axis thrust components are minimal (i.e. less than 100nN). Appendix F directionalizes the miss distances and quantifies both the desired and off-axis thrust components for a giving firing scenario and solar cycle period.

As discussed in Chapter 3, the phase of the solar cycle at the time of firing will effect the overall miss distance due to fluctuations of the atmospheric density. Figure 27 quantifies the effects that a varying solar cycle can have on the overall miss distance of a macron firing scenario. Figure 27 highlights that the fore of drag counters the orbital motions which tend to increase a macron's overall miss distance. A macron collection device must be adequately large to capture all macrons during all phases of the solar cycle while maintaining a reasonable margin of error. Therefore, the radius of the collection device needs to be several times larger the largest miss distance to ensure the prevention of orbital debris accumulation.

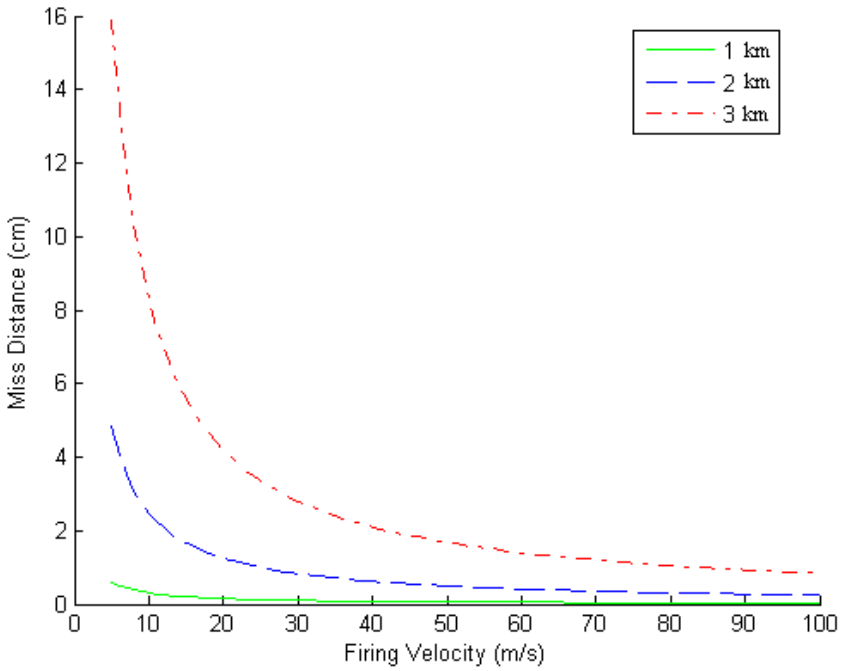

Figure 26. Overall miss distance for varying firing velocities as a function of separation distance

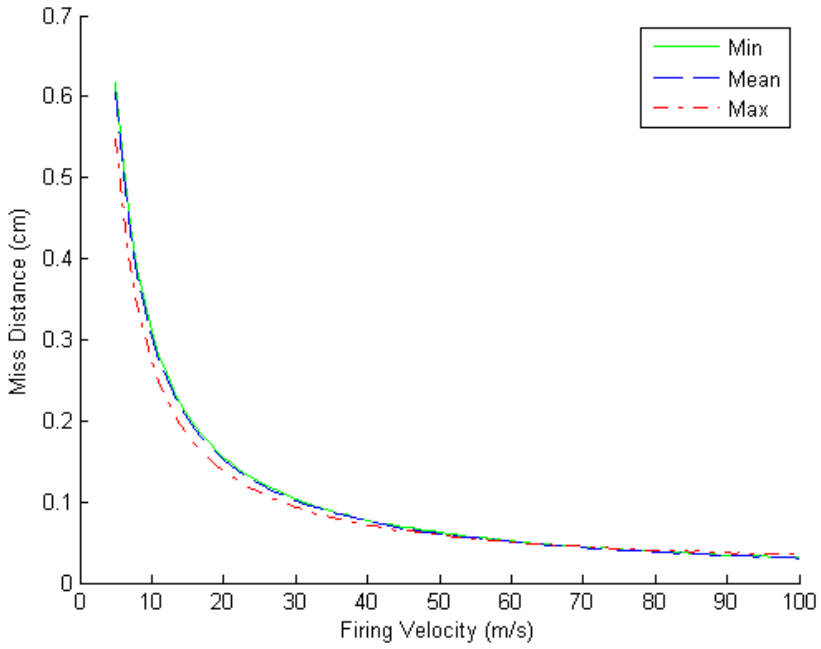

Figure 27. Miss distance for varying firing velocities as a function of the solar cycle for a 1km separation distance

D. MLP System Configuration Effects

When selecting a MLP system configuration for a tandem satellite formation, the two driving parameters are the momentum and the firing frequency of a macron. The firing frequency of a MLP system determines the change in separation distance between satellites overtime. The momentum per macron in turn determines the mass and exit velocity of a macron, the energy per firing, the power input required, and the amount of macrons in transit (i.e. the mass of the propellant required). All tandem satellite formation analysis conducted in this chapter assumed a formation of two 100kg satellites with a 1km separation distance in a near polar orbit at 400km altitude.

The change in separation distance (Δy) between satellites assumes that each firing will at minimum produce the amount of station-keeping thrust required to counter the attractive force of gravity (α) according to Eq. (2). Utilizing this assumption, the change in separation distance of the satellite formation is solely dependent upon the firing frequency as seen in Figure 28. At approximately 0.5Hz, any increase in firing frequency will result in a diminishing return with respect to an overall decrease in satellite separation distance. At any given firing frequency, the momentum per macron is constant, for a constant thrust, dictating a linearly proportional relationship between a macron's mass and exit velocity.

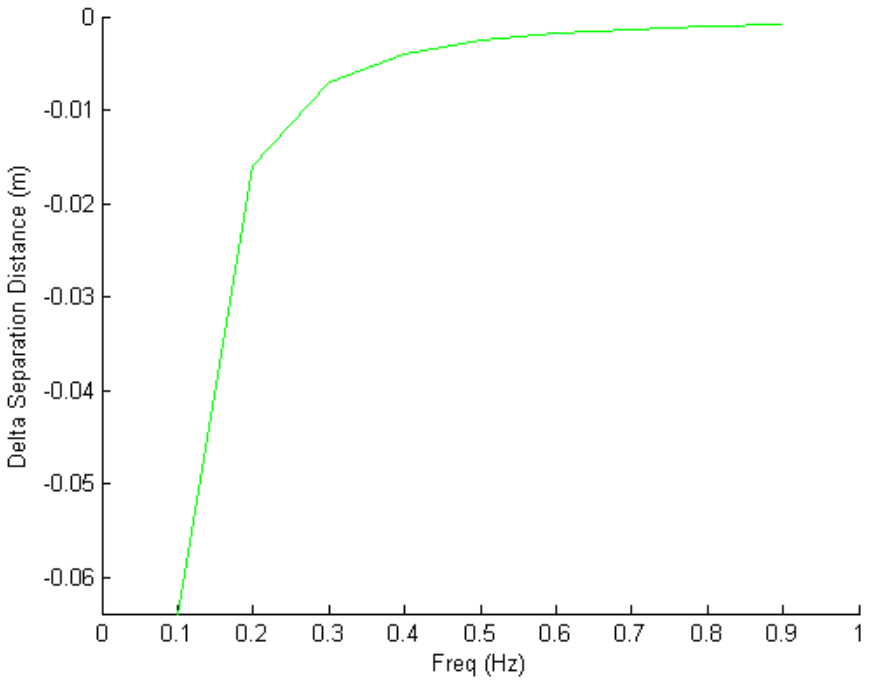

Figure 28. Change is satellite formation separation distance as a function of firing frequency

The required force of thrust to maintain tandem flight is equal in magnitude but opposite in direction from α. Therefore if α is known, the required exit velocity of a macron can be determined through the use of Eq. (9) and by applying macron mass (i.e. 0.1, 1, and 10g) and firing frequency (0.01 to 1Hz) limitations as seen in Figure 29.

$$\alpha = F_T = mvf \tag{9}$$

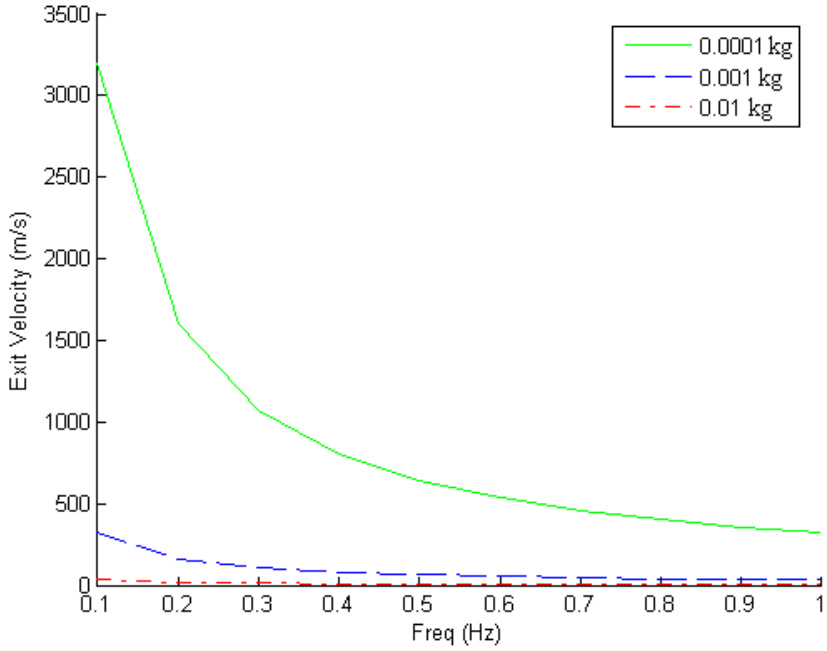

Figure 29. Macron exit velocities as a function of firing frequencies for various masses

Knowledge of a macron's exit velocity, allows for the determination of the number of macrons in transition for a given satellite separation distance at any given time as seen in Figure 30. When computing the number of transitioning macrons, it is important to take into account the accelerating force of gravity. Once a macron is fired, it will continue to accelerate until it crosses the centerline of Earth at which point it will decelerate until captured by the opposing satellite. Therefore, the maximum velocity of a macron is actually greater than its initial exit velocity. This increase in macron velocity creates a decrease in the expected travel time between satellites. A decreased travel time correlates to a decreased propellant mass required.

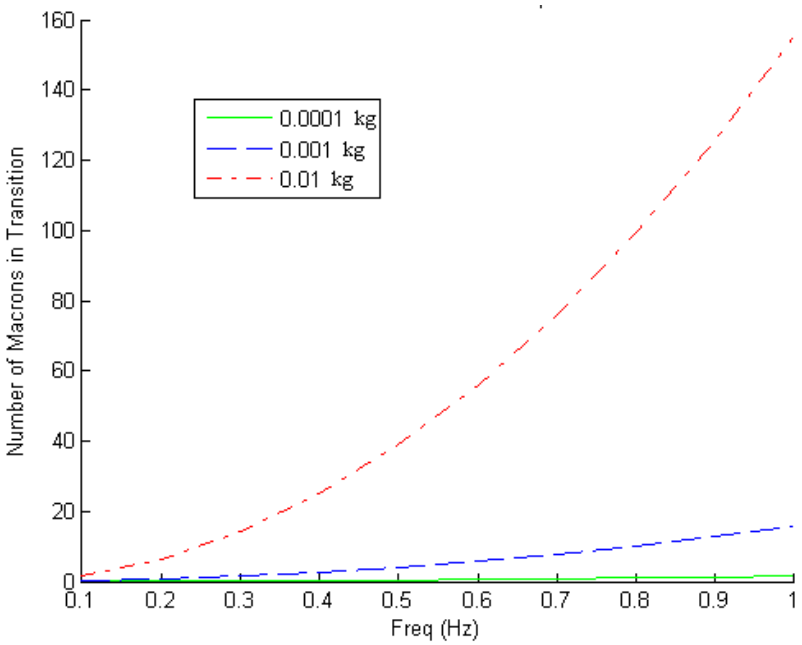

Figure 30. Number of macrons in transit for various firing frequencies as a function of macron mass

The number of transitioning macrons at any given time is an important parameter because it dictates the required propellant mass of the satellite formation system. Multiplying the number of macron in transition by the respective mass of a macron will determine the amount of propellant mass in transition. According to Figure 30, a MLP system operating at 1Hz will require 1.56kg of propellant for a 10g macron configuration, 15.6g of propellant for a 1g macron configuration, and 0.156g of propellant for a 0.1g macron configuration due to increasing exit velocities, respectively.

The impulse (i.e. momentum) of a fired macron is directly proportional to the amount of propellant required. Assuming that each macron provides the required station-keeping force necessary, the momentum per macron decreases as firing frequency increases. The momentum per macron is directly correlated to the importance of capturing a given macron. In other words, as momentum increases, each macron is responsible for imparting an increased percentage of the overall station-keeping force required. Therefore, if a high momentum macron is not captured, the satellite formation will experience an increased change in separation distances as compared to a low momentum macrons that is not captured.

The energy required for a given macron firing scenario can be determined by Eq. (10). In terms of a constant energy per firing MLP system configuration, the mass of a macron is inversely proportional to exit velocity squared. Therefore, a decrease in the exit velocity correlates to a dramatic increase in the

required mass of a given macron. The general range of energy per firing of a MLP system for a momentum exchange implementation is approximately between 1 and 500J.

$$E = \frac{1}{2}mv^2 \tag{10}$$

The input power required for a given macron firing scenario is a function of the energy per firing, firing frequency, and the thruster's efficiency as seen in Eq. (11). Rearranging Eq. (9) to solve for the exit velocity and plugging the resulting relation in to Eq. (11) allows for an alternative derivation of the input power required for a MLP system as seen in Eq. (12) The nominal MLP thruster efficiency for firing a macron size projectile with exit velocities less than 1km/s is approximately 70%. Figure 31 depicts the MLP input power requirements for a given firing frequency and mass combination assuming a minimal station-keeping thrust.

$$P_{in} = Ef\eta^{-1} = \frac{1}{2}mv^2 f\eta^{-1} \tag{11}$$

$$P_{in} = \frac{1}{2}{F_T}^2(mf\eta)^{-1} \tag{12}$$

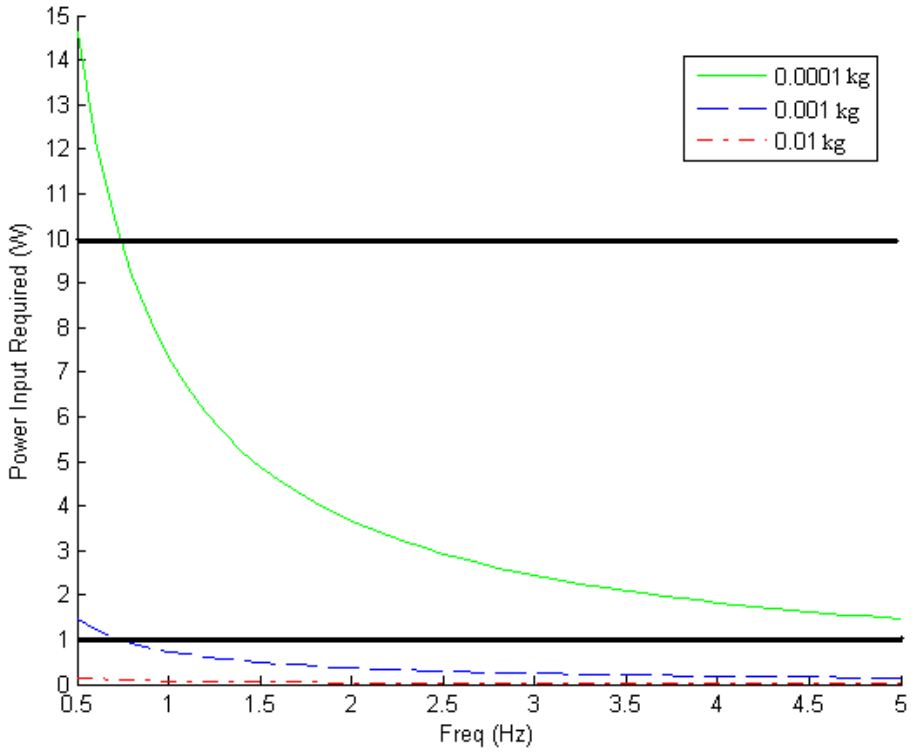

Figure 31. Required power input for various firing frequencies as a function of macron mass

In general, microsatellites are capable of producing 1W/kg of power. For a 100kg satellite, approximately 1W (i.e. 10%) might be available for constant propulsion. Therefore, a firing frequency of at least 0.85Hz is required to satisfy microsatellite power limitations for all macron masses investigated. Power supply limitations would further increase the required firing frequencies to greater than 5Hz to satisfy all macron masses. However, a macron mass of 1g satisfies the input power limitations for all firing frequencies greater than approximately 0.75Hz. The maximum sustainable firing frequencies are bound by propulsion system limitations. Firing frequencies greater than 2Hz are generally achievable but hard to sustain for long durations due to power cycling and material fatigue issues. However, an increase in macron mass (i.e. from 0.1 to 1g), results in dramatically decreased input power requirements (i.e. less than 10W) for all firing frequencies.

The optimum MLP system configuration is highly dependent on the satellite formation's mission objectives and in turn varies from mission to mission. Therefore, there is no single optimized MLP system configuration. However, based upon the trends displayed in the data and prior knowledge of a satellite formation's mission objectives, general guidance can be provided to direct spacecraft operators towards the optimal MLP system configuration and can be viewed in Table 8.

Optimized Parameter	**Required Changes**						**Trade-offs**				
	V_e	**Freq.**	**mv**	**F_d**	**A**	**M_{macron}**	**Miss Dis.**	**Δy**	**M_{prop}**	**E**	**P**
↓ Miss Dis.	↑	↓	↑	↑	↑	↓	NA	↑	↓	↑	↑
↓ Δy	↓	↑	↓	↓	↓	↑	↑	NA	↑	↓	↓
↓ M_{prop}	↑	↓	↑	↓	↓	↓	↓	↑	NA	↑	↑
↓ E	↓	↑	↓	↓	↓	↑	↑	↓	↑	NA	↓
↓ P	↓	↑	↓	↓	↓	↑	↑	↓	↑	↓	NA

Table 8: Momentum exchange MLP System optimization guide

Assuming adequate power supply and propellant storage capabilities, the optimal MLP system configuration utilizes increased masses and firing frequencies to minimize the change in satellite separation distance, exit velocity, energy per firing, and the importance of a single macron on the overall satellite formation (i.e. decreased impulse per macron) at the cost of an increased propellant mass and material fatigue rates. If power and propellant storage capabilities are limited, the optimal MLP system

configuration utilizes decreased macron masses and firing frequencies to minimize the power and propellant storage requirements at the cost of increased satellite separation distances, exit velocities, energies required per firing, and the importance of a single macron on the overall satellite formation (i.e. minimizing the number of uncaptured macrons becomes mission critical).

The nominal MLP system under investigation in this study is capable of achieving exit velocities less than or equal to 10km/s with an overall system mass of approximately 245kg. The MLP system mass is directly related to the energy and power requirements (i.e. macron mass, exit velocity, and firing frequency combination) of the system. The experimental MLP system was developed to operate solely in a laboratory environment and therefore, overall system mass was not optimized. A MLP system designed for spaceflight will be less massive than 245kg with the exact mass being a function of the desired energy and power outputs. For the tandem satellite formation under consideration, the corresponding required energy range is approximately between 1 and 500J. If a 50kJ (i.e. 1g-10km/s) MLP system has a system mass of 245kg, then a 500J MLP system will have a system mass of approximately 3kg according to linear scaling. In reality linear scaling is not an accurate estimation of a MLP system; however, it provides an approximate order of magnitude estimation of the required mass for a nominal 500J MLP system.

The trajectory analysis provided by the miss distance code supports the implementation of macron propulsion technology as a momentum exchange device for tandem satellite formations. Using traditional propulsion methods and techniques, the lifetime of any satellite formation is limited to the amount of propellant available. Once the propellant supply has been exhausted, the satellite formation will enter into free body motion and relative satellite positioning tolerances will be uncorrectable. Utilizing macron propulsion technology to provide a constant momentum exchange of mass is a more sustainable method of satellite formation station-keeping than traditional propulsion technologies. Furthermore, the operational lifetime of a tandem satellite formation utilizing a MLP system as a means of momentum exchange is theoretically infinite.

CHAPTER 6

COMPARISON OF SYSTEMS

When selecting a propulsion system, the primary selection criteria must be geared towards the fulfillment of the overall mission requirements. There are two general categories of propulsion systems used for in-space maneuvers (i.e. chemical and electric) which offer a wide range of cost, reliability, and performance parameters.

Table 9 provides general characteristics of common propulsion systems and highlights the versatility of a MLP system (i.e. propulsion duration) and a MLP system's capability of maintaining competitive performance parameters with all categories of in-space propulsion systems.

Engine Type	Isp (s)	Thrust-to-Weight Ratio	Propulsion Duration	Specific Power (kW/kg)	Typical Working Fluid	Status of Technology
Chemical (solid or liquids)	200-410	10^{-2}-100	Seconds-Minutes	10^{-1}-10^{3}	Liquid or Solid Propellants	Flight Proven
Liquid Monopropellant	180-223	10^{-1}-10^{-2}	Seconds-Minutes	$2x10^{-2}$-200	N_2H_4	Flight Proven
Resistojet	150-300	10^{-2}-10^{-4}	Days	10^{-3}-10^{-1}	H_2, N_2H_4	Flight Proven
Arch Heating (Electrothermal)	280-1200	10^{-4}-10^{-2}	Days	10^{-3}-1	H_2, N_2H_4, NH_3	Flight Proven
Electromagnetic (Pulsed Plasma)	700-2500	10^{-6}-10^{-4}	Weeks	10^{-3}-1	H_2	Flight Proven
Hall Thruster	1000-1700	10^{-4}	Weeks	10^{-1}-$5x10^{-1}$	Xe	Flight Proven
Ion Engine (Electrostatic)	1200-5000	10^{-6}-10^{-4}	Months	10^{-3}-1	Xe	Several have flown
Macron Propulsion*	500-1000	$>10^{-2}$	Seconds-Months	$>10^{-4}$	Al	In Development

Table 9. Typical performance parameters of common propulsion systems[53]

**Macron propulsion parameters added by author*

There is no propulsion system which is universally applicable or optimal for all orbital maneuvers. A thorough analysis of any propulsion system will stress that there is a balance of advantages and

disadvantages. All propulsion systems are developed to fulfill a specific category of mission profiles (e.g. orbital maneuvers, attitude control, interplanetary transfers, etc.) and are generally inapplicable outside of their intended mission niche. The potential disadvantages of a macron propulsion system (i.e. exhausting macrons into the space environment) are evident. The remainder of this chapter is devoted to identifying the disadvantages of traditional propulsion systems and quantifying their effects with respect to the effects of a MLP system.

A. Solid Rocket Motors

An extensive characterization of SRM debris characteristics is provided in Ref. [10]. The primary source of mission related space debris resulting from SRM firings occur in the form of slag and "dust" particles.[10] Slag is a solid particle produced as a byproduct of smelting which occurs during a combustion process involving a metallic substance. Slag particles are primarily produced through ablation of the nozzle and thrust chamber walls during a SRM firing. The size of a typical slag particle ranges between 0.1 and 30mm in diameter. Ablation is a process where materials erode, chip, or vaporize when subjected to intense heat. When a material ablates, the ablating particle removes heat from the spacecraft and can be used as a method of thermal regulation. The majority of slag particles are released in the exhaust plume during the final stages of thrusting when the pressure in the combustion chamber decreases dramatically. Due to slag particles being released during the final stages of thrusting, particles are ejected with minimal exit velocities (i.e. Isp). Therefore, the resulting velocity profile of ejected slag particles is nearly equivalent to the velocity of the ejecting spacecraft. This results in the majority of slag particles entering into orbital trajectories.

Dust particles refer to the numerous solid molecules which are exhausted into the space environment during a chemical combustion process. Table 10 provides various performance parameters for common SRM propellants and highlights that the majority of SRM propellants contain metal particles which will ultimately contribute to the sub-10μm orbital debris particle population size and impact the space environment.

In addition to slag and dust, SRM systems exhaust gaseous molecules which collectively account for the majority of the mass in an exhaust plume. Gaseous molecules are the smallest byproduct of a combustion process and typically have diameters in the nanometer to picometer range. The mass fraction of

gaseous molecules in an exhaust plume is approximately 60% of the overall exhaust plume mass. In other words, for an IUS with a solid propellant mass of 9,709kg, approximately 5,800kg of gaseous molecule will be ejected in its exhaust plume with the remaining 3,909kg of mass being exhausted as complex particles in various states of matter (e.g. slag or dust particles).

Propellant Type	Isp (s)	Specific Gravity	Metal Content (mass %)
DB-AP-Al	260-265	1.8	20-21
DB-AP-HMX-Al	265-270	1.8	20
PVC-AP-Al	260-265	1.78	21
PU-AP-Al	260-265	1.78	16-20
PBAN-AP-Al	260-263	1.78	14
CTPB-AP-Al	260-265	1.78	15-17
HTPB-AP-Al	260-265	1.86	4-17
PBAA-AP-Al	260-265	1.78	14

Table 10. Characteristics of some operational solid propellants[53]

Table 11 quantifies the relative contributions of SRM slag and dust particles to the overall MMOD environment. In terms of space environment impact, SRM slag is responsible for approximately 30% of all 1cm orbital debris particles, 46% of all 1mm orbital debris particles, and 76% of all 10mm orbital debris particles. SRM dust accounts for 99% of all orbital debris particles less than 10μm in diameter. In terms of mass contributions, SRM slag accounts for 30% of the overall orbital debris mass in 1cm size particles.

It is assumed that during the 1,032 SRM firings that occurred prior to June 2001, approximately 907×10^3kg of propellant (i.e. approximately 880kg per SRM vehicle) was released into space.[10] Based on the hypotheses of physical and mathematical models approximately 290×10^3kg of the released dust particles (i.e. approximately 280kg per SRM vehicle) were solid Al_2O_3 particles and 3.6×10^3kg were slag particles (i.e. 3.5kg per SRM vehicle) composed of Al_2O_3, metallic Al, and motor liner material.[10] Although the average size and mass of a dust particle may seem insignificant, it still represents an accumulation of mass being exhausted into the space environment.

Source Type	Orbit Regime	>1μm	>10μm	>0.1mm	>1mm	>1cm	>10cm	>1m
Launch/MRO	LEO	--	--	5,156	4,487	3,118	3,007	2,028
	LEO+MEO+GEO	--	--	45,342	30,561	5,171	5,128	3,808
Fragments	LEO	--	1.64E+11	2.37E+10	1.30E+08	149,266	6,602	228
	LEO+MEO+GEO	--	2.14E+11	3.20E+10	3.20E+08	382,719	12,704	462
NaK	LEO	--	--	--	35,280	15,012	0	0
	LEO+MEO+GEO	--	--	--	35,280	15,012	0	0
SRM Slag	LEO	--	8.33E+09	7.66E+09	8.23E+06	22,065	0	0
	LEO+MEO+GEO	--	5.06E+11	4.13E+11	1.52E+08	171,046	0	0
SRM Dust	LEO	2.88E+13	1.92E+13	0	0.00E+00	--	--	--
	LEO+MEO+GEO	7.22E+15	1.39E+14	0	0.00E+00	--	--	--
Paint Flakes	LEO	5.03E+12	1.27E+12	3.15E+10	0.00E+00	--	--	--
	LEO+MEO+GEO	4.23E+13	1.51E+13	9.63E+10	0.00E+00	--	--	--
Ejecta	LEO	1.37E+09	1.33E+09	1.01E+08	7.96E+05	--	--	--
	LEO+MEO+GEO	7.15E+10	1.44E+10	2.52E+08	1.10E+06	--	--	--
Total Count	LEO	3.39E+13	2.06E+13	6.30E+10	1.39E+08	189,461	9,679	2,256
	MEO+GEO	7.22E+15	1.33E+14	4.78E+11	1.92E+08	384,484	8,153	2,014
	LEO+MEO+GEO	7.26E+15	1.54E+14	5.41E+11	3.31E+08	573,945	17,832	4,270

Table 11. Orbital debris contributions by micro and macro objects (*MASTER-2001 reference population for May 2001)*[10]

B. Other Traditional Propulsion Methods

In addition to SRMs, liquid and EP systems are widely used in the space environment. Liquid propulsion systems rely on the chemical combustion of liquid propellants to provide thrust; whereas, EP systems rely on electrical means of accelerating particles.

The exhaust plume of a liquid propulsion system primarily consists of gaseous particles with minimal byproducts. The primary byproduct of a liquid propulsion system is liquid droplets which are not combusted and then expelled in the exhaust plume. These liquid droplets tend to coalesce into liquid droplet clusters which could adversely affect to the orbital debris environment. The threat imposed by liquid droplet or a liquid droplet cluster are comparable to solid MMOD particles of similar size due to the nature of HVIs being relatively independent of particle density (i.e. state of matter). However, due to the high vapor pressures of most liquid propellants, liquid droplets and droplet clusters typically vaporize when exposed to the vacuum of space. This phenomenon minimizes the impact a liquid droplet or a droplet cluster has on the space environment.

Based on the exit velocities achieved by EP systems, all exhausted mass is placed on escape trajectories in accordance with Figure 10. The primary advantage of all EP technology is the capability of conducting a plethora of in-space maneuvers without placing any mass into orbital trajectories. In general, EP systems exhibit minimal impact on the space environment.

C. MLP System Comparison

The MLP system currently being developed is categorized as an EP system due to its reliance on electrical power and acceleration techniques. The primary difference between a MLP system and a traditional EP system is the size and nature of the particles being accelerated (i.e. exhausted). Macron propulsion systems accelerate macroscopic size particles whereas, EP systems accelerate atomic size particles (e.g. xenon). As a result of their overall system similarities, a MLP system and traditional EP systems share a common advantage of exhaust plume trajectory control.

In comparison to a MLP system, the greatest disadvantage of a chemical propulsion system is the lack of completely directionalized exhaust flow. When a MLP system is fired, the macron will exit the system in the exact direction it was fired. The worst possible implementation of a MLP system is as an anti-RAM firing, LEO to GEO propulsion system because this type of maneuver results in the creation of 160kg of orbital debris.

During a maneuver in the vacuum of space using a chemical propulsion system, the exhaust flow experiences Prandtl-Meyer type expansion waves which are attached to the lip of the nozzle causing the exhaust flow to be bent up to a theoretical limit of 129deg off the axis of the nozzle.[53] Figure 32 shows a density profile for a chemical propulsion system's exhaust plume expansion profile in a vacuum. This phenomenon creates a wide distribution of exhaust plume constituents (i.e. dust and gaseous molecules) with final trajectories being reentry and orbital.

According to past orbital debris contributions, every LEO to GEO transfer utilizing a SRM will on average place approximately 1,160kg (i.e. 880kg of dust and 280kg of slag) of mass into the space environment. In comparison, a MLP system being utilized in the worst way possible to conduct a LEO to GEO transfer (i.e. anti-RAM firings) results in 160kg of orbital debris. This is approximately 13% of the orbital debris mass produced by a SRM. Furthermore, a SRM is incapable of being operated in a manner which does not result in the production of orbital debris whereas, a MLP system can utilize maneuvering

techniques (i.e. off-axis thrusting and increased exit velocities) to negate orbital debris contributions. Therefore, a MLP system can theoretically have less of an impact on the space environment than a SRM.

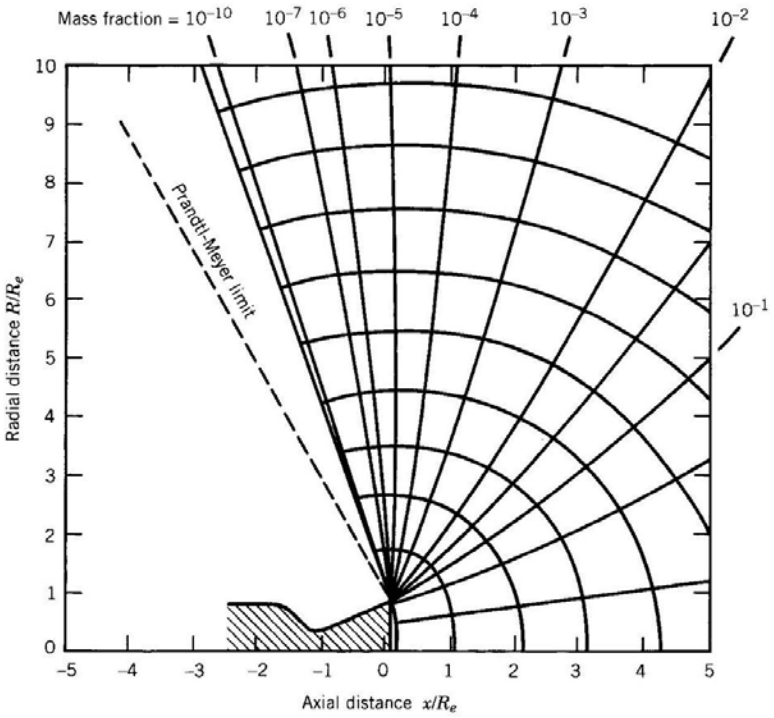

Figure 32. Density profile for vacuum plume expansion (*k=1.25, exit mach = 4, and nozzle cone half angle = 19deg*)[53]

CHAPTER 7

CONCLUSION

It is critically important for a MLP system or any macron propulsion device to be implemented in a manner which minimizes its impact on the space environment. Macrons which are placed into orbital trajectories will adversely contribute to the MMOD environment and increase the MMOD flux experienced by satellites. Any increase in the MMOD flux equates to an increased probability that a satellite will experience a HVI with a MMOD object during the satellite's operational lifetime. According to mathematical models and simulations, the average velocity of a MMOD impact (i.e. stray orbital macron) is approximately between 11 and 16km/s for prograde orbital macrons. Macrons which are placed in retrograde orbital trajectories experience increased collision velocities which results in an increased hazard to spacecrafts. HVIs occurring with orbital macrons possess adequate destructive capability to induce a catastrophic failure on even the most heavily shielded spacecrafts. Before a maneuvering scenario is conducted using a macron propulsion device, a trajectory analysis must be conducted to ensure that a fired macron does not achieve an orbital trajectory.

Ultimately, the combination of a macron's firing angle, exit velocity, and altitude determine its overall energy level which defines a given firing scenario's trajectory outcome. These three parameters combined dictate a fired macron's level of impact on the space environment. Trajectory analysis studies of fired macrons highlighted that, in general, macrons which are fired with the majority of their velocity directed in either the RAM or anti-RAM directions minimized the potential impact on the space environment. RAM fired macrons primarily result in escaping trajectories whereas, anti-RAM firing usually enter into reentry or escaping trajectories. The one exception being anti-RAM firings in MEO which result in orbital trajectories.

Before an orbital maneuver is conducted, it is critical that spacecraft operators take precautions to ensure avoidance of not only macron orbital trajectories but also collision course trajectories with neighboring spacecraft. Therefore, the timing of a maneuver is deemed significant in addition to the firing

angle, exit velocity, and altitude combination. The timing of a macron's firing dictates the relative position of neighboring spacecrafts which, if poorly timed, could result in a collision trajectory with an operational satellite. For LEO maneuvers, reentry trajectories are more desirable than escaping due to the decreased probabilities of collisions and vice versa for GEO maneuvers.

Orbital analysis studies support the implementation of a MLP system as an intra-LEO, LEO to GEO and GEO inclination changing propulsion system. Operating a MLP system at GEO minimizes the potential impact of a macron due to the decreased energy levels required to place a macron on an escape trajectory. Based on the analysis conducted in this study, it can be reasonable assumed that a MLP system could also be implemented as a GEO insertion, phasing, and rendezvous propulsion system while maintaining minimal impact on the space environment.

In addition to traditional orbital maneuvers, a MLP system can be implemented as a momentum exchange device to enable satellite formation which are impossible to sustain through the use of traditional propulsion techniques. A sustained tandem satellite formation with a constant separation distance between satellites is not only achievable through the implementation of MLP systems but it can also significantly benefit the field of remote sensing by enabling bistatic SAR operations with a theoretically infinite operational lifetime. Trajectory analysis of macrons fired between tandem satellites shows that the effects of orbital perturbation forces are minimal and result in manageable macron miss distances. Furthermore, the thrust and optimal system configuration requirements to sustain a tandem satellite formation are well within the operational performance range of a MLP system.

A systems analysis of both traditional and macron propulsion technologies highlight a macron propulsion system's greatest advantage, its ability to accurately control and predict the final trajectory of its exhaust plume. When conducting a LEO to GEO transfer, a MLP system being implemented in the worst case scenario will contribute 160kg of mass to the orbital debris environment; whereas, historical averages dictate that a SRM will contribute approximately 1,160kg of mass. Therefore, implementing a MLP system as a LEO to GEO propulsion system will be approximately seven times less impactful on the space environment than a SRM. In comparison to traditional EP systems, a MLP system is capable of efficiently conducting a LEO to GEO transfer 95% faster due increased thrust.

The data presented in this paper outlines the performance parameters of a MLP system and serves as a guide for spacecraft operators to effectively implement and utilize a macron propulsion system. All spacecraft propulsion systems have the potential to adversely impact the space environment. The research conducted within the study supports the claim that a macron propulsion system's level of impact on the space environment is no greater than current operational propulsion methods. If implemented in the most precautious manner, a macron propulsion system is theoretically capable of operating in the space environment with a near zero level of impact. Macron propulsion technology has numerous distinct performance parameters and the potential to be implemented as a primary in-space propulsion system capable of conducting numerous orbital maneuvering scenarios with minimal space environment impact.

REFERENCES

[1] Harrison, E R. "The problem of producing energetic macrons (macroscopic particles)." *Plasma Physics* **9** (2) (1967): 183.

[2] Pancotti, Anthony P. *A Study of Ignition Effects on Thruster Performance of a Multi-Electrode Capillary Discharge Using Visible Emission Spectroscopy Diagnostics*. Thesis. University of Southern California, 2009.

[3] Kirtley, David, John Slough, Jacob Schonig, and Andrew Ketsdever. "Pulsed Inductive Macron Propulsion," 57th Joint Army-Navy-NASA-Air Force Propulsion Meeting, Colorado Springs, CO, May 3-7, 2010.

[4] Slough, John, Arthur Blair, Chris Pihl, and George Votroubek, "Magnetically Accelerated Plasmoid (MAP) Thruster – Initial Results and Future Plans", IEPC paper 2007-16, 30th International Electric Propulsion Conference, Florence, Italy, September 17-20, 2007.

[5] Wertz, James R., and Wiley J. Larson, eds. *Space Mission Analysis and Design*. Dordrecht [u.a.: Kluwer Academic Publ.], 2008.

[6] Sellers, Jerry Jon., William J. Astore, Robert B. Giffen, Wiley J. Larson, Douglas H. Kirkpatrick, Dale Gay, and Anita Shute. *Understanding Space: an Introduction to Astronautics*. New York: McGraw-Hill Companies, 2005.

[7] Bate, Roger R., Donald D. Mueller, and Jerry E. White. *Fundamentals of Astrodynamics*. New York: Dover Publications, 1971.

[8] Prussing, John E., and Bruce A. Conway. *Orbital Mechanics*. New York, NY, 1993.

[9] Belk, C.A. , Robinson, J.H., Alexander, M.B, Cooke, W.J., Pavelitz, S.D. Meteoroids and Orbital Debris: Effects on Spacecraft, NASA Reference Publication No. 1408, August 1997.

[10] Klinkrad, Heiner, and H. Stokes. *Space Debris: models and Risk Analysis.* Praxis Publishing Ltd, Chichester, 2006.

[11] National Research Council: "Orbital Debris A Technical Assessment." National Academy Press, Washington, DC, 1995.

[12] Meshishnek, M.J. Overview of the space debris environment. Technical report, 1995. Aerospace report no. TR-95(5231)-3.

[13] Millman, Peter M. "Meteor News." *Journal of the Royal Astronomical Society of Canada.* Vol 55 (1961): 265.

[14] Theall, J. "Service Module Micrometeoroid and Orbital Debris (MMOD) Shielding", Briefing presented to the Stafford Task Force by the ISS MMOD Team, NASA Johnson Space Center, July 23, 1997. 174.

[15] Tribble, Alan C. *The Space Environment: Implications for Spacecraft Design*. Princeton, NJ: Princeton UP, 1995.

[16] J. Bendisch, K.D. Bunte, H. Krag, H. Sdunnus, P. Wegener, R. Walker, C. Wiedemann and. H. Klinkrad : Final Report Upgrade of ESA's MASTER Model, 2002

[17] Coombs, C. R., Atkinson, D. R. , Allbrooks, M. K., Watts, A. J., Hennessy, C. J., and Wagner, J. D., "Damage Areas on Selected LDEF Aluminum Surfaces," NASA CP 3194, Part 2, p 595-618 (1993).

[18] Kemp, W., Bloemker, C., Resner, G., Watts, A., and White, F. "LDEF Space Optics Handbook," Phillips Laboratory Report, September 1993.

[19] "Hypervelocity Impact Technology Facility." *National Aeronautics and Space Administrati*

[20] Torvik, Peter J. *Critical Technologies for National Defense*. Washington, DC: American Institute of Aeronautics and Astronautics, 1991. 287-303.

[21] Lamontagne CG, Manuelpillai GN, Taylor EA, Tennyson RC. Normal and oblique hypervelocity impacts on carbon fiber/PEEK composites. *Int. J. of Impact Engineering*, 1999; 23: 519-532.

[22] Kessler, D.J. , Reynolds, R.C. and Ans-Meador, P.D. "Orbital Debris Environment for Spacecraft Designed to Operate in Low Earth Orbit," NASA TM-100-471, April 1989. See also D.J. Kessler, Orbital Debris Technical Interchange Meeting, Phillips Laboratory presentation, 2-3 April 1991.

[23] Schonberg, W.P., Bean, A.J. and Darzi, K. *Hypervelocity Impact Physics*. NASA Contractor Report 4343, 1991.

[24] "Meteoroid and Orbital Debris Environment." *NASA Orbital Debris Program Office*. 03 Feb. 2010.

[25] "The Future of Civil Explosives." *Federation of European Explosives Manufacturers.* <http://www.feem-europe.org.

[26] Clark, Philip S., "Space debris incidents involving Soviet/Russian launches", *Journal of the British Interplanetary Society*, Vol 47, No 9,1994,

[27] "The Olympus Failure." *European Space Agency*. 26 Aug. 1993.

[28] Alby, F., E. Lansard, T. Michal. *Collision of Cerise with Space Debris.* 2nd European Conference on Space Debris, pp. 589-596, ESA SP-393 (1997)

[29] "Russian Satellite Failure Caused By Space Garbage." *Space Daily*. 17 Apr. 2006.

[30] Iannotta, Becky, and Tariq Malik. "U.S. Satellite Destroyed in Space Collision." *Space.com*. 11 Feb. 2009.

[31] NASA. Lyndon B Johnson Space Center. *Meteoroid and Debris Impact Features Documented on the Long Duration Exposure Facility (1998)*. 19980302-056.

[32] "Space Mission Software - Analytical Graphics, Inc." *Analytical Graphics, Inc. (AGI): Analysis Software for Land, Sea, Air, and Space*. Web. 07 June 2010. <http://www.stk.com >.

[33] Carrico, John. *Analytic Graphics Inc. Orbital Maneuver Planning*. Proc. of STK Users' Conference. 2002. <http://www.stk.com >.

[34] The National Science and Technology Council Committee on Transportation Research and Development: "Interagency Report on Orbital Debris." Washington, DC, 1995.

[35] Hastings, Daniel, and Henry Garrett. *Spacecraft-Environment Interactions* (Cambridge Atmospheric and Space Science Series). Cambridge: Cambridge University Press, 1996.

[36] Prolss, Gerd W. *Physics of the Earth's Space Environment*. Berlin: Springer, 2004.

[37] Picone, J. M. , Hedin, A. E. , Drob, D. P., and Aikin, A. C. "NRLMSISE-00 empirical model of the atmosphere: statistical comparisons and scientific issues," J. Geophys. Res. **107** (A12), 1468–1483 (2002).

[38] Shindell, Drew, David Rind, Nambeth Balachandran, Judith Lean, and Patrick Lonergan. "Solar Cycle Variability, Ozone, and Climate." *Science* **284.5412** (1999): 305-08.

[39] Larson, Wiley J., and James Richard. Wertz. *Space Mission Analysis and Design*. El Segundo, Calif.: Microcosm, 2006. 207.

[40] Vallado, David A., and Wayne D. McClain. *Fundamentals of Astrodynamics and Applications*. Hawthorne, Calif. 2007.

[41] Larson, Wiley J., and James Richard. Wertz. *Space Mission Analysis and Design*. El Segundo, CA: Microcosm, 2006.

[42] Free, B., *High Altitude Orbit Raising with On- Board Electric Power*, IEPC-93-205, Sept. 1993.

[43] Wright, D., "Space Debris," Physics Today, October 2007, pages 35-40.

[44] Kelso, TS, "Analysis and Implications of the Iridium 33/Cosmos 2251 Collision", Advanced Maui Optical and Space Surveillance Technologies Conference, 1-4 Sept, 2009.

[45] Kessler, DJ., R.C. Reynolds, and P.D. Anz-Mexdor, "Orbital Debris Environment for Spacecraft Designed to Operate in Low Earth Orbit," NASA TM l00-471, April 1988.

[46] Joslyn, Thomas and Andrew Ketsdever. "Constant Momentum Exchange Between Microspacecraft Using Liquid Droplet Thrusters", 46th joint Propulsion Conference, Nashville, TN, July 25-28 2010.

[47] Tragesser, S., Static Formations Using Momentum Exchange Between Satellites, J. Guidance, Control, and Dynamics, Vol. 32, pp. 1277-1286 (2009).

[48] Krieger, G., et al. TanDEM-X: A satellite formation for high-resolution SAR interferometry. *IEEE Transactions on Geoscience and Remote Sensing*, **45**, 11, 1 (2007), 3317—3341.

[49] Zink, Manfred; Krieger, Gerhard; Fiedler, Hauke; Moreira, Alberto (2008): The TanDEM-X Mission Concept, In: Proceedings of the European Conference on Synthetic Aperture Radar (EUSAR), S. 4, Friedrichshafen, Germany, 2008-06-02 - 2008-06-05.

[50] Moccia, A., Salzillo, G., D'Errico, M., Rufino, G. and Alberti, G. "Performance of spaceborne bistatic synthetic aperture radar," *IEEE Trans. Aerosp. Electron. Syst.*, vol. 41, no. 4, pp. 1383–1395, Oct. 2005.

[51] Horne, A. M., and Yates, G. Bistatic synthetic aperture radar. *IEE Radar 2002*, (Oct. 2002), 6–10.

[52] Zink, M., Krieger G., Fiedler H., and Moreira L., The TanDEM-X Mission:Overview ans Status, Proceedings of the Geoscience and Remote Sensing Symposium, IEEE International, pp. 1383-1395, Oct. 2005.

[53] Sutton, George Paul., and Oscar Biblarz. *Rocket Propulsion Elements*. New York: John Wiley & Sons, 2001. 28.

APPENDIX A

SUPPLEMENTAL MMOD FLUX EQUATIONS

The following equation can be utilized to determine the MMOD flux for a given mass (i.e. MMOD object size) if the density of the object is known[15]

$$Flux = 3.156 \times 10^{7}[A^{-4.38} + B + C]$$

where flux has units of particles/(m^2year), m is the micrometeoroid mass in grams and[15]

$$A = 15 + 2.2 \times 10^{3} m^{0.306}$$

$$B = 1.3 \times 10^{-9}(m + 10^{11} m^2 + 10^{27} m^4)^{-.0306}$$

$$C = 1.3 \times 10^{-16}(m + 10^{6} m^2)^{-0.85}$$

The representative mass density distribution of MMOD objects can be approximated as follows[15]

$$\rho = 2\frac{g}{cm^3}; \qquad m < 10^{-6} g$$

$$\rho = 1\frac{g}{cm^3}; \qquad 10^{-6} \leq m < 0.01 g$$

$$\rho = 0.5\frac{g}{cm^3}; \qquad m > 0.01 g$$

In General, the MMOD flux in LEO is slightly greater than in MEO or GEO due to the focusing effect of Earth's gravity. All micrometeoroids must pass through MEO and GEO to contribute to the LEO MMOD flux and in the process of doing so, micrometeoroids also contribute to the MEO and GEO fluxes.

APPENDIX B

SUPPLEMENTAL HVI INFORMATION

HVIs do not occur naturally on Earth but can be replicated by using the acceleration techniques shown in the table below.

Accelerator Type	Mass and Velocity Ranges Covered		
Powder guns	1,200g at 1.0km/s	→	160g at 3.8km/s
Single-stage light gas guns	1,200g at 0.8km/s	→	160g at 2.0km/s
Two-stage light gas guns	80g at 3.0km/s	→	0.2g at 9.5km/s
Modified light gas guns	5g at 10.0km/s	→	0.1g at 15.0km/s
Electromagnetic rail guns	20g at 1.5km/s	→	1.0g at 7.5km/s
Electrostatic guns	6g at 2.0km/s	→	0.05g at 18.0km/s
Shaped charges	10g at 10.0km/s	→	1.0g at 11.5km/s

Performance ranges of hypervelocity accelerators[10]

According to Figure 6, equatorial orbits (i.e. inclination = 0deg) experience the greatest flux of MMOD particles. Due to orbital mechanics, all orbiting objects in unpowered flight (i.e. restricted two-body motion) must cross the equator two times per orbit; once traveling North (i.e. ascending node) and once traveling South (i.e. descending node). Equatorially orbiting spacecrafts are threatened by all objects that have an ascending or descending node altitude equivalent to their own orbital altitude. Similarly, polar orbits (i.e. inclination = 90deg) experience the highest relative velocities with MMOD objects as seen in Figure 6. The hazards of MMOD objects on polar orbits are catastrophic in nature and hinder remote sensing operations.

Pure crater damage will occur when the impacting surface thickness (t_t) is much greater than the predicted crater depth (D_c) (i.e. $t_t > 3D_c$). Spallation of the rear wall occurs when $t_t \approx 2.2D_c$ and complete perforation of the impacting surface will usually occur when $t_t \approx 1.8D_c$.[10] Spallation is a phenomenon induced by the stress waves created during a HVI and can result in the separation of the rear wall of the

impacting material. The figure below shows pure crater, spallation and perforation impact geometries resulting from HVIs of aluminum spheres on typical space-faring material.

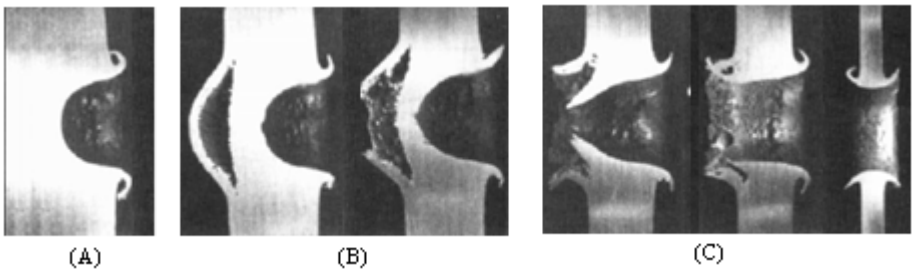

Impact geometries for a 6km/s Al-particle impacting various target thicknesses[9]
(A) Pure crater (B) Spallation (C) Perforation

In addition to the size and velocity, the shape and orientation of an impacting particle have significant effects on the resulting crater size and geometry. For a slender projectile with high velocity, the peak pressure and temperature during a HVI can reach levels of 100GPa and 10,000K, respectively. These conditions are comparable to the Earth's core where pressures and temperatures are approximately 365GPa and 6,000K, respectively.[10] As seen in the Figure below, cylindrical particles have a greater penetration capability than spherical or flat plate particles. Likewise, the impacting surface's material composition plays a significant role in the determination of the overall crater size. In general, ductile materials (i.e. the majority of space-faring materials) experience less damage than brittle materials (e.g. solar arrays, telescope mirrors, or the space shuttle's windows). Experiments have also shown that the overall impact damage for a solid aluminum particle with the same mass and velocity as a liquid aluminum particle are nearly equivalent.[10] The independence of a particle's state of matter prior to impact forms the core definition of a HVI (i.e. impacts of sufficient velocity to cause both the impacting particle and the impacting surface to behave like fluids).

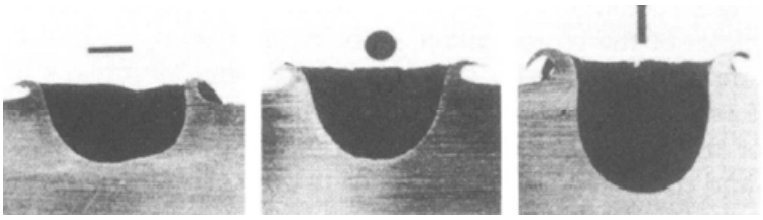

Impact crater geometry for various aluminum particles and surfaces[10]

APPENDIX C

SUPPLEMENTAL HVI DAMAGE EQUATIONS AND COEFFICIENTS

The non-normalized collision velocity distribution (i.e. most probably impact velocity between and MMOD object and a satellite) relative to an orbiting spacecraft with a given inclination (i) is given by[12]

$$(v) = (2vv_o - v^2)\left(Ge^{-\left(\frac{v-Av_o}{Bv_0}\right)^2}\right) + \left(Fe^{-\left(\frac{v-Dv_o}{Ev_0}\right)}\right) + HC(4vv_o - v^2)$$

where v is the collision velocity in km/s and the values for A, B, C, D, E, F, G, H and v_o are functions of the satellite's orbital inclination given by[12]

A = 2.5

B = 0.5 ; i < 60
0.5 - 0.01 (i - 60) ; 60 < i < 80
0.3 ; i > 80

C = 0.0125 ; i < 100
0.0125 + 0.00125 (i - 100) ; i > 100

D = 1.3 - 0.01 (i-30)

E = 0.55 + 0.005 (i - 30)

F = 0.3 + 0.0008 (i - 50)^2 ; i < 50
0.3 - 0.01 (i - 50) ; 50 < i < 80
0.0 ; i > 80

G = 18.7 ; i < 60
18.7 + 0.0289 (i - 60)^3 ; 60 < i < 80
250.0 ; i > 80

H = 1.0 - 0.0000757 (i - 60)^2

Vo = 7.25 + 0.015 (i-30) ; i < 60
7.7 ; i > 60

Once the most probable impact velocity is established, an estimation of the resulting damage from and MMOD impact can be approximated. The impact crater diameter (d_c) on a semi-infinite single-walled surface and the minimum impacting surface thickness ($t_{t\,min}$) required to withstand a MMOD impact can be described by the following equation[10]

$$d_c = t_{t\,min} = K_1 d_p^{\lambda} \rho_p^{\beta} \rho_t^{\kappa} v_p^{\gamma} \left(\cos \alpha_p\right)^{\xi}$$

with corresponding calibration parameters λ, β, κ, γ, and γ in accordance with the table and the end of Appendix B.

The corresponding impact crater depth (D_c) can be described by[23]

$$D_c = Am^{\alpha} v^{\beta}$$

where α = 1.02, β = 0.7 and A is a parameter with values typically ranging between 0.2 and 0.25. The exact value of A is defined as[10]

$$A = 6.97\left(\frac{V\rho_p}{\sqrt{\sigma_t\rho_t}}\right)^{-0.271}\left(\frac{\sigma_t}{\sigma_{Al}}\right)^{-0.217} {t_t}^{-0.053}$$

where v is in km/s.

The above impact crater diameter equation can be can be rewritten to indicate the maximum diameter particle a given spacecraft surface can defeated during a HVI through the following equation[10]

$$d_{p\,max} \leq \left[\frac{t_t}{K_1\rho_p^{\beta}\rho_t^{\kappa}v_p^{\gamma}(\cos\alpha_p)^{\xi}}\right]^{\frac{1}{\lambda}}$$

Determining the maximum defeatable particle MMOD particle size during a HVI becomes fundamental when designing passive spacecraft protection measures (i.e. shielding).

Equation	Target	K_1	λ	β	γ	ξ	κ
ESA	thick plate	0.36–0.99	1.056	0.519	2/3	2/3	0
ESA	thin plate	0.26–0.64	1.056	0.519	0.875	0.875	0
Pailer & Gruen	any	0.77	1.212	0.737	0.875	0.875	–0.5
Frost	any	0.43	1.056	0.519	0.875	0.875	0
Naumann et al.	any	0.65	1.056	0.5	0.875	0.875	–0.5
Naumann	any	0.326	1.056	0.499	2/3	2/3	0
McHugh et al.	thick glass	1.18–4.48	1.2	0	2/3	2/3	0.5
Cour-Palais	thick glass	0.98–3.17	1.06	0.5	2/3	2/3	0

Calibrated parameters for a single-wall ballistic limit equation, according to different sources[10]

APPENDIX D

PARAMETRIC TIME STEP STUDY

An analysis was conducted to determine the optimal time step of the EOV code to produce highly accurate data with minimal time costs. Reduced time steps allow for greater accuracy as seen in the figure below

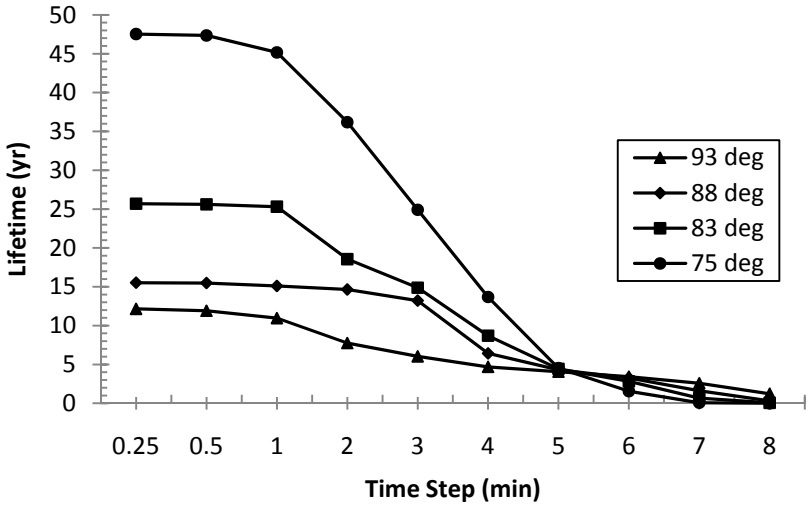

Resulting orbital lifetime data for various orbital trajectory firing angles as a function of EOV code time step.

However, reduced time steps also equate to an increased overall computation time as seen in the figure below

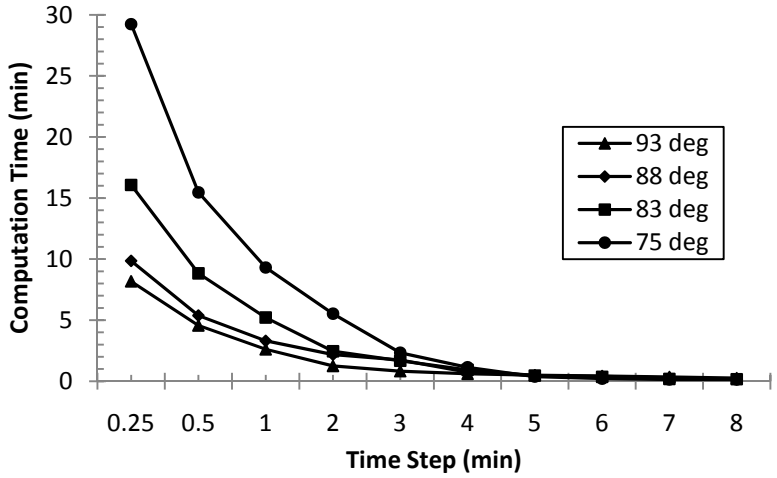

Overall computation time for various orbital trajectory firing angles as a function of EOV code time step

The parametric time step yielded a standardized time step of 60 seconds based on the trade-offs between orbital lifetime accuracy and overall computation times.

A standardized computer was used throughout all parametric time step studies with the following performance parameters: Intel® Core ™ 2 Duo CPU, E8500 @3.16GHz, and 3.25GB of RAM.

APPENDIX E

MATLAB MISS DISTANCE CODE

```
function miss_dis_drag_MMM

%%%%%%%%%%%%%%%%%%%%%%%%%%%%%%%%%%%%%%%%%%%%%%%%%%%%%%%%%%%%%%%%%%%%%%%%%%%%
% Author: Jacob A. Schonig                                                     %
%                                                                             %
% Required Inputs:                                                            %
%    -Excel spreadsheet containing atmospheric density data for solar %
%     min, mean and max periods                                                %
%    -Exit velocity range                                                     %
%    -Satellite separation distance range
%
%    -Orbital altitude                                                        %
%    -Macron and satellite parameters (cross-sectional area,                  %
%      coefficient of drag and mass                                           %
%                                                                             %
% Outputs:                                                                    %
%    -Overall and directionalized miss distances                              %
%    -Impact velocity components                                              %
%    -Deviations from expected impulse                                        %
%                                                                             %
%%%%%%%%%%%%%%%%%%%%%%%%%%%%%%%%%%%%%%%%%%%%%%%%%%%%%%%%%%%%%%%%%%%%%%%%%%%%

%%%%%%%%%%%%%%%%%%%%%%%%%%%%%%%%%%%%%%%%%%%%%%%%%%%%%%%%%%%%%%%%%%%%%%%%%%%%

%(dv in m/s, dx in km)
dv_min=5;     %dv_min >= 1m/s
dv_max=100;
dx_min=1;     %dx_max-dx_min=integer<=4...for legend
dx_max=dx_min;     %dx_max=5
orbit_alt=400;

%Macron parameters
%Setting A, Cd or M = 0...propagates purely orbital mechanics
A1=.00006235169878;  %m^2
Cd1=2;
M1=.001;         %kg

%Satellite parameters
%Setting A, Cd or M = 0...propagates purely orbital mechanics
A2=.1082974536;  %m^2
Cd2=2;
M2=100;         %kg

%%%%%%%%%%%%%%%%%%%%%%%%%%%%%%%%%%%%%%%%%%%%%%%%%%%%%%%%%%%%%%%%%%%%%%%%%%%%

%constants for scenario (1=macron, 2=satellite)
C1_1=-.5*Cd1*A1;    %m^2
C2_1=1/M1*1/1000;   %km/(kg m)
C1_2=-.5*Cd2*A2;    %m^2
C2_2=1/M2*1/1000;   %km/(kg m)
pi2=2*pi;
```

```
mu=398600.5;        %km^3/s^2
R_earth=6378.137;   %km

%Propagations are less than 2yrs sim time...therefore, only the current
%solar cycle spreadsheet is needed. (reduces computation time)
Alt_Roe_min=[xlsread('Atmospheric Density (SPENVIS-
400).xlsx',1,'A6:A3006'),...
    xlsread('Atmospheric Density (SPENVIS-400).xlsx',1,'Q6:Q3006')];
Alt_Roe_mean=[xlsread('Atmospheric Density (SPENVIS-
400).xlsx',1,'U6:U3006'),...
    xlsread('Atmospheric Density (SPENVIS-400).xlsx',1,'AK6:AK3006')];
Alt_Roe_max=[xlsread('Atmospheric Density (SPENVIS-
400).xlsx',1,'AN6:AN3006'),...
    xlsread('Atmospheric Density (SPENVIS-400).xlsx',1,'BD6:BD3006')];

%Sets up blank matrices with correct dimensions
miss_dis_min=zeros(dv_max-dv_min+1,dx_max-dx_min+2);
miss_dis_x_min=zeros(dv_max-dv_min+1,dx_max-dx_min+2);
miss_dis_y_min=zeros(dv_max-dv_min+1,dx_max-dx_min+2);
miss_dis_z_min=zeros(dv_max-dv_min+1,dx_max-dx_min+2);

miss_dis_mean=zeros(dv_max-dv_min+1,dx_max-dx_min+2);
miss_dis_x_mean=zeros(dv_max-dv_min+1,dx_max-dx_min+2);
miss_dis_y_mean=zeros(dv_max-dv_min+1,dx_max-dx_min+2);
miss_dis_z_mean=zeros(dv_max-dv_min+1,dx_max-dx_min+2);

miss_dis_max=zeros(dv_max-dv_min+1,dx_max-dx_min+2);
miss_dis_x_max=zeros(dv_max-dv_min+1,dx_max-dx_min+2);
miss_dis_y_max=zeros(dv_max-dv_min+1,dx_max-dx_min+2);
miss_dis_z_max=zeros(dv_max-dv_min+1,dx_max-dx_min+2);

v_impact_min=zeros(dv_max-dv_min+1,dx_max-dx_min+2);
v_impact_x_min=zeros(dv_max-dv_min+1,dx_max-dx_min+2);
v_impact_y_min=zeros(dv_max-dv_min+1,dx_max-dx_min+2);
v_impact_z_min=zeros(dv_max-dv_min+1,dx_max-dx_min+2);

v_impact_mean=zeros(dv_max-dv_min+1,dx_max-dx_min+2);
v_impact_x_mean=zeros(dv_max-dv_min+1,dx_max-dx_min+2);
v_impact_y_mean=zeros(dv_max-dv_min+1,dx_max-dx_min+2);
v_impact_z_mean=zeros(dv_max-dv_min+1,dx_max-dx_min+2);

v_impact_max=zeros(dv_max-dv_min+1,dx_max-dx_min+2);
v_impact_x_max=zeros(dv_max-dv_min+1,dx_max-dx_min+2);
v_impact_y_max=zeros(dv_max-dv_min+1,dx_max-dx_min+2);
v_impact_z_max=zeros(dv_max-dv_min+1,dx_max-dx_min+2);

%Populates Velocity Column
for x=1:dv_max-dv_min+1
    miss_dis_min(x,dx_max-dx_min+2)=x+dv_min-1;
    miss_dis_x_min(x,dx_max-dx_min+2)=x+dv_min-1;
    miss_dis_y_min(x,dx_max-dx_min+2)=x+dv_min-1;
    miss_dis_z_min(x,dx_max-dx_min+2)=x+dv_min-1;

    miss_dis_mean(x,dx_max-dx_min+2)=x+dv_min-1;
    miss_dis_x_mean(x,dx_max-dx_min+2)=x+dv_min-1;
```

```
    miss_dis_y_mean(x,dx_max-dx_min+2)=x+dv_min-1;
    miss_dis_z_mean(x,dx_max-dx_min+2)=x+dv_min-1;

    miss_dis_max(x,dx_max-dx_min+2)=x+dv_min-1;
    miss_dis_x_max(x,dx_max-dx_min+2)=x+dv_min-1;
    miss_dis_y_max(x,dx_max-dx_min+2)=x+dv_min-1;
    miss_dis_z_max(x,dx_max-dx_min+2)=x+dv_min-1;

    v_impact_min(x,dx_max-dx_min+2)=x+dv_min-1;
    v_impact_x_min(x,dx_max-dx_min+2)=x+dv_min-1;
    v_impact_y_min(x,dx_max-dx_min+2)=x+dv_min-1;
    v_impact_z_min(x,dx_max-dx_min+2)=x+dv_min-1;

    v_impact_mean(x,dx_max-dx_min+2)=x+dv_min-1;
    v_impact_x_mean(x,dx_max-dx_min+2)=x+dv_min-1;
    v_impact_y_mean(x,dx_max-dx_min+2)=x+dv_min-1;
    v_impact_z_mean(x,dx_max-dx_min+2)=x+dv_min-1;

    v_impact_max(x,dx_max-dx_min+2)=x+dv_min-1;
    v_impact_x_max(x,dx_max-dx_min+2)=x+dv_min-1;
    v_impact_y_max(x,dx_max-dx_min+2)=x+dv_min-1;
    v_impact_z_max(x,dx_max-dx_min+2)=x+dv_min-1;
end

%Solar Cycle Phase ('min', 'mean' or 'max')
for phase=1:3
    if phase==1
        MMM='min';
    elseif phase==2
        MMM='mean';
    elseif phase==3
        MMM='max';
    end
    %For separation distances...dx_min to dx_max
    for dx=dx_min:dx_max

        ri_macron = [0, -dx/2 ,R_earth+orbit_alt];
        vi_macron = [sqrt(mu/mag(ri_macron)),0,0];

        %For velocities... dv_min to dv_max
        for dv=dv_min:dv_max

            %r & v for fired macron
            ri_macron_fired = ri_macron;
            Rmag1 = mag(ri_macron_fired);
            vi_macron_fired = vi_macron + [0, dv/1000, 0];
            Vmag1000_1 = mag(vi_macron_fired)*1000;

            %checks to make sure initial dx is correct
            ri_rel = ri_macron_fired-[0, dx/2, R_earth+orbit_alt];
            r_rel = ri_rel;

            %COEs for fired macron
            [a1,e1,i1,raan1,w1,nu1]=convert_vec_IJK2COE(mu,ri_macron_fi
            red,vi_macron_fired);
```

```
            E1=acos((e1+cos(nu1))/(1+e1*cos(nu1))); %rad
            E1=mod(E1,pi);

            %r & v for satellite
            ri_sat = [0, 0, R_earth+orbit_alt];
            Rmag2 = mag(ri_sat);
            vi_sat = [sqrt(mu/mag(ri_sat)), 0, 0];
            Vmag1000_2 = mag(vi_sat)*1000;

            %COEs for satellite
            [a2,e2,i2,raan2,w2,nu2] =
            convert_vec_IJK2COE(mu,ri_sat,vi_sat);
            E2=acos((e2+cos(nu2))/(1+e2*cos(nu2))); %rad
            E2=mod(E2,pi);

            N=0;
            time=0;

            %Progress indicator
            disp(' ');
            disp(' ');
            disp(' ');
            disp(' ');
            disp ('  dv             MMM')
            disp([num2str(dv),'             ' char(MMM)])
            disp(' ');

%Have to take into account the accel due to gravity in the y-
direction...causes Vy to increase as the macron gets closer to the
equator and decrease as it gets further away from the equator. The
overall Vy_avg is greater than the initial firing vel which decreases
the "ideal...d=rt" transit time. ex) Ve=40m/s, dx=1km
t_ideal=d/r=1km/((40m/s)*(1km/1000m))

%Coordinate system: x-RAM, y-firing direction, z-radial direction

            %time to travel dx (no gravity (y))
            dt_ideal=dx/(dv/1000);
            %max velocity taking into account Fg in y-direction (m/s)
            dv_gravity_max=dv+(abs(9.81*sin(i1-pi/2))*dt_ideal);
            %avg velocity taking into account Fg in y-direction (m/s)
            dv_gravity=(dv_gravity_max+dv)/2;
            %avg time to travel dx with gravity
            dt_gravity_o=dx/(dv_gravity/1000);
            dt_gravity=0;

            %Stops when y-coordinate of macron is within .01cm of dx/2
            while abs(r_rel(2))*1000*100 > .01

%%%%%%%%%%%%%%%%%%%%%%%%%%%%    TIME STEP    %%%%%%%%%%%%%%%%%%%%%%%%%%%%

                %Prop .1s until the total prop time is near the total
                time required to travel dx then...
                if time+dt_gravity<dt_gravity_o && N==0
                    dt_gravity=.1;
```

```
                    %prop in 1cm incriments until sep dist is within .01cm
                    of dx/2
                else
                    %time to travel .01cm (no gravity (y))
                    dt_ideal=.01/(dv*100);
                    %max velocity taking into account Fg in y-direction
                   (m/s)
                    dv_gravity_max=dv+(abs(9.81*sin(i1-pi/2))*dt_ideal)
                   %avg velocity taking into account Fg in y-direction
                   (m/s)
                    dv_gravity=(dv_gravity_max+dv)/2;
                    %avg time to travel .01cm with gravity
                    dt_gravity=.01/(dv_gravity*100);
                    N=N+1;
                end

                time=time+dt_gravity;

%%%%%%%%%%%%%%%%%%%%%%%%%%%%%%%%      MACRON      %%%%%%%%%%%%%%%%%%%%%%%%%%%%%%%%

                p1=a1*(1-e1*e1);  %km

                %Determines Rho for macron
                Alt1=round((Rmag1-R_earth)*100)/100;
                if strcmp(MMM,'min')
                    Roe1=Alt_Roe_min(round((Alt1-390)*100+1),2);
                elseif strcmp(MMM,'mean')
                    Roe1=Alt_Roe_mean(round((Alt1-390)*100+1),2);
                elseif strcmp(MMM,'max')
                    Roe1=Alt_Roe_max(round((Alt1-390)*100+1),2);
                end

                %EOVs for macron
                T1=Roe1*Vmag1000_1*Vmag1000_1*C1_1;   %N

                nu_dot1=sqrt(mu*p1)/(Rmag1*Rmag1);     %s^-1

                 a_dot1=((2*a1*a1)/(sqrt(mu*p1))*((1+e1*cos(nu1))*T1))*C
                 2_1; %km/s
                e_dot1=sqrt(p1/mu)*((cos(nu1)+cos(E1))*T1)*C2_1;%s^-1

                nu1=mod(nu_dot1*dt_gravity+nu1,pi2);    %rad
                a1=a1+a_dot1*dt_gravity;    %km
                E1=acos((e1+cos(nu1))/(1+e1*cos(nu1))); %rad
                E1=mod(E1,pi);
                e1=e1+e_dot1*dt_gravity;    %rad

                 %Don't include w_dot..w changes drastically for near
                 circular orbits

%%%%%%%%%%%%%%%%%%%%%%%%%%%%%%%%      SATELLITE      %%%%%%%%%%%%%%%%%%%%%%%%%%%%%%%%

                p2=a2*(1-e2*e2);    %km
```

```
        %Determines Rho for satellite
        Alt2=round((Rmag2-R_earth)*100)/100;
        if strcmp(MMM,'min')
            Roe2=Alt_Roe_min(round((Alt2-390)*100+1),2);
        elseif strcmp(MMM,'mean')
            Roe2=Alt_Roe_mean(round((Alt2-390)*100+1),2);
        elseif strcmp(MMM,'max')
            Roe2=Alt_Roe_max(round((Alt2-390)*100+1),2);
        end

        %EOVs for satellite
        T2=Roe2*Vmag1000_2*Vmag1000_2*C1_2; %N

        nu_dot2=sqrt(mu*p2)/(Rmag2*Rmag2);  %s^-1

         a_dot2=((2*a2*a2)/(sqrt(mu*p2))*((1+e2*cos(nu2))*T2))*C
         2_2; %km/s
         e_dot2=sqrt(p2/mu)*((cos(nu2)+cos(E2))*T2)*C2_2; %s^-1

        nu2=mod(nu_dot2*dt_gravity+nu2,pi2);    %rad
        a2=a2+a_dot2*dt_gravity;    %km
        E2=acos((e2+cos(nu2))/(1+e2*cos(nu2))); %rad
        E2=mod(E2,pi);
        e2=abs(e2+e_dot2*dt_gravity);   %rad

         %Don't include w_dot..w changes drastically for near
         circular orbits

%%%%%%%%%%%%%%%%%%%%%%%%     RELATIVE POSITIONING     %%%%%%%%%%%%%%%%%%%%%%%%

         %macron and satellite position and velocity after time
         step
         [rf1,vf1]=convert_vec_coe2ijk(mu,a1,e1,i1,raan1,w1,nu1)
        [rf2,vf2]=convert_vec_coe2ijk(mu,a2,e2,i2,raan2,w2,nu2)
        rf2 = rf2 + [0; dx/2; 0];

        Rmag1=mag(rf1);
        Vmag1000_1=mag(vf1);
        Rmag2=mag(rf2);
        Vmag1000_2=mag(vf2);

        %relative positioning after current time step
        r_rel = rf1-rf2;
    end

    %final separation distance (cm) for dv,dx combination
    r=mag(r_rel)*1000*100;

    if phase==1
      miss_dis_min(dv-dv_min+1,dx-dx_min+1)=r;
      miss_dis_x_min(dv-dv_min+1,dx-dx_min+1)=r_rel(1)*1000*100;
      miss_dis_y_min(dv-dv_min+1,dx-dx_min+1)=r_rel(2)*1000*100;
      miss_dis_z_min(dv-dv_min+1,dx-dx_min+1)=r_rel(3)*1000*100;
    elseif phase==2
```

```
                miss_dis_mean(dv-dv_min+1,dx-dx_min+1)=r;
                miss_dis_x_mean(dv-dv_min+1,dx-dx_min+1)=r_rel(1)*1000*100;
                miss_dis_y_mean(dv-dv_min+1,dx-dx_min+1)=r_rel(2)*1000*100;
                miss_dis_z_mean(dv-dv_min+1,dx-dx_min+1)=r_rel(3)*1000*100;
            elseif phase==3
                miss_dis_max(dv-dv_min+1,dx-dx_min+1)=r;
                miss_dis_x_max(dv-dv_min+1,dx-dx_min+1)=r_rel(1)*1000*100;
                miss_dis_y_max(dv-dv_min+1,dx-dx_min+1)=r_rel(2)*1000*100;
                miss_dis_z_max(dv-dv_min+1,dx-dx_min+1)=r_rel(3)*1000*100;
            end

            %final relative velocity for dv,dx combination (direction
            of force received)
            v_rel = abs(vf1-vf2);
            v = mag(v_rel);

            if phase==1
            v_impact_min(dv-dv_min+1,dx-dx_min+1)=v*1000;
            v_impact_x_min(dv-dv_min+1,dx-dx_min+1)=v_rel(1)*1000;
            v_impact_y_min(dv-dv_min+1,dx-dx_min+1)=v_rel(2)*1000-dv;
            v_impact_z_min(dv-dv_min+1,dx-dx_min+1)=v_rel(3)*1000;
            elseif phase==2
            v_impact_mean(dv-dv_min+1,dx-dx_min+1)=v*1000;
            v_impact_x_mean(dv-dv_min+1,dx-dx_min+1)=v_rel(1)*1000;
            v_impact_y_mean(dv-dv_min+1,dx-dx_min+1)=v_rel(2)*1000-dv;
            v_impact_z_mean(dv-dv_min+1,dx-dx_min+1)=v_rel(3)*1000;
            elseif phase==3
            v_impact_max(dv-dv_min+1,dx-dx_min+1)=v*1000;
            v_impact_x_max(dv-dv_min+1,dx-dx_min+1)=v_rel(1)*1000;
            v_impact_y_max(dv-dv_min+1,dx-dx_min+1)=v_rel(2)*1000-dv;
            v_impact_z_max(dv-dv_min+1,dx-dx_min+1)=v_rel(3)*1000;
            end
        end
    end
end

%%%%%%%%%%%%%%%%%%%%%%%%%%%    PLOTS   %%%%%%%%%%%%%%%%%%%%%%%%%%%%%%%%

%Miss Distance vs Firing Velocity
figure(1)
hold on

A=plot(miss_dis_min(:,dx_max-dx_min+2), miss_dis_min(:,1));
set(A,'Color','green');
B=plot(miss_dis_mean(:,dx_max-dx_min+2), miss_dis_mean(:,1));
set(B,'Color','blue','linestyle', '--');
C=plot(miss_dis_max(:,dx_max-dx_min+2), miss_dis_max(:,1));
set(C,'Color','red','linestyle', '-.');
legend('Min','Mean','Max')
xlabel('Firing Velocity (m/s)')
ylabel('Miss Distance (cm)')
title('Miss Distance as a fxn Firing Velocity')

%Miss Distance (XZ) vs Firing Velocity
figure(2)
hold on
```

```
grid on
axis square

A=plot3(miss_dis_x_min(:,1),
miss_dis_z_min(:,1),miss_dis_x_min(:,dx_max-dx_min+2));
set(A,'Color','green');
text(miss_dis_x_min(1,1),miss_dis_z_min(1,1),miss_dis_z_min(1,2),'
\leftarrow Min','HorizontalAlignment','left')
grid on
axis square

B=plot3(miss_dis_x_mean(:,1),
miss_dis_z_mean(:,1),miss_dis_x_mean(:,dx_max-dx_min+2));
set(B,'Color','blue','linestyle', '--');

text(miss_dis_x_mean(1,1),miss_dis_z_mean(1,1),miss_dis_z_mean(1,2),'
\leftarrow Mean','HorizontalAlignment','left')
grid on
axis square

C=plot3(miss_dis_x_max(:,1),
miss_dis_z_max(:,1),miss_dis_x_max(:,dx_max-dx_min+2));
set(C,'Color','red','linestyle', '-.');
text(miss_dis_x_max(1,1),miss_dis_z_max(1,1),miss_dis_z_max(1,2),'
\leftarrow Max','HorizontalAlignment','left')
grid on
axis square

legend('Min','Mean','Max')
xlabel('Miss Distance (X) (cm)')
ylabel('Miss Distance (Z) (cm)')
Zlabel('Firing Velocity (m/s)')
title('Miss Distance (XZ) as a fxn Firing Velocity')

%Impact Velocities in XZ-plane (aka undesired force vectors)
figure(3)
hold on
grid on
axis square

A=plot3(v_impact_x_min(:,1), v_impact_z_min(:,1),
miss_dis_x_min(:,dx_max-dx_min+2)); set(A,'Color','green');
text(v_impact_x_min(1,1),v_impact_z_min(1,1),v_impact_z_min(1,2),'
\leftarrow Min','HorizontalAlignment','left')
B=plot3(v_impact_x_mean(:,1), v_impact_z_mean(:,1),
miss_dis_x_mean(:,dx_max-dx_min+2)); set(B,'Color','blue','linestyle',
'--');
text(v_impact_x_mean(1,1),v_impact_z_mean(1,1),v_impact_z_mean(1,2),'
\leftarrow Mean','HorizontalAlignment','left')

C=plot3(v_impact_x_max(:,1), v_impact_z_max(:,1),
miss_dis_x_max(:,dx_max-dx_min+2)); set(C,'Color','red','linestyle', '-
.');
text(v_impact_x_max(1,1),v_impact_z_max(1,1),v_impact_z_max(1,2),'
\leftarrow Max','HorizontalAlignment','left')
```

```
legend('Min','Mean','Max')
xlabel('Impact Velocity (X) (m/s)')
ylabel('Impact Velocity (Z) (m/s)')
Zlabel('Firing Velocity (m/s)')
title('Impact Velocity (XZ) as a fxn Firing Velocity')

%deviation from expected desired thrust component (Y) vs Firing
Velocity
figure(4)
hold on

A=plot(v_impact_y_min(:,2), v_impact_y_min(:,1));
set(A,'Color','green');
B=plot(v_impact_y_mean(:,2), v_impact_y_mean(:,1));
set(B,'Color','blue','linestyle', '--');
C=plot(v_impact_y_max(:,2), v_impact_y_max(:,1));
set(C,'Color','red','linestyle', '-.');

legend('Min','Mean','Max')
xlabel('Firing Velocity (m/s)')
ylabel('Deviation from Expected Thrust (y) (m/s)')
title('Deviation from Expected Thrust (y)')
```

APPENDIX F

TANDEM SATELLITE FORMATION MISS DISTANCES

Directionalized miss distances as a function of firing velocity for varying separation distances during solar mean.

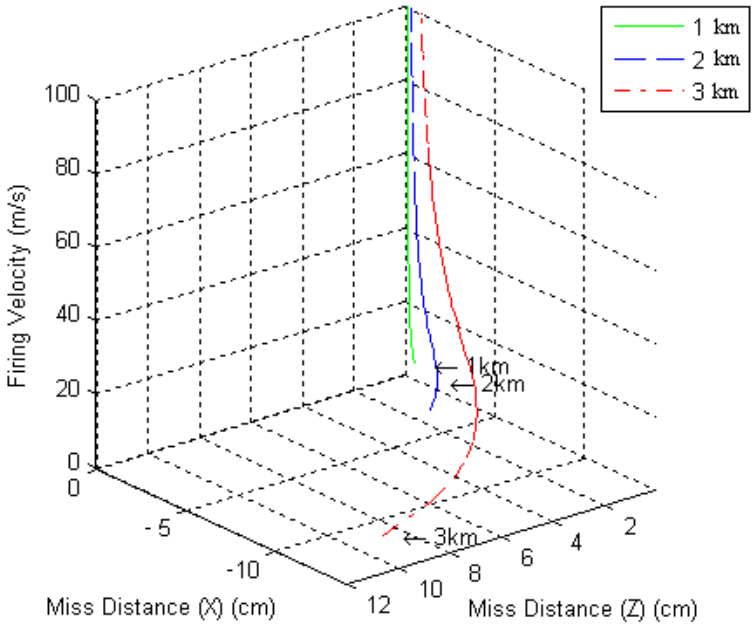

Off-axis thrust components as a function of firing velocity for varying separation distances during solar mean.

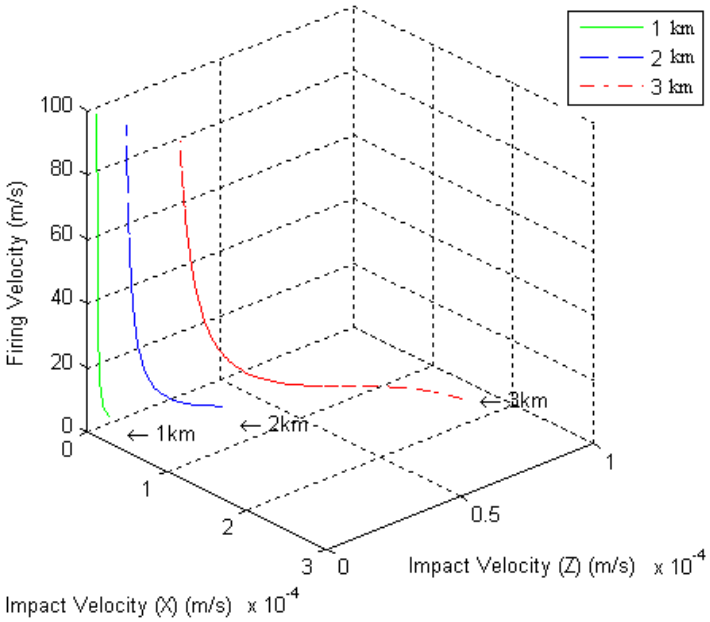

Deviation from expected thrust components in the desired direction (i.e. y-axis) as a function of firing velocity for varying separation distances during solar mean.

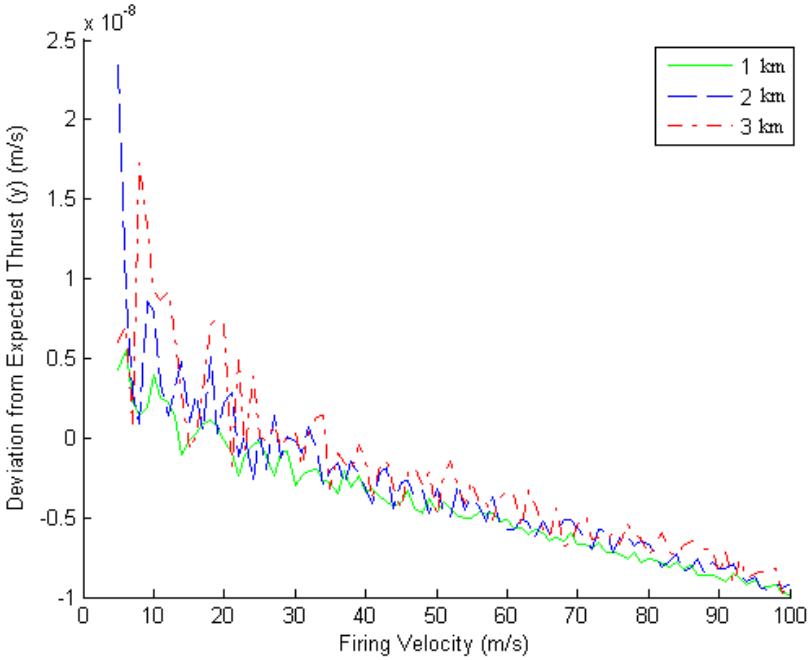

Directionalized miss distances as a function of firing velocity for varying separation distances during solar min, mean, and max periods.

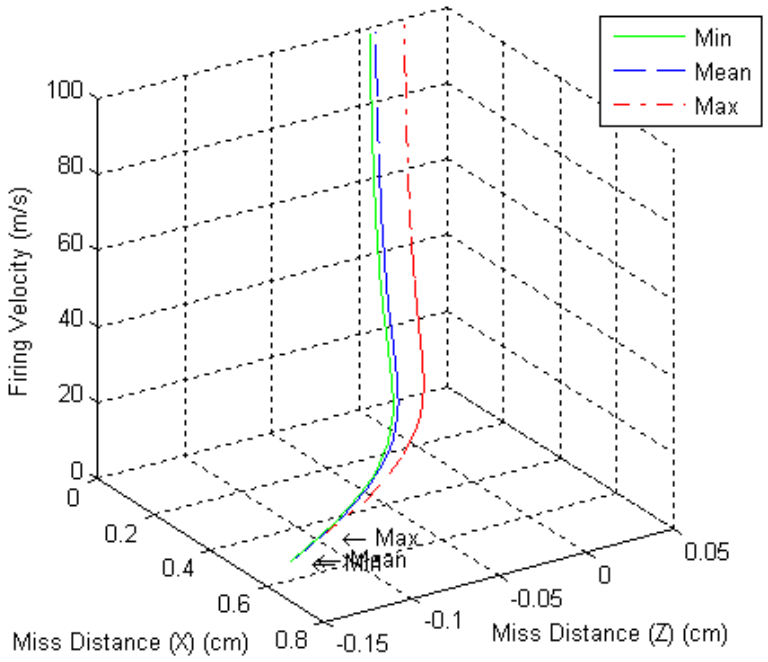

Off-axis thrust components as a function of firing velocity for varying separation distances during solar min, mean, and max periods.

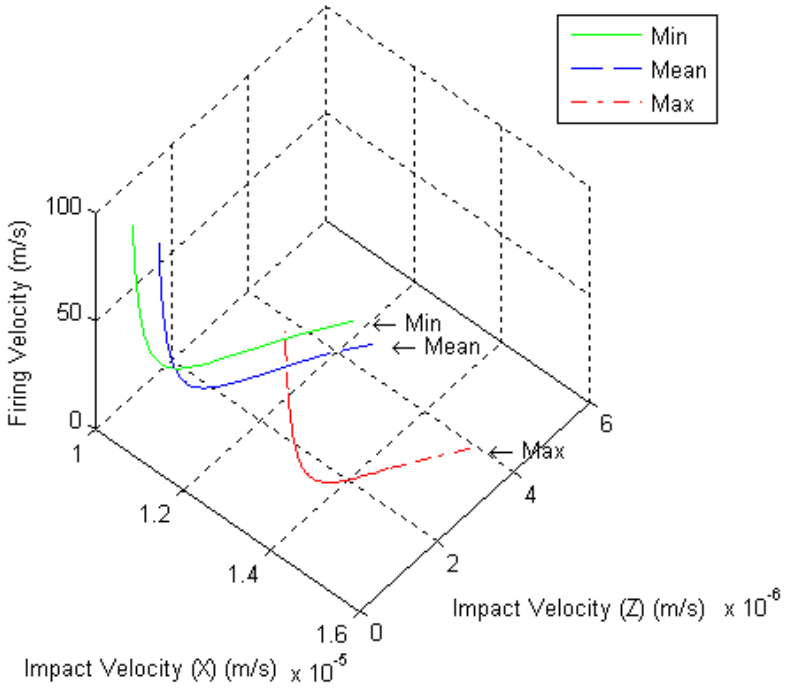

Deviation from the expected thrust components in the desired direction (i.e. y-axis) as a function of firing velocity for varying separation distances during solar min, mean, and max periods.